

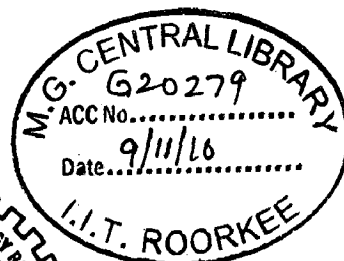
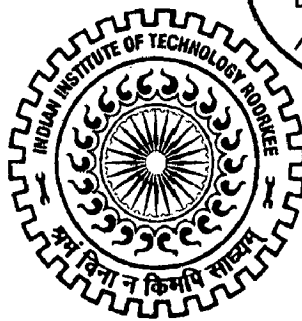
**VARIABLE SPEED GENERATOR FOR HYDRO
POWER PLANT UNDER VARYING HEAD
AND DISCHARGE CONDITIONS**

A DISSERTATION

*Submitted in partial fulfillment of the
requirements for the award of the degree*
of
MASTER OF TECHNOLOGY
in
WATER RESOURCES DEVELOPMENT

By

MUKESH KUMAR LODHA



**DEPARTMENT OF WATER RESOURCES DEVELOPMENT AND MANAGEMENT
INDIAN INSTITUTE OF TECHNOLOGY ROORKEE
ROORKEE -247 667 (INDIA)
JUNE, 2010**

CANDIDATE'S DECLARATION

I hereby certify that the work which is being presented in this Dissertation entitled, "Variable Speed generator for hydro power plant under varying head and discharge conditions", is in partial fulfilment of the requirement for the award of the Degree of Master of Technology and submitted to the Department of Water Resources Development and Management (WRD&M), Indian Institute of Technology, Roorkee. This is an authentic record of my own work carried out under the supervision of Prof. Devedutta Das, WRD&M, and Prof. S.P.Singh Department of Electrical Engineering IIT, Roorkee, Uttarakhand, India.

The matter presented in this Dissertation has been submitted by me for the award of any other degree.

Dated: 30/06/10

Place: Roorkee



(MUKESH KUMAR LODHA)

Enrolment no-08548016

CERTIFICATE

This is to certify that the above statement made by the candidate is correct to the best of my knowledge.



Prof. S.P.Singh
Deptt. Of Elect. Engg.
IIT, Roorkee



Prof. Devedutta Das
Deptt. Of WRD&M,
IIT, Roorkee

ACKNOWLEDGEMENT

First of all I praise the God, the cherisher and sustainers of the world.

I feel privileged to express my deep sense of gratitude and sincere regards to Prof. Devadutta Das, Department of Water Resource Development and Management and Prof. S.P. Singh Department of Electrical Engineering, Indian Institute of Technology Roorkee for their keen interest, invaluable guidance and constant encouragement throughout the course of present study.

I am also pleased to extend my sincere gratitude to Dr. Nayan Sharma, Professor and Head of Department and also Dr. M.L. Kansal, faculty members of WRD&M, IIT Roorkee for their valuable suggestions and encouragement.

Place : Roorkee
Date : 30/06/10



(MUKESH KUMAR LODHA)
M.Tech.(WRD&M)
Enrollment No. 08548016

CONTENTS

<i>S.N.</i>	<i>SUBJECT</i>	<i>PAGE NO.</i>
1.	INTRODUCTION	1
1.1	Functional block diagram of power generation and control system	2
2.	LITERATURE REVIEW	3
2.1	Simulation models of the hydro power plants in Macedonia and Yugoslavia	3
2.2	Power Interchange Control of Frequency Converter using Adjustable Speed Generator/Motor Taking Into Account Multiple Power Flow Conditions	4
2.3	The Design of Control Configuration of Variable Speed Generator System	5
2.4	Adjustable Speed Drive and Variable Speed Generation System with Reduced Power Converter Requirements	6
3.	METHODOLOGY	8
3.1	Hydraulic Turbine	9
3.1.1	Hydraulic Turbine Transfer Function	9
3.1.2	Non-ideal turbine	13
3.1.3	Non linear Turbine Model Assuming Inelastic water column	13
3.2	Governors for Hydraulic Turbines	18
3.2.1	Requirement for a transient droop	18
3.2.2	Mechanical- Hydraulic governor	19

3.2.3	Electro hydraulic governor	21
3.3	Generator Modelling	22
3.3.1	Fundamentals of Speed Governing	25
3.3.2	Generator response to load change	25
4.	SIMULATION	28
4.1	Data Used In Model	28
4.1.1	Synchronous Machine data	28
4.1.2	Turbine Data	28
4.1.3	Governor Data	29
4.1.4	Excitation System Data	29
4.2	Hydraulic Turbine Simulation	30
4.3	Governor Simulation	31
4.4	Overall block diagram	32
4.5	Complete overall Block Diagram	33
4.6	Simulation Output Table	34
4.7	Simulation Output Response	40
4.7.1	For 50 MW Active Power and 50 MVAR Reactive Power Load at 1 p.u. Head	40
4.7.2	For 60 MW Active Power and 50 MVAR Reactive Power Load at 1 p.u. Head	45
4.7.3	For 50 MW Active Power and 50 MVAR Reactive Power Load at 0.9 p.u. Head	50
4.7.4	For 60 MW Active Power and 50 MVAR Reactive Power Load at 0.9 p.u. Head	55
4.7.5	For 50 MW Active Power and 50 MVAR Reactive Power Load at 0.8 p.u. Head	60
4.7.6	For 50 MW Active Power and 50 MVAR Reactive Power Load at 0.7 p.u. Head .	65
4.7.7	For 50 MW Active Power and 50 MVAR Reactive Power Load at 0.6	

	p.u. Head	70
5.	CONCLUSION	75
6.	REFERENCES	76

ABSTRACT

Since a long time, it is known that hydraulic machines can work with an increased efficiency at partial load when the speed can be adapted to this partial load. In a standard configuration when the hydraulic machine is coupled to the electric grid this speed variation is not possible at all. So for variable speed generator operation some modifications have to be made in hydro power plant. Speed governor may not be used to control frequency of isolated plant. Depending upon the type of generator whether it is synchronous or induction the suitable topology of converter need to be selected to convert variable voltage or frequency output into the constant voltage or frequency output. The variable speed concept of electrical machines is the optimum solution in the case of large variation in the turbine and pumping heads enables load control in pumping mode, results in the best overall efficiency and improves the stability in the power system. The reason for these advantages comes from the ability to run the group at the optimum speed (in a given speed range) of the hydraulic machine for all hydraulic conditions. The control systems proposed for a variable speed generator becomes nowadays more and more complicated. When the load is suddenly decreased by a step reduction in conductance, the current does not change instantly; however, the voltage across the load suddenly increases because of the reduction in conductance (or increase in resistance). This causes the output power to suddenly increase initially. With a rate determined by the inductance, the current decreases exponentially until a new steady value is reached establishing the new steady output power. The responses of current, voltage and power are very similar to those of velocity, head and power for a step reduction in gate position. Speed governor performs speed control functions for satisfactory operation of power plant. The main part of the dissertation is dedicated to the behavior of this variable speed generator system under varying head and discharge conditions in respect of grid stability and grid transients.

1. INTRODUCTION

One of the most important aspects of the hydro power plant is the efficiency of the energy conversion. The Prime sources of Electrical Energy supplied by utilities are the kinetic Energy of water. The prime movers convert these sources of energy into mechanical energy that is, in turn, converted to electrical energy by synchronous generators. The prime mover governing systems provide a means of controlling power and frequency, a function commonly referred to as load frequency control or automatic generation control. Synchronous generators form the principle source of electric energy in power systems. Many large loads are driven by synchronous motors. Synchronous condensers are sometimes used as a means of providing reactive power compensation and controlling voltage. These devices operate on the same principle and are collectively referred to as synchronous machines. The power system stability problem is largely one of keeping interconnected synchronous machines in synchronism.

The basic function of an excitation system is to provide direct current to the synchronous machine field winding. In addition, the excitation system performs control and protective functions essential to the satisfactory performance of the power system by controlling the field voltage and thereby the field current.

The flows of active power and reactive power in a transmission networks are fairly independent of each other and are influenced by different control actions. Active power control is closely related to frequency control, and reactive power control is closely related to voltage control. As constancy of frequency and voltage are important factors in determining the quality of power supply, the control of active power and reactive power is vital to the satisfactory performance of power systems.

As frequency is a common factor throughout the system, a change in active power demand at one point is reflected throughout the system by a change in frequency. Because there are many generators supplying power into the system, some means must be provided to allocate change in demand to the generators. A speed governor on each generating unit provides the primary speed control function, while supplementary control origination at a central control centre allocates generation.

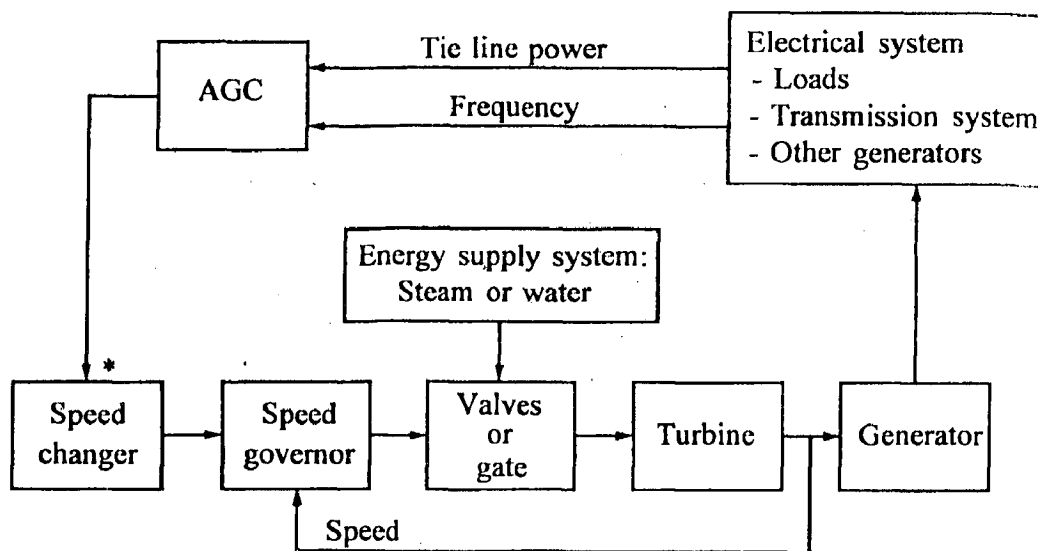
However for variable speed generator operation some modifications have to be made in hydro power plant. Speed governor may not be used to control frequency of isolated plant. Depending upon the type of generator whether it is synchronous or induction the suitable topology of converter need to be selected to convert variable voltage or frequency output into the constant voltage or frequency output. In case of synchronous generator as-dc-ac scheme may be adopted on stator side. But in case of induction generator the same converter topology may be considered on rotor side to harness power under large variations in head or discharge conditions.

Such complex power conversion process includes potential, mechanical and electromechanical phenomena each with different, characteristic time scale.

Block diagrams are obtained by modeling using equations for different components. They are connected with each other as per requirement. Then they are simulated using MATLAB software.

Simulation is done for mechanical power, active power, speed, gate opening, excitation voltage etc. for different load power. Their transient response and steady state response are studied, and then stability is studied. Further, this study is extended for different head and discharge conditions also.

1.1 Functional block diagram of power generation and control system



2. LITERATURE REVIEW

2.1 Simulation models of the hydro power plants in Macedonia and Yugoslavia

By H. Weber and F. Prillwitz

In hydro power plants of Macedonia and Yugoslavia there is a lack of knowledge and information about the static and dynamic behavior of the units for each contingency that could occur. In that sense the inevitable task was the creation of simulation models of the hydro power plants which can be used on the one hand by experts for analysis of the static and dynamic behavior and on the other hand by the staff involved with the operation and maintenance of the plant for their training. This contribution presents the most important steps for the reality oriented creation of mathematical models of hydro power plants which can be used for such investigations. According to the joint project DYSIMAC (Dynamic Simulation of the Macedonian and Yugoslavian power plants in a new technological and market environment), the authors investigated dynamic characteristics of units in HPP "Vrutok" and "Tikves" in Macedonia and also HPP "Zvornik" and "Bajina Basta" in Yugoslavia. It will be shown, that a model structure developed using the documentations of the power plants together with parameter estimations after suitable experiments will lead to comparatively small simulation models which can guarantee a very good dynamic behavior compared with the behavior of real power plants. With this method the modeling was performed for hydro power plants with Pelton Turbin, HPP "Vrutok" (FYROM), with Francis turbine, HPP "Tikves" (FYROM), HPP "Bajina Basta"(YU) and with Kaplan turbine, HPP "Zvornik"(YU).

2.2 Power Interchange Control of Frequency Converter using Adjustable Speed Generator/Motor Taking Into Account Multiple Power Flow Conditions(IEEE paper 2000)

By R.Kobayashi, A.Yokoyama , S. Ogawa, S.C.Verma

Adjustable Speed Generator/ Motor can control active power and reactive power independently by the AC excitation. It can also change the rotor speed. Because of the above characteristics, ASGM can be applied to frequency converter, where two ASGMs are used. The rotor shaft of their ASGMs is common. Here, it is necessary to design a control system in order to adjust active power to the specified value quickly.

Adjustable Speed Generator/Motor is excited by AC voltage and has the same structure as 3-phase induction motor. ASGM has two important characteristics. One is the ability to control active power and reactive power independently by the AC excitation. The other is the ability to vary the rotor speed.

Recently, ASGM is applied to large-capacity pumped storage power plants, which can control the frequency of the power system. ASGM can also applied to frequency converter station inherent to Japan, where two ASGMs are connected with the shaft mechanically. This frequency converters will be able to have a function of power system stabilization because it can make use of the stored energy by the rotor. And it may have the advantage of the low construction cost compared with the conventional power electronics based frequency converter.

The main purpose of this paper is a design of power interchange control system with relatively large interchanged power. First, two-state eigenvalue control technique is proposed to determine the control parameters in this paper. Then digital dynamic simulation is performed to illustrate effectiveness of the proposed method. Finally, the reverse control system of interchanged power flow is designed by using three-state eigenvalue control technique. The future work is to design the power system stabilizing control system.

2.3 The Design of Control Configuration of Variable Speed Generator System(IEEE paper 1997)

By Yuzo ITOH and Nobuhito NOZAWA

In this paper a new designing method for variable Rotating speed Generator system is presented. On the other hand the rotor speed of the traditional Synchronous generator system is exactly regulated to the power system frequency by the manner of mechanical governor control, VSGS has no necessity of frequency controlling by a mechanical Control system. The machine employed in VSGS is a wound type induction machine.

Nowadays, VSGS is applied for the pumped storage generator which elevates a running efficiency. And the system with large rotating inertia is used to improve the stability for the step load variation in the power system. As the other utilization, it can be applied for asynchronous rotary machine which can provide not only electrical reactive power but active power. So, a variable speed generator will be more used as the device of Flexible AC Transmission system. For those application of VSGS, the stable and quick response for the system references and step change of power output are required. In order to obtain the steady and transient state behavior of VSGS, the instantaneous vector analysis is employed. To design control system for VSGS, a developed optimal control theory is applied.

The system response of VSGS designed by the proposed method is simulated and is experimented on the case of constant generating mode while the shaft input is increasing. Finally, the effectiveness of the proposed control method for VSGS is confirmed.

In order to be put VSGS to practical use, some important problems which should be solved are remained. Some of those are as follows.

1. To remove noise of the measured data, a filter may be employed.
2. A two directional power converter system should be used to work at region of the lower and upper side of synchronous speed.

The effectiveness of elevating the stability of electrical power line applied VSGS should be developed in the future.

2.4 Adjustable Speed Drive and Variable Speed Generation System with Reduced Power Converter Requirements (IEEE paper 1993)

By Alan K. Wallace, Rene Spee, Gerald C. Alexander

This Paper described the physical configuration of the brushless doubly-fed machine and its potential as an alternative low cost adjustable speed drive. Particular interest in this type of machine is now being shown because of its flexibility as a variable speed generator. The projected advantages of the brushless double fed machine system for adjustable-speed drives and, more particularly, for variable-speed generators are being established by design improvement verified by laboratory tests. Application oriented designs must now be pursued to establish the benefits of the systems.

A single-frame self-cascaded induction machine, which is capable of operation in both an induction mode and form of synchronous mode, has attracted the attention of many researchers since the concept was first developed by Hunt at the turn of this century. This type of machine evolved, both physically and conceptually, from two induction machines with cross-connected rotor phase-windings on the same shaft, thus avoiding the use of brush gear. The advent of power electronic converters capable of adjustable frequency, adjustable voltage and bidirectional power-flow operation has revived interest in the self-cascaded induction machine. This interest is promoted by the demonstrated adjustable speed drive and variable speed generation capability in which one of the stator windings is supplied via a converter of a rating significantly smaller than that of the machine. This configuration is now referred to as a brushless doubly-fed machine.

To avoid direct transformer coupling, it is essential that the two windings on the stator have different numbers of poles. Although many pole-number combinations are possible, laboratory demonstration machines have, so far, concentrated on 6-pole power windings and 2-pole control windings. The rotor has a specified cage structure with the number of identical sections, or nests, equal to the sum of the pole-pairs of the two stator windings. Specialized single stator windings connections have been developed for induction motors to produce two magnetic fields of different pole numbers. For pole-changing machines these type of stator windings enable more effective use of slot space and hence increase available conductor area. However, for the BDFM, it has been shown that parallel

winding imbalance results in the lower pole-number connection giving rise to internal circulation currents, causing both additional losses and instability in certain areas of the speed range. In consequence, two isolated 3-phase stator windings are preferred as they enable a better overall performance compromise and can be individually rated depending upon the machine applications.

3. METHODOLOGY

3.1 Hydraulic Turbines

Hydraulic turbines are of two basic types: impulse turbines and reaction turbines.

The impulse-type turbine (also known as Pelton wheel) is used for high heads 300 meters or more. The runner is at atmospheric pressure, and the whole of the pressure drop takes place in stationary nozzles that convert potential energy to kinetic energy. The high-velocity jets of water impinge on spoon-shaped buckets on the runner, which deflect the water axially through about 160° ; the change in momentum provides the torque to drive the runner, the energy supplied being entirely kinetic.

In a reaction turbine the pressure within the turbine is above atmospheric; the energy is supplied by the water in both kinetic and potential (pressure head) forms. The water first passes from a spiral casing through stationary radial guide vanes and gates around its entire periphery. The gates control water flow. There are two subcategories of reaction turbines: Francis and propeller.

The Francis turbine is used for heads up to 360 meters. In this type of turbine, water flows through guide vanes impacting on the runner tangentially and exiting axially.

The propeller turbine, as the name implies, uses propeller-type wheels. It is for use on low heads-up to 45 meters. Either fixed blades or variable-pitch blades may be used. The variable-pitch blade propeller turbine, commonly known as the Kaplan wheel, has high efficiency at all loads.

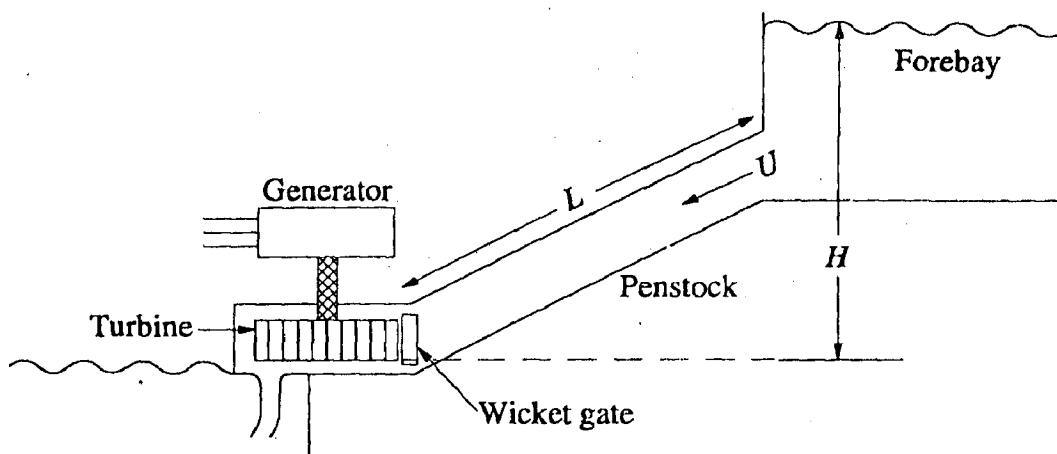
The performance of a hydraulic turbine is influenced by the characteristic of the water column feeding the turbine; these include the effects of water inertia, water compressibility, and pipe wall elasticity in the penstock. The effect of water inertia is to cause changes in turbine flow to lag behind changes in turbine gate opening.

3.1.1 Hydraulic Turbine Transfer Function

The representation of the hydraulic turbine and water column in stability studies is usually based on the following assumptions:

1. The hydraulic resistance is negligible.
2. The penstock pipe is inelastic and the water is incompressible.
3. The velocity of the water varies directly with the gate opening and with the square root of the net head.
4. the turbine output power is proportional to the product of head and volume flow.

The essential elements of the hydraulic plant are depicted in Figure.



The turbine and penstock characteristics are determined by three basic equations relating to the following:

- (a) Velocity of water in the penstock
- (b) Turbine mechanical power
- (c) Acceleration of water column

The velocity of the water in the penstock is given by

$$U = K_u G \sqrt{H} \quad \text{----- (1)}$$

Where

U = water velocity

G = gate position

H = hydraulic head at gate

K_u = a constant of proportionality

For small displacement about an operating point,

$$\Delta U = \frac{\partial U}{\partial H} \Delta H + \frac{\partial U}{\partial G} \Delta G \quad \text{----- (2)}$$

Substituting the appropriate expressions for the partial derivatives and dividing through by $U = K_u G_o H_o^{1/2}$ yields

$$\frac{\Delta U}{U_o} = \frac{\Delta H}{2H_o} + \frac{\Delta G}{G_o} \quad \text{----- (3)}$$

Or

$$\Delta \bar{U} = \frac{1}{2} \Delta \bar{H} + \Delta \bar{G} \quad \text{----- (4)}$$

Where the subscript o denotes initial steady-state values, the prefix Δ denotes small deviations, and the superbar “-” indicates normalized values based on steady-state operating values.

The turbine mechanical power is proportional to the product of pressure and flow; hence,

$$P_m = K_p H U \quad \text{----- (5)}$$

Linearizing by considering small displacements, and normalizing by dividing both sides by $P_{m0} = K_p H_o U_o$ we have

$$\frac{\Delta P_m}{P_{m0}} = \frac{\Delta H}{H_o} + \frac{\Delta U}{U_o} \quad \text{----- (6)}$$

Or

$$\Delta \bar{P}_m = \Delta \bar{H} + \Delta \bar{U} \quad \text{----- (7)}$$

Substituting for from equation

$$\Delta \bar{P}_m = 1.5 \Delta \bar{H} + \Delta \bar{G} \quad \text{----- (8)}$$

Alternatively, by substituting for ΔH from equation we may write

$$\Delta \bar{P}_m = 3 \Delta \bar{U} - 2 \Delta \bar{G} \quad \text{----- (9)}$$

The acceleration of water column due to a change in head at the turbine, characterized by Newton's second law of motion, may be expressed as

$$(\rho LA) \frac{d\Delta U}{dt} = -A(\rho a_g) \Delta H \quad \text{----- (10)}$$

Where

L = Length of conduit

A = Pipe area

ρ = Mass density

a_g = acceleration due to gravity

ρLA = Mass of water in the conduit

$\rho a_g \Delta H$ = incremental change in pressure at turbine gate

t = time in seconds

By dividing both sides by $A\rho a_g H_0 U_0$ the acceleration equation in normalized form becomes

$$\frac{LU_0}{a_g H_0} \frac{d}{dt} \left(\frac{\Delta U}{U_0} \right) = -\frac{\Delta H}{H_0} \quad \text{----- (11)}$$

$$T_w \frac{d\Delta \bar{U}}{dt} = -\Delta \bar{H} \quad \text{----- (12)}$$

Where by definition,

$$T_w = \frac{LU_0}{a_g H_0} \quad \text{----- (13)}$$

Here T_w is referred to as the water starting time. It represents the time required for a head H to accelerate the water in the penstock from standstill to the velocity U . It should be noted that T_w varies with load. Typically, T_w at full load lies between 0.5 s and 4.0 s.

Equation represents an important characteristic of the hydraulic plant. A descriptive explanation of the equation is that if back pressure is applied at the end of the penstock by closing the gate, then the water in the penstock will decelerate. That is, if there is a positive pressure change, there will be a negative acceleration change.

The relationship between change in velocity and change in gate position as

$$T_w \frac{d\Delta\bar{U}}{dt} = 2(\Delta\bar{G} - \Delta\bar{U}) \quad \text{----- (14)}$$

Replacing d/dt with the Laplace operator s , we may write

$$T_w s \Delta\bar{U} = 2(\Delta\bar{G} - \Delta\bar{U}) \quad \text{----- (15)}$$

Or

$$\Delta\bar{U} = \frac{1}{1 + \frac{1}{2} T_w s} \Delta\bar{G} \quad \text{----- (16)}$$

Substituting for $\Delta\bar{U}$ from Equation and rearranging, we obtain

$$\frac{\Delta\bar{P}_m}{\Delta\bar{G}} = \frac{1 - T_w s}{1 + \frac{1}{2} T_w s} \quad \text{----- (17)}$$

Equation represents the “classical” transfer function of a hydraulic turbine. It shows how the turbine power output changes in response to a change in gate opening for an ideal lossless turbine.

3.1.2 Non-ideal turbine

The transfer function of a non-ideal turbine may be obtained by considering the following general expression for perturbed values of water velocity (flow) and turbine power:

$$\Delta \bar{U} = a_{11} \Delta \bar{H} + a_{12} \Delta \bar{\omega} + a_{13} \Delta \bar{G}$$

----- (18)

$$\Delta \bar{P}_m = a_{21} \Delta \bar{H} + a_{22} \Delta \bar{\omega} + a_{23} \Delta \bar{G}$$

----- (19)

Where $\bar{\omega}$ is the per unit speed deviation. The speed deviations are small, especially when the unit is synchronized to a large system; therefore, the terms related to $\bar{\omega}$ may be neglected. Consequently,

$$\Delta \bar{U} = a_{11} \Delta \bar{H} + a_{13} \Delta \bar{G}$$

----- (20)

$$\Delta \bar{P}_m = a_{21} \Delta \bar{H} + a_{23} \Delta \bar{G}$$

----- (21)

The coefficients a_{11} and a_{13} are partial derivatives of flow with respect to head and gate opening, and the coefficients a_{21} and a_{23} are partial derivatives of turbine power output with respect to head and gate opening. These coefficients depend on machine loading and may be evaluated from the turbine characteristics at the operating point.

$$\frac{\Delta \bar{P}_m}{\Delta \bar{G}} = a_{23} \frac{1 + (a_{11} - a_{13} a_{21} / a_{23}) T_w s}{1 + a_{11} T_w s}$$

----- (22)

3.1.3 Non linear Turbine Model Assuming Inelastic water column

The linear model given by equation represents the small-signal performance of the turbine. It is useful for control system tuning using linear analysis techniques (frequency response, root locus, etc.). Because of the simplicity of its structure, this model provides insight into the basic characteristic of the hydraulic system.

We consider a simple hydraulic system configuration with unrestricted head and tail race, and with either a very large or no surge tank.

Assuming a rigid conduit and incompressible fluid, the basic hydrodynamic equations are

$$U = K_u G \sqrt{H} \quad \text{----- (23)}$$

$$P = K_p H U \quad \text{----- (24)}$$

$$\frac{dU}{dt} = -\frac{a_g}{L}(H-H_0) \quad \text{----- (25)}$$

$$Q = AU \quad \text{----- (26)}$$

Where

U = water velocity

G = ideal gate opening

H = hydraulic head at gate

H₀ = initial steady-state value of H

P = turbine power

Q = water-flow rate

A = pipe area

l = length of conduit

a_g = acceleration due to gravity

t = time in seconds

Since we are interested in the large-signal performance, we normalize the above equations based on rated values.

$$\frac{U}{U_r} = \frac{G}{G_r} \left(\frac{H}{H_r} \right)^{\frac{1}{2}} \quad \text{----- (27)}$$

$$\frac{P}{P_r} = \frac{U}{U_r} \frac{H}{H_r} \quad \text{----- (28)}$$

Where the subscript r denotes rated values. In per unit notation, the above equations may be written as

$$\bar{U} = \bar{G}(\bar{H})^{1/2} \quad \text{----- (29)}$$

$$\bar{P} = \bar{U}\bar{H} \quad \text{-----} \quad (30)$$

$$\bar{H} = \left(\frac{\bar{U}}{\bar{G}}\right)^2 \quad \text{-----} \quad (31)$$

Similarly, the per unit form of Equation

$$\frac{d}{dt}\left(\frac{U}{U_r}\right) = -\frac{a_g}{L} \frac{H_r}{U_r} \left(\frac{H}{H_r} - \frac{H_0}{H_r}\right) \quad \text{-----} \quad (32)$$

$$\frac{d\bar{U}}{dt} = -\frac{1}{T_w}(\bar{H} - \bar{H}_0) \quad \text{-----} \quad (33)$$

Or in Laplace notation

$$\frac{\bar{U}}{\bar{H} - \bar{H}_0} = \frac{-1}{T_w s} \quad \text{-----} \quad (34)$$

Where T_w is the water starting time at rated load. It has a fixed value for a given turbine-penstock unit and is given by

$$T_w = \frac{LU_r}{a_g H_r} = \frac{LQ_r}{a_g A H_r} \quad \text{-----} \quad (35)$$

The mechanical power output P_m is

$$P_m = P - P_L \quad \text{-----} \quad (36)$$

Where P_L represents the fixed power loss of the turbine given by

$$P_L = U_{NL} H \quad \text{-----} \quad (37)$$

With U_{NL} representing the no-load water velocity. In normalized form, we have

$$\frac{P_m}{P_r} = \frac{P}{P_r} - \frac{P_L}{P_r} = \left(\frac{U}{U_r} - \frac{U_{NL}}{U_r}\right) \frac{H}{H_r} \quad \text{-----} \quad (38)$$

Or

$$\bar{P}_m = (\bar{U} - \bar{U}_{NL})\bar{H} \quad \text{----- (39)}$$

The above equation gives the per unit value of the turbine power output on a base equal to the turbine MW rating. In system stability studies, solution of the machine swing equation requires turbine mechanical torque on a base equal to either the generator MVA rating or a common MVA base. Hence,

$$\bar{T}_m = \left(\frac{\omega_0}{\omega}\right)\bar{P}_m \left(\frac{P_r}{\text{MVA}_{base}}\right) = \frac{1}{\omega}(\bar{U} - \bar{U}_{NL})\bar{H}\bar{P}_r \quad \text{----- (40)}$$

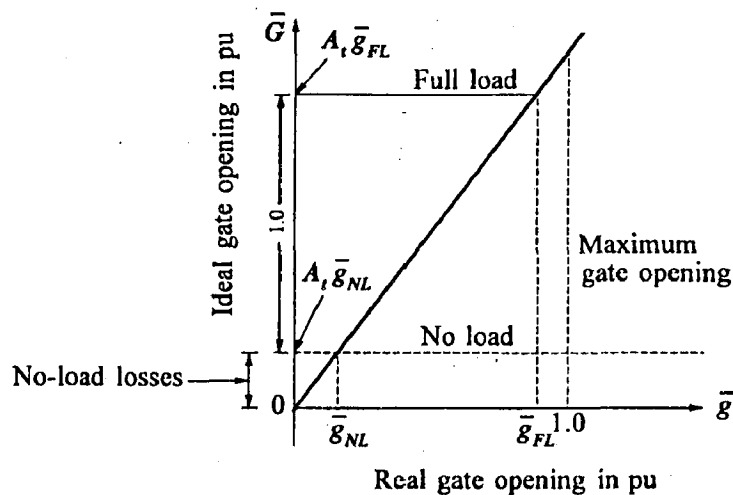
Where

$\bar{\omega}$ = per unit speed

MVA_{base} = base MVA on which turbine torque is to be made per unit

P_r = per unit turbine rating = turbine MW rating/ MVA_{base}

In the above equations, G is the ideal gate opening based on the change from no load to full load being equal to 1 per unit. This is related to the real gate opening g as shown in figure. The real gate opening is based on the change from the fully closed to the fully open position being equal to 1 per unit.



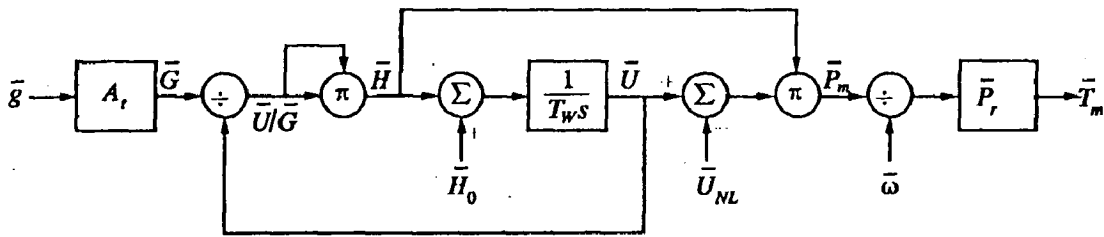
The ideal gate opening is related to real gate opening as follows

$$\bar{G} = A_t \bar{g}$$

Where A is the turbine gain given by

$$A_t = \frac{1}{\bar{g}_{FL} - \bar{g}_{NL}}$$

Hydraulic turbine block diagram assuming inelastic water column



$$A_t = \frac{1}{\bar{g}_{FL} - \bar{g}_{NL}}$$

$$\bar{P}_r = \frac{\text{turbine MW rating}}{\text{base MVA}}$$

$$T_w = \frac{LU_r}{a_g H_r}$$

$$\bar{U}_{NL} = A_t \bar{g}_{NL} (\bar{H}_0)^{1/2}$$

The turbine and penstock model may be rearranged and expressed in terms of two equations, one representing the water column and the other the turbine.

Water column equation:

$$\frac{d\bar{U}}{dt} = -\frac{1}{T_w} (\bar{H} - \bar{H}_0) = -\frac{1}{T_w} \left[\left(\frac{\bar{U}}{A_t \bar{g}} \right)^2 - \bar{H}_0 \right]$$

----- (41)

Turbine equation:

$$\bar{T}_m = \frac{\bar{U} - \bar{U}_{NL}}{\bar{\omega}} \left(\frac{\bar{U}}{A_t \bar{g}} \right)^2 \bar{P}_r \quad \text{----- (42)}$$

The steady-state condition corresponding to no load, we have

$$\bar{U}_{NL} = A_t \bar{g}_{NL} (\bar{H}_0)^{1/2} \quad \text{----- (43)}$$

Usually

$$\bar{H}_0 = 1.0.$$

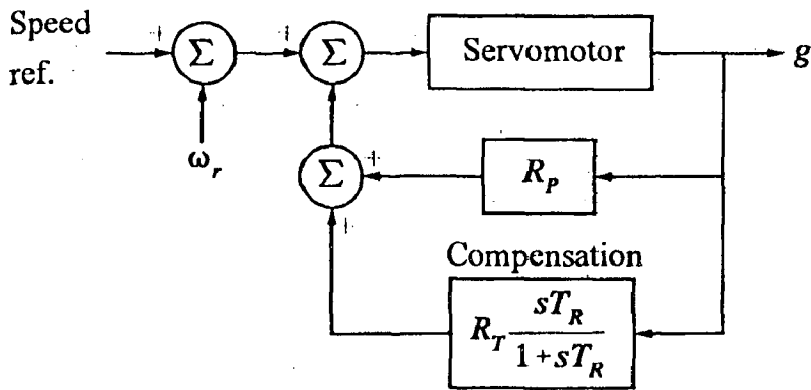
3.2 Governors for Hydraulic Turbines

The basic function of a governor is to control speed and /or load. The primary speed/load control function involves feeding back speed error to control the gate position. In order to ensure satisfactory and stable parallel operation of multiple units, the speed governor is provided with a droop characteristic. The purpose of the droop is to ensure equitable load sharing between units. Typically, the steady-state droop is set at about 5%, such that a speed deviation of 5% cause 100% change in gate position or power output; this corresponds to a gain of 20. For a hydro turbine, however, such a governor with a simple steady-state droop characteristic would be unsatisfactory.

3.2.1 Requirement for a transient droop

Hydro turbines have a peculiar response due to water inertia: a change in gate position produces an initial turbine power change which is opposite to that sought. For stable control performance, a large transient(temporary) droop with a long resetting time is therefore required. This is accomplished by the provision of a rate feedback retards or limits the gate movement until the water flow and power output have time to catch up. The result is a governor which exhibits a high droop (low gain) for fast speed deviations, and the normal low droop (high gain) in the steady state.

Governor with transient droop compensation

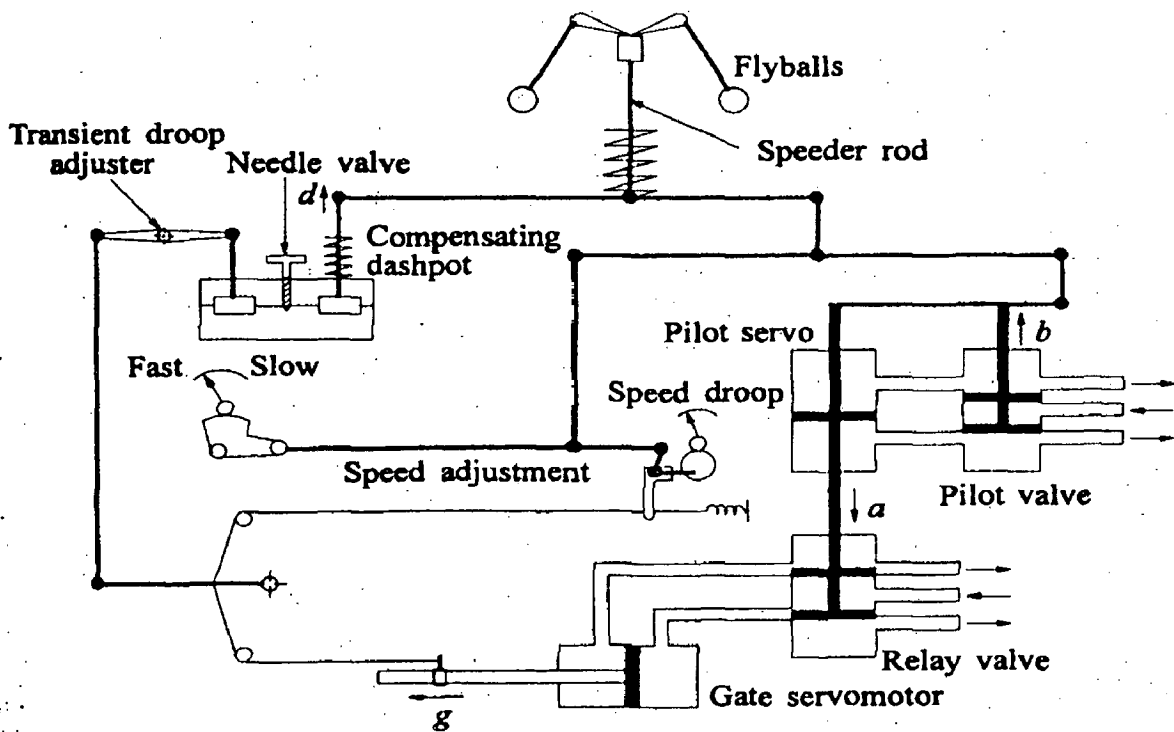


R_p = Permanent droop

R_T = Temporary droop

T_R = Reset time

3.2.2 Mechanical- Hydraulic governor



On older units the governing function is realized using mechanical and hydraulic components. Figure shows a simplified schematic of a mechanical-hydraulic governor. Speed sensing, permanent droop feedback, and computing functions are achieved through hydraulic components. A dashpot is used to provide transient droop compensation. A bypass arrangement is usually provided to disable the dashpot if so desired.

The transfer function of the relay valve and gate servomotor is

$$\frac{g}{a} = \frac{K_1}{s}$$

The transfer function of the pilot valve and pilot servo is

$$\frac{a}{b} = \frac{K_2}{1+sT_p}$$

Where K_2 is determined by the feed back lever ration, and T_p by port areas of the pilot valve and K_2 . Combining Equations yields

$$\frac{g}{b} = \frac{K_1 K_2}{s(1+sT_p)} = \frac{K_s}{s(1+sT_p)}$$

Where K_s is the servo gain and T_p is the pilot valve/servomotor time constant. The servo gain K_s is determined by the pilot valve feedback lever ratio.

Assuming that the dashpot fluid flow through the needle valve is proportional to the dashpot pressure, the dashpot transfer function is

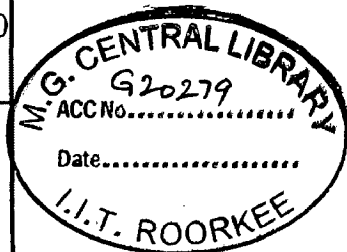
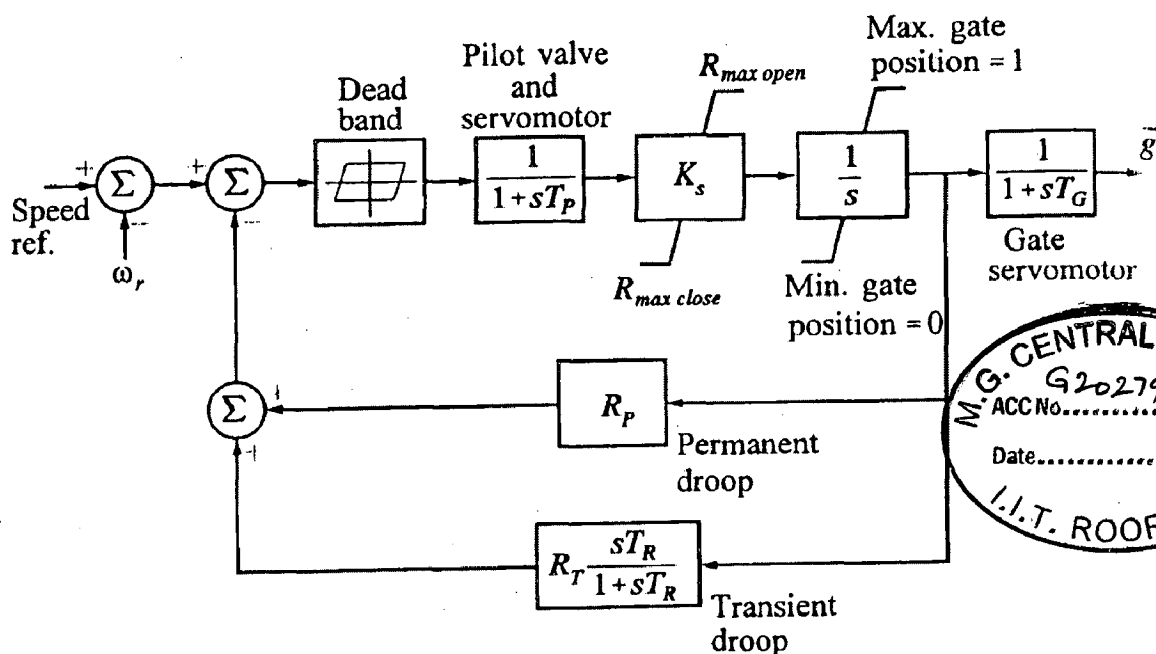
$$\frac{d}{g} = R_T \frac{sT_R}{1+sT_R}$$

The temporary droop R_T is determined by the lever ratio, and the reset or washout time T_R is determined by the needle valve setting.

Water is not a very compressible fluid; if the gate is closed too rapidly, the resulting pressure could burst the penstock. Consequently, the gate movement is rate limited. Often, the rate of gate movement is limited even further in the buffer region near full closure to provide cushioning.

A block diagram representation of the governing system suitable for system stability studies is shown in Figure. This diagram together with the diagram of Figure provides a complete model of the hydraulic turbine and speed-governing system.

The governor model shown in Figure has provision for representing the effects of dead bands. However, it is usually difficult to get data that identify their magnitude and locations. Consequently, dead band effects are not usually modeled in system studies.



3.2.3 Electro hydraulic governor

Modern speed governors for hydraulic turbines use electro hydraulic systems. Functionally, their operation is very similar to that of mechanical-hydraulic governors. Speed sensing, permanent droop, temporary droop, and other measuring and computing functions are performed electrically. The electric components provide greater flexibility and improved performance with regard to dead bands and time lags. The dynamic characteristics of electric governors are usually adjusted to be essentially similar to those of the mechanical-hydraulic governors.

3.3 Generator Modelling

For balanced steady-state operation, the stator phase voltages may be written as

$$e_a = E_m \cos(\omega_s t + \alpha) \quad \text{----- (44)}$$

$$e_b = E_m \cos(\omega_s t - \frac{2\pi}{3} + \alpha) \quad \text{----- (45)}$$

$$e_c = E_m \cos(\omega_s t + \frac{2\pi}{3} + \alpha) \quad \text{----- (46)}$$

Where ω_r is the angular frequency and α is the phase angle of e_a with respect to the time origin.

Applying the dq transformation gives

$$e_d = E_m \cos(\omega_s t + \alpha - \theta) \quad \text{----- (47)}$$

$$e_q = E_m \sin(\omega_s t + \alpha - \theta) \quad \text{----- (48)}$$

The angle θ by which the d-axis leads the axis of phase a is given by

$$\theta = \omega_r t + \theta_0$$

Where θ_0 is the value of θ at $t=0$.

With ω_r equal to ω_s at synchronous speed, substitution for in equations

$$e_d = E_m \cos(\alpha - \theta_0) \quad \text{----- (49)}$$

$$e_q = E_m \sin(\alpha - \theta_0) \quad \text{----- (50)}$$

In the above equations, E_m is the peak value of phase voltage. In steady-state analysis, we are interested in RMS values and phase displacements rather than instantaneous or peak values. Using E_r to denote per unit RMS value of armature terminal voltage and noting that in per unit RMS and peak values are equal,

$$e_d = E_r \cos(\alpha - \theta_0) \quad \text{----- (51)}$$

$$e_q = E_r \sin(\alpha - \theta_0) \quad \text{----- (52)}$$

The dq components of armature voltage are scalar quantities. However, in view of the trigonometric relationship between them, they can be expressed as phasors in a complex plane having d- and q-axes as coordinates. This is illustrated in Figure (a) and (b) and is conceptually similar to phasor representation of alternating quantities varying sinusoidally with respect to time. Thus the armature terminal voltage may be expressed in complex form as

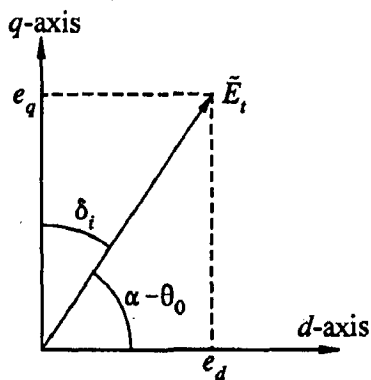
$$\begin{aligned}\tilde{E}_t &= e_d + je_q \\ e_d &= E_t \sin \delta_i \\ e_q &= E_t \cos \delta_i\end{aligned}\tag{53}$$

Similarly, the dq components of armature terminal current I_t can be expressed as phasors. If ϕ is the power factor angle, we can write

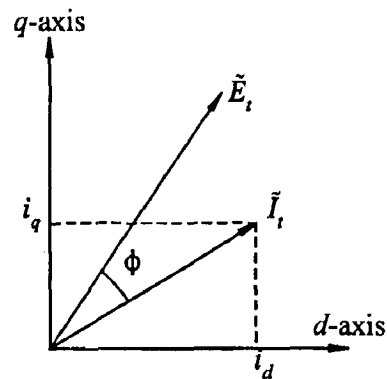
$$\begin{aligned}i_d &= I_t \sin(\delta_i + \phi) \\ i_q &= I_t \cos(\delta_i + \phi)\end{aligned}$$

And

$$\tilde{I}_t = i_d + ji_q$$



(a) Voltage components



(b) Current components

From the above analysis, it is clear that in phasor form with dq axes as reference, the RMS armature phase current and voltage can be treated the same way as is done with

phasor representation of alternating voltages and currents. This provides the link between the steady-state values of dq components of armature quantities and the phasor representation used in conventional ac circuit analysis.

The relationships between dq components of armature terminal voltage and current are defined by

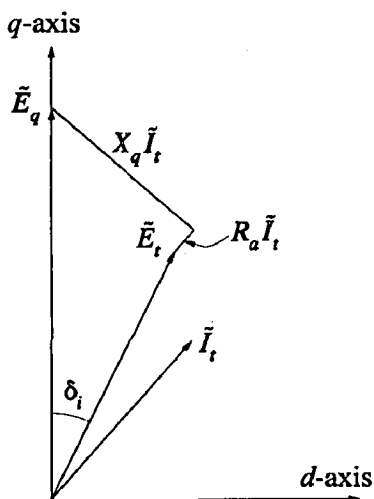
$$\begin{aligned}
 e_d &= -\omega_r \psi_q - R_a i_d \\
 &= \omega_r L_q i_q - R_a i_d \\
 &= X_q i_q - R_a i_d
 \end{aligned}
 \tag{54}$$

$$\begin{aligned}
 e_q &= \omega_r \psi_d - R_a i_q \\
 &= -X_d i_d + X_{ad} i_{fd} - R_a i_q
 \end{aligned}
 \tag{55}$$

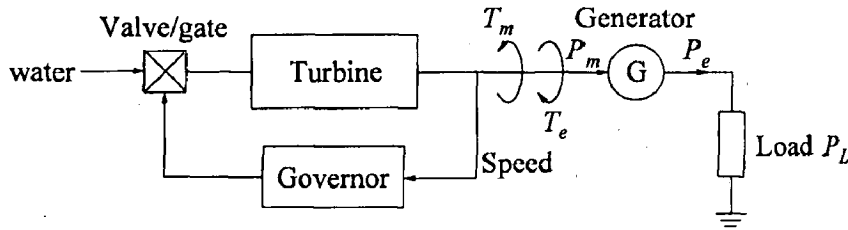
The reactances X_d and X_q are called the direct- and quadrature-axis synchronous reactances, respectively. They represent the inductive effects of the armature mmf wave by separately accounting for its d- and q-axis components.

$$\begin{aligned}
 \tilde{E}_q &= \tilde{E}_t + (R_a + jX_q)\tilde{I}_t \\
 &= (e_d + je_q) + (R_a + jX_q)(i_d + ji_q)
 \end{aligned}
 \tag{56}$$

$$\tilde{E}_d = j[X_{ad}i_{fd} - (X_d - X_q)i_d]
 \tag{57}$$



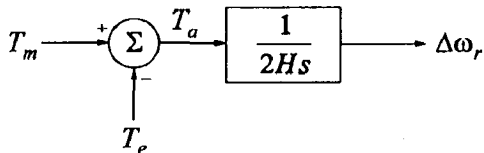
3.3.1 Fundamentals of Speed Governing



T_m = mechanical torque T_e = electrical torque
 P_m = mechanical power P_e = electrical power P_L = load power

3.3.2 Generator response to load change

When there is a load change, it is reflected instantaneously as a change in the electrical torque output T_e of the generator. This causes a mismatch between the mechanical torque T_m and the electrical torque T_e which in turn results in speed variations as determined by the equation of motion. The following transfer function represents the relationship between rotor speed as a function of the electrical and mechanical torques.



s = Laplace operator
 T_m = Mechanical torque (pu)
 T_e = Electrical torque (pu)
 T_a = Accelerating torque (pu)
 H = Inertia constant (MW-Sec/MVA)
 $\Delta\omega_r$ = Rotor speed deviation (pu)

For load-frequency studies, it is preferable to express the above relationship in terms of mechanical and electrical power rather than torque. The relationship between power P and torque T is given by

$$P = \omega_r T \quad \text{----- (58)}$$

$$P = P_0 + \Delta P \quad \text{----- (59)}$$

$$T = T_0 + \Delta T \quad \text{-----} \quad (60)$$

$$\omega_r = \omega_0 + \Delta\omega_r$$

$$P_0 + \Delta P = (\omega_0 + \Delta\omega_r)(T_0 + \Delta T) \quad \text{-----} \quad (61)$$

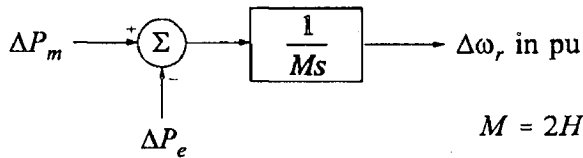
The relationship between the perturbed values, with higher-order terms neglected, is given by

$$\begin{aligned} \Delta P &= \omega_0 \Delta T + T_0 \Delta\omega_r \\ \Delta P_m - \Delta P_e &= \omega_0 (\Delta T_m - \Delta T_e) + (T_{m0} - T_{e0}) \Delta\omega_r \end{aligned} \quad \text{-----} \quad (62)$$

Since, in the steady state, electrical and mechanical torques are equal, $T_{m0} = T_{e0}$.

With speed expressed in pu, $w=1$. Hence,

$$\Delta P_m - \Delta P_e = \Delta T_m - \Delta T_e \quad \text{-----} \quad (63)$$



Load response to frequency deviation

In general, power system loads are a composite of a variety of electrical devices. For resistive loads, such as lighting and heating loads, the electrical power is independent of frequency. In the case of motor loads, such as fans and pumps, the electrical power changes with frequency due to changes in motor speed. The overall frequency-dependent characteristic of a composite load may be expressed as

$$\Delta P_e = \Delta P_L + D \Delta\omega_r \quad \text{-----} \quad (64)$$

The damping constant is expressed as a percent change in load for one percent in frequency. Typical values of D are 1 to 2 percent. A value of $D=2$ means that a 1% change in frequency would cause a 2% change in load.

4. SIMULATION

4.1 Data Used In Model

4.1.1 Synchronous Machine data

Power	200MVA
Voltage	13.8kV
Frequency	50Hz
Stator Resistance	0.0028544 p.u.
Coeff. Of Inertia	3.2
Friction Factor	0
Poles Pairs	10
Exciter Voltage (initial)	1 p.u.
Rotor speed deviation	0 p.u.
Stator Current I_a, I_b, I_c	All are 0 p.u.
Reactance X_d	1.305 p.u.
Reactance X_d'	0.296 p.u.
Reactance X_d''	0.252 p.u.
Reactance X_q	0.474 p.u.
Reactance X_q''	0.243 p.u.
Rotor Type	Salient

4.1.2 Turbine Data

Water Starting Time T_w	2.67 sec.
Full Load Gate Opening	0.84 p.u.
No Load Gate Opening	0.16 p.u.
No Load Water Velocity U_{NL}	0.068 p.u.

4.1.3 Governor Data

Permanent Droop R_p	0.05
Temporary Droop R_T	0.4
Reset Time T_R	5.0 sec
Servo gain K_a	3.33
Servo Time constant T_a	0.07 s
Max. Gate opening Rate	-0.1 p.u.
Max. Gate closing Rate	0.1 p.u.
Initial Mechanical Power P_m	1 p.u.

4.1.4 Excitation System Data

Initial Value of Terminal Voltage V_{t0}	1 p.u.
Initial Value of Field Voltage V_{f0}	1 p.u.
Minimum Excitation Voltage $V_{fmin.}$	-11.5 V
Maximum Excitation Voltage V_{fmax}	11.5 V

4.2 Hydraulic Turbine Simulation

Block Diagram

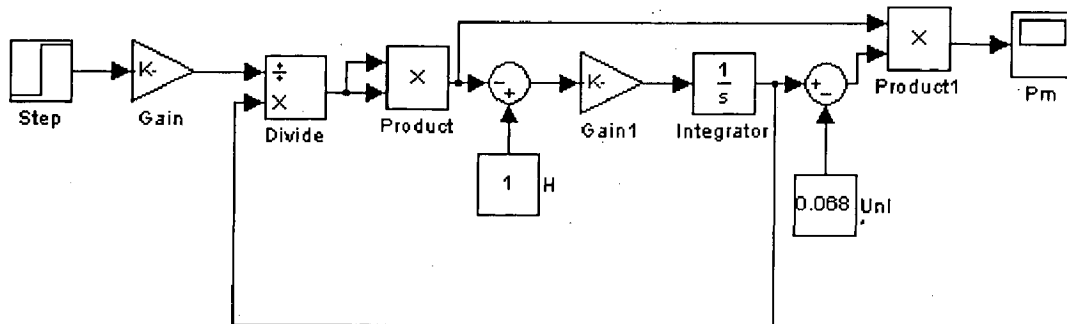
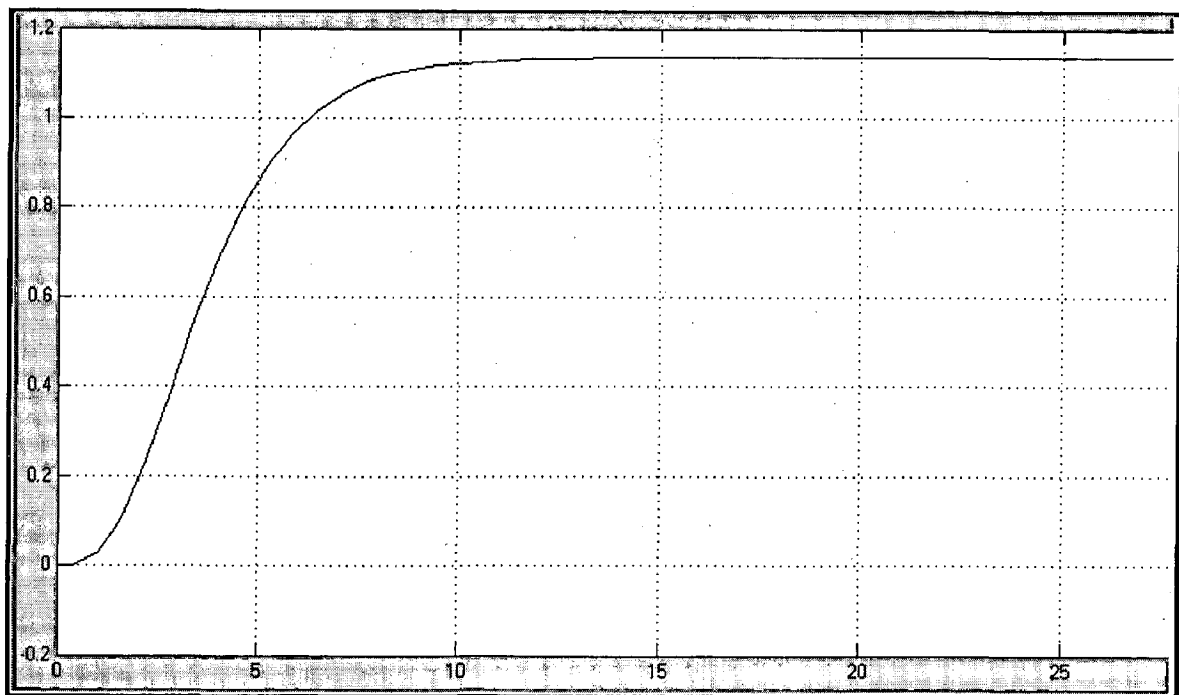


Fig. 4.1 Output (Mechanical Power)



Here from block diagram of Hydraulic turbine gate opening is input and mechanical power is output. For step input gate opening the mechanical power show transient response for some time (second) after that it stabilized and show steady-state response. System behaves as stable system.

4.3 Governor Simulation

Block Diagram

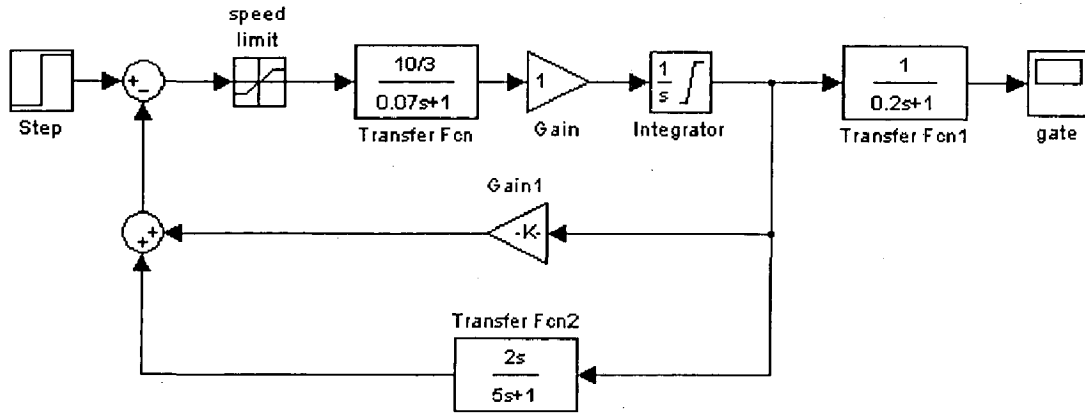
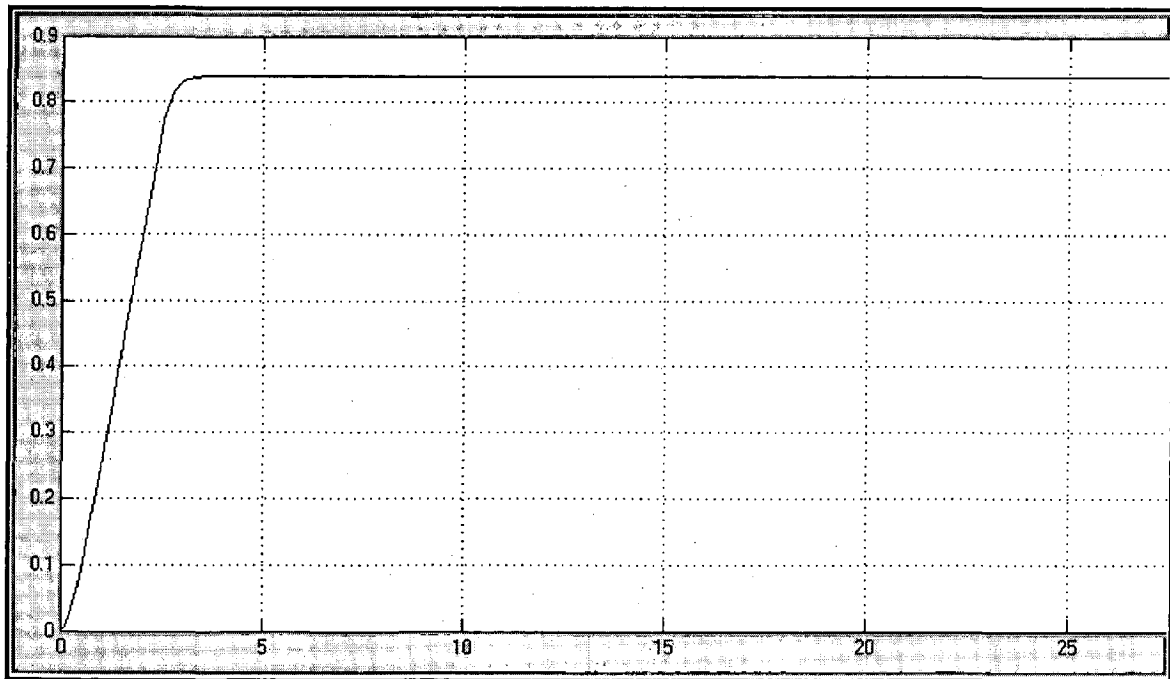


Fig. 4.2 Output (gate)



Here from block diagram of Governor speed error with respect to reference speed is input and gate opening is output. For step input speed error the gate opening show transient response for some time (second) after that it stabilized and show steady-state response. System behaves as stable system.

4.4 Overall block diagram

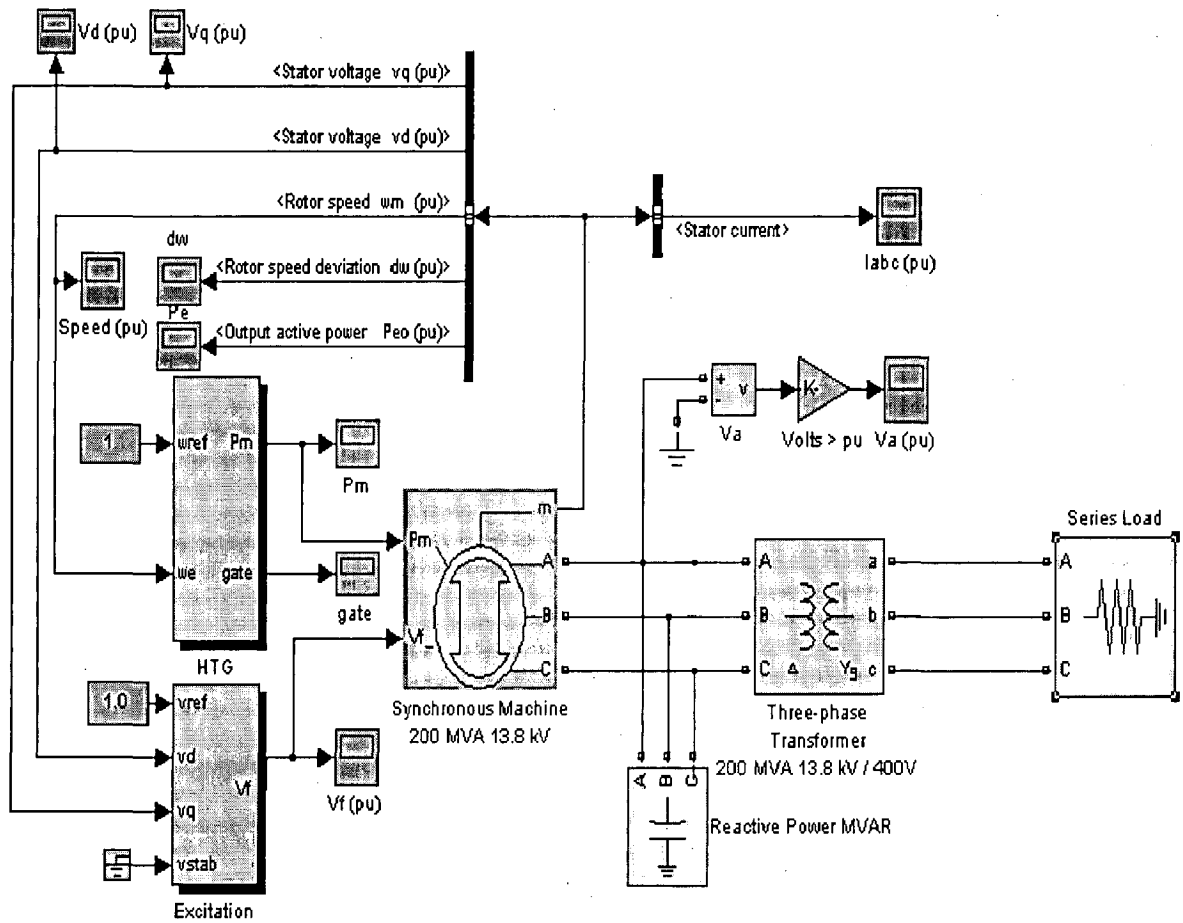


Fig. 4.3 Overall Block Diagram for Hydro Power Plant

4.5 Complete overall Block Diagram

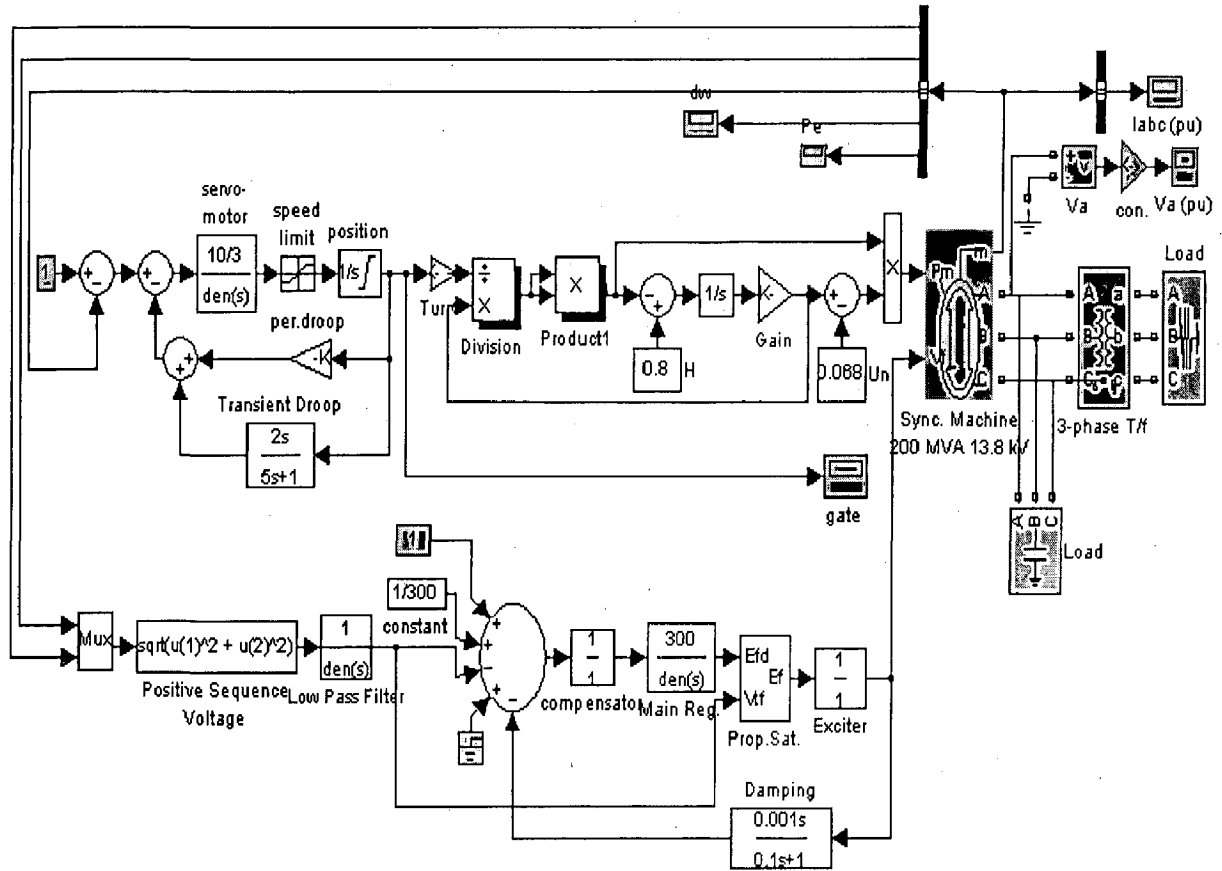


Fig. 4.4 Complete Overall Block Diagram for Hydro Power Plant

4.6 Simulation Output Table

Table 1

Reactive Power = 50MVAR; Head = 1 p.u.

Head (p.u.)	Load P _L	Gate (p.u.)	Excitation Voltage V _f (p.u.)	Rotor Speed (p.u.)	Variation in Speed, dw (p.u.)	vd (p.u.)	vq (p.u.)	Mech. Power P _m (p.u.)	Electric Power, p _{eo} (p.u.)
1	40MW	0.2245	0.725	0.988	-0.0115	0.106	0.995	0.2023	0.2
1	50MW	0.2655	0.745	0.9867	-0.013	0.131	0.993	0.252	0.25
1	60MW	0.3068	0.77	0.9845	-0.0153	0.155	0.988	0.3017	0.3
1	70MW	0.348	0.8	0.9825	-0.0175	0.18	0.985	0.351	0.35
1	80MW	0.388	0.82	0.98	-0.019	0.203	0.98	0.401	0.4
1	90MW	0.43	0.85	0.975	-0.021	0.225	0.975	0.452	0.45
1	100MW	0.47	0.9	0.97	-0.025	0.245	0.97	0.495	0.5
1	140MW	Oscilla.	Oscilla.	Oscilla.	Oscilla.	Oscilla.	Oscill.	Oscill.	Oscill.
1	160MW	Oscilla.	Oscilla.	Oscilla.	Oscilla.	Oscilla.	Oscill.	Oscill.	Oscill.
1	180MW	Oscilla.	Oscilla.	Oscilla.	Oscilla.	Oscilla.	Oscill.	Oscill.	Oscill.
1	200MW	0.84	0.935	0.105	-0.895	0.05	0.971	0.944	0.942

Table 2

Reactive Power =50MVAR; Head = 0.9 p.u.

Head (p.u.)	Load P_L	Gate (p.u.)	Excitation Voltage V_f (p.u.)	Rotor Speed (p.u.)	Variation in Speed, dw (p.u.)	vd (p.u.)	vq (p.u.)	Mech. Power, P_m (p.u.)	Electric Power, p_{eo} (p.u.)
0.9	40MW	0.2562	0.725	0.9872	-0.0128	0.106	0.995	0.2023	0.2
0.9	50MW	0.3045	0.745	0.9848	-0.0153	0.131	0.993	0.252	0.25
0.9	60MW	0.3527	0.77	0.9825	-0.017	0.155	0.9885	0.3017	0.3
0.9	70MW	0.4	0.8	0.98	-0.02	0.18	0.985	0.351	0.35
0.9	80MW	0.442	0.825	0.9755	-0.0225	0.203	0.98	0.401	0.4
0.9	100MW	Oscill.	Oscill.	Oscill.	Oscill.	Oscill.	Oscill.	Oscil.	Oscill.
0.9	140MW	Oscill.	Oscill.	Oscill.	Oscill.	Oscill.	Oscill.	Oscil.	Oscill.
0.9	160MW	Oscill.	Oscill.	Oscill.	Oscill.	Oscill.	Oscill.	Oscil.	Oscill.
0.9	180MW	0.84	E_{fmax}	0.083	-0.917	0.033	0.945	0.803	0.8
0.9	200MW	0.84	E_{fmax}	0.078	-0.9215	0.033	0.895	0.803	0.8

Table 3

Reactive Power =50MVAR; Head = 0.8 p.u.

Head (p.u.)	Load P_L	Gate (p.u.)	Excitation Voltage, V_f (p.u.)	Rotor Speed (p.u.)	Variation in Speed, dw (p.u.)	v_d (p.u.)	v_q (p.u.)	Mech.Pow er, P_m (p.u.)	Electric. Power, p_{eo} (p.u.)
0.8	40MW	0.2977	0.73	0.985	-0.015	0.106	0.995	0.2023	0.2
0.8	50MW	0.355	0.75	0.983	-0.017	0.131	0.993	0.252	0.25
0.8	60MW	0.41	0.77	0.9795	-0.020	0.155	0.988	0.3017	0.3
0.8	70MW	0.47	0.79	0.979	-0.021	0.18	0.985	0.351	0.35
0.8	80MW	0.84	E_{fmax}	0.081	-0.9185	0.039	0.926	0.944	0.942
0.8	90MW	Oscill.	Oscill.	Oscill.	Oscill.	Oscill.	Oscill.	Oscil.	Oscil.
0.8	100MW	Oscill.	Oscill.	Oscill.	Oscill.	Oscill.	Oscill.	Oscil.	Oscil.
0.8	140MW	0.84	7.64	0.129	-0.871	0.042	0.977	0.67	0.668
0.8	160MW	0.84	E_{fmax}	0.08	-0.92	0.0275	0.915	0.6697	0.668
0.8	180MW	0.84	E_{fmax}	0.0754	-0.923	0.0276	0.862	0.67	0.668
0.8	200MW	0.84	E_{fmax}	0.0717	-0.9282	0.0276	0.818	0.67	0.668
0.8	220MW	0.84	E_{fmax}	0.0685	-0.9315	0.0276	0.78	0.67	0.668

Table 4

Reactive Power =50MVAR; Head = 0.7 p.u.

Head (p.u.)	Load P_L	Gate (p.u.)	Excitation Voltage, V_f (p.u.)	Rotor Speed (p.u.)	Variation in Speed, dw (p.u.)	vd (p.u.)	vq (p.u.)	Mech.Power, P_m (p.u.)	Electric. Power, p_{eo} (p.u.)
0.7	40MW	0.3542	0.735	0.9823	-0.0177	0.105	0.995	0.202	0.2
0.7	50MW	0.425	0.755	0.9787	-0.0213	0.13	0.992	0.252	0.25
0.7	60MW	0.49	0.78	0.975	-0.026	0.154	0.989	0.31	0.3
0.7	70MW	Oscill.	Oscill.	Oscill.	Oscill.	Oscill.	Oscill.	Oscil.	0.35
0.7	80MW	Oscill.	Oscill.	Oscill.	Oscill.	Oscill.	Oscill.	Oscil.	0.4
0.7	90MW	Oscill.	Oscill.	Oscill.	Oscill.	Oscill.	Oscill.	Oscil.	0.4473
0.7	100MW	Oscill.	Oscill.	Oscill.	Oscill.	Oscill.	Oscill.	Oscil.	0.5
0.7	140MW	0.84	E_{fmax}	0.077	-0.923	0.0225	0.882	0.5451	0.543
0.7	160MW	0.84	E_{fmax}	0.072	-0.938	0.0225	0.825	0.5451	0.543
0.7	180MW	0.84	E_{fmax}	0.068	-0.932	0.0225	0.778	0.5451	0.543
0.7	200MW	0.84	E_{fmax}	0.0645	-0.9353	0.0225	0.738	0.5451	0.543
0.7	220MW	0.84	E_{fmax}	0.0618	-0.9383	0.0225	0.705	0.5451	0.543

Table 5

Reactive Power =50MVAR; Head = 0.6 p.u.

Head (p.u.)	Load P_L	Gate (p.u.)	Excitation Voltage, V_f (p.u.)	Rotor Speed (p.u.)	Variation in Speed, dw (p.u.)	vd (p.u.)	vq (p.u.)	Mech.Pow er, P_m (p.u.)	Electric. Power, p_e o (p.u.)
0.6	40MW	0.4339	0.74	0.9782	-0.022	0.105	0.995	0.202	0.2
0.6	50MW	0.52	0.76	0.97	-0.03	0.13	0.992	0.252	0.25
0.6	60MW	Oscill.	Oscill.	Oscill.	Oscill.	Oscill.	Oscill.	Oscil.	0.3
0.6	70MW	Oscill.	Oscill.	Oscill.	Oscill.	Oscill.	Oscill.	Oscil.	0.35
0.6	80MW	Oscill.	Oscill.	Oscill.	Oscill.	Oscill.	Oscill.	Oscil.	0.4
0.6	90MW	0.84	8.3	0.1175	-0.8825	0.0245	0.975	0.4295	0.428
0.6	100MW	0.84	E_{fmax}	0.08	-0.92	0.0177	0.925	0.4295	0.428
0.6	140MW	0.84	E_{fmax}	0.0684	-0.9315	0.0177	0.782	0.4295	0.428
0.6	160MW	0.84	E_{fmax}	0.064	-0.9359	0.0177	0.733	0.4295	0.428
0.6	180MW	0.84	E_{fmax}	0.0605	-0.94	0.0177	0.691	0.4295	0.428
0.6	200MW	0.84	E_{fmax}	0.057	-0.943	0.0177	0.655	0.4295	0.428
0.6	220MW	0.84	E_{fmax}	0.055	-0.9452	0.0177	0.625	0.4295	0.428

Table 6

Reactive Power =50MVAR; Head = 0.5 p.u.

Head (p.u.)	Load P_L	Gate (p.u.)	Excitation Voltage, V_f (p.u.)	Rotor Speed (p.u.)	Variation in Speed, dw (p.u.)	vd (p.u.)	vq (p.u.)	Mech.Power, P_m (p.u.)	Electric. Power, p_{eo} (p.u.)
0.5	40MW	0.555	0.745	0.972	-0.275	0.105	0.995	0.202	0.2
0.5	50MW	Oscill.	Oscill.	Oscill.	Oscill.	Oscill.	Oscill.	Oscil.	0.25
0.5	60MW	Oscill.	Oscill.	Oscill.	Oscill.	Oscill.	Oscill.	Oscil.	0.3
0.5	70MW	0.84	E_{fmax}	0.0836	-0.9165	0.0134	0.96	0.3238	0.323
0.5	80MW	0.84	E_{fmax}	0.07835	-0.9217	0.0133	0.898	0.3238	0.323
0.5	90MW	0.84	E_{fmax}	0.074	-0.926	0.0133	0.847	0.3238	0.323
0.5	100MW	0.84	E_{fmax}	0.07	-0.93	0.0133	0.805	0.3238	0.323
0.5	140MW	0.84	E_{fmax}	0.0595	-0.9405	0.0133	0.68	0.3238	0.323
0.5	160MW	0.84	E_{fmax}	0.0556	-0.9444	0.0133	0.636	0.3238	0.323
0.5	180MW	0.84	E_{fmax}	0.0525	-0.9475	0.0133	0.6	0.3238	0.323
0.5	200MW	0.84	E_{fmax}	0.05	-0.95	0.0133	0.57	0.3238	0.323
0.5	220MW	0.84	E_{fmax}	0.0475	-0.9525	0.0133	0.543	0.3238	0.323

4.7 Simulation Output Response

4.7.1 For 50 MW Active Power and 50 MVAR Reactive Power Load at 1 p.u. Head

Here X- axis represent time (sec.)

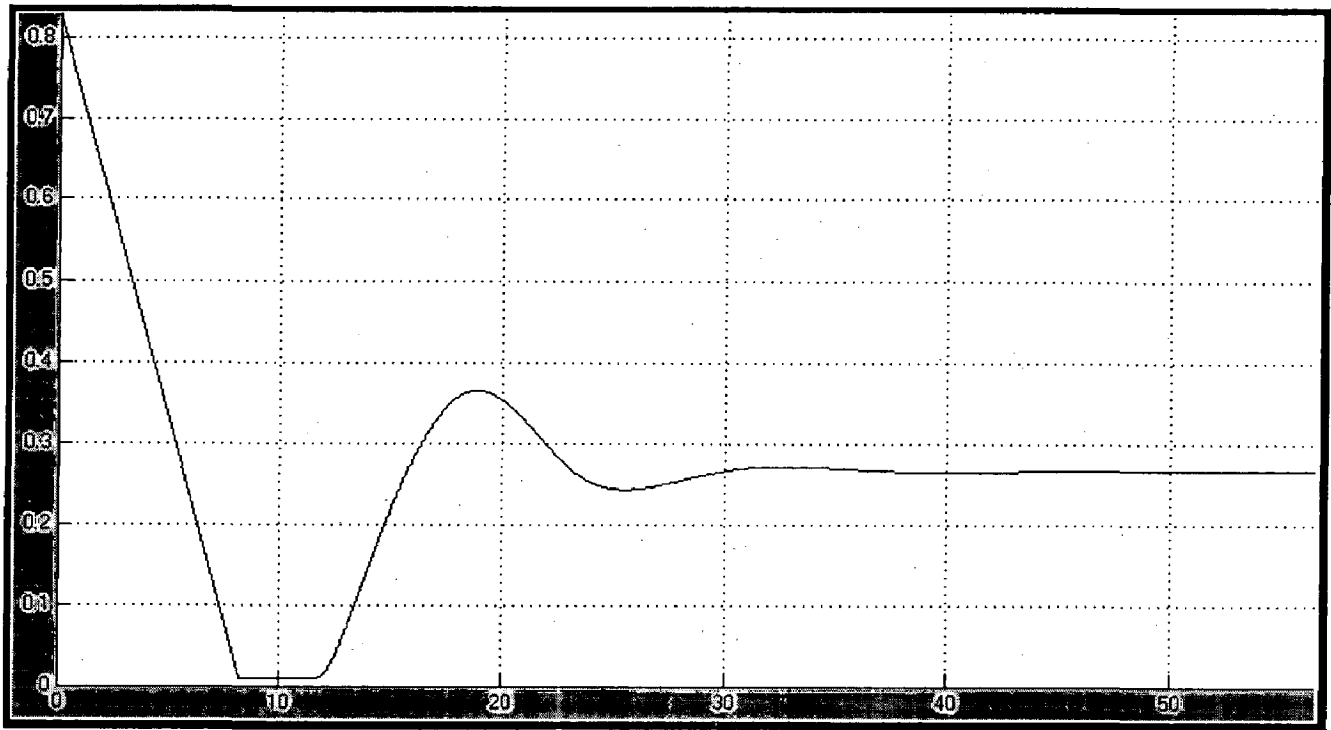


Fig.(4.5) Gate Opening (p.u.)

When 50 MW active power and 50 MVAR Reactive Power Load is applied at 1 p.u. Head then at that moment gate opening increases from 0.16 p.u. to 0.2655 p.u. Here 0.16 p.u. is gate opening at no load condition.

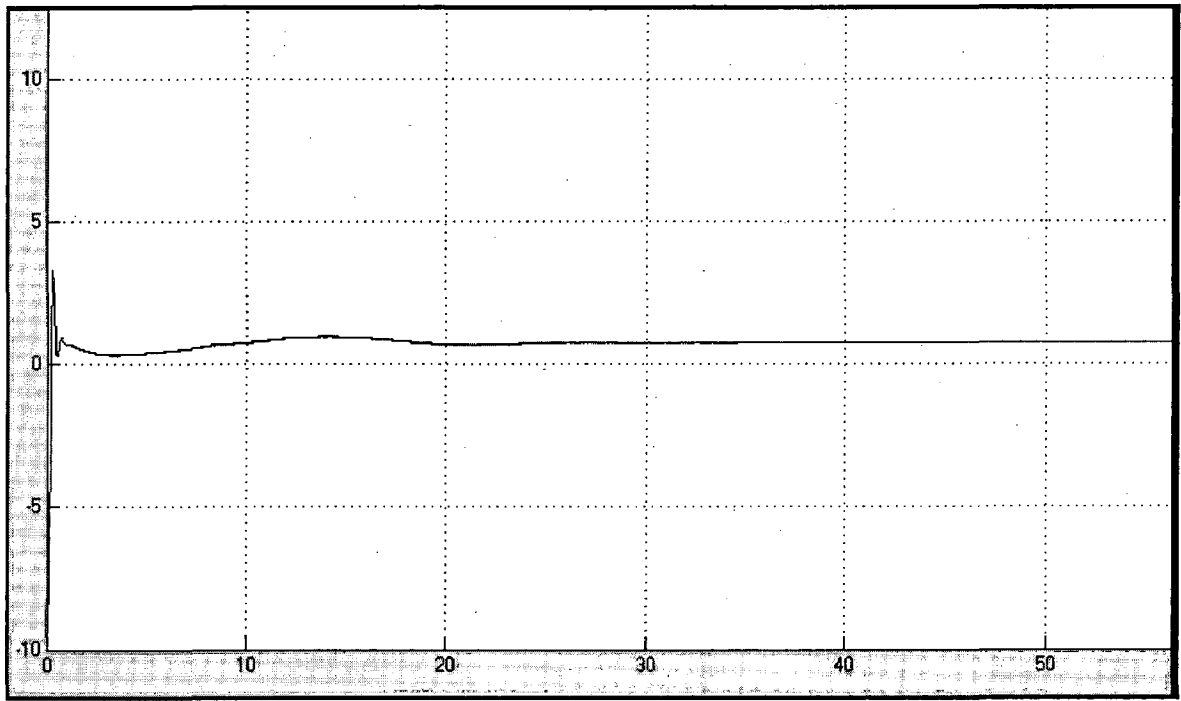


Fig. (4.6) Excitation Voltage V_f (p.u.)

When 50 MW active power and 50 MVAR Reactive Power Load is applied at 1 p.u. Head then Excitation Voltage increases upto 0.745 p.u. It is used to increase rotor speed.

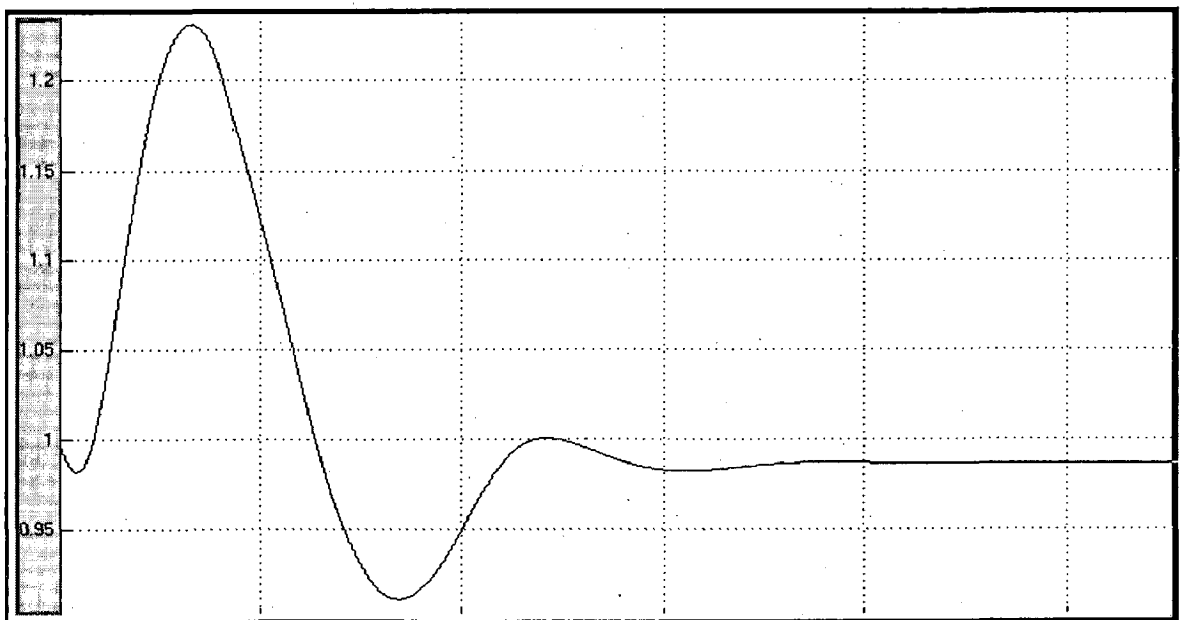


Fig. (4.7) Rotor Speed (p.u.)

When 50 MW active power and 50 MVAR Reactive Power Load is applied at 1 p.u. Head then at that moment speed decrease from 1 p.u. to 0.9867 p.u.

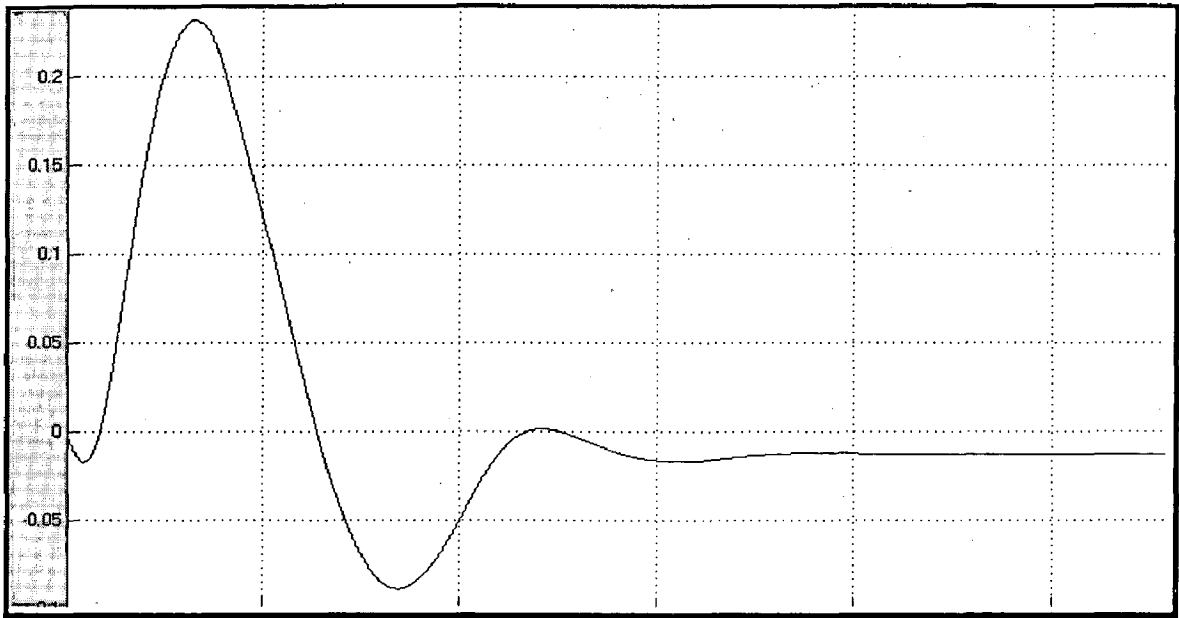


Fig. (4.8) Speed Deviation (p.u.)

When 50 MW active power and 50 MVAR Reactive Power Load is applied at 1 p.u. Head then speed deviation decrease from 0 p.u. to -0.013 p.u.

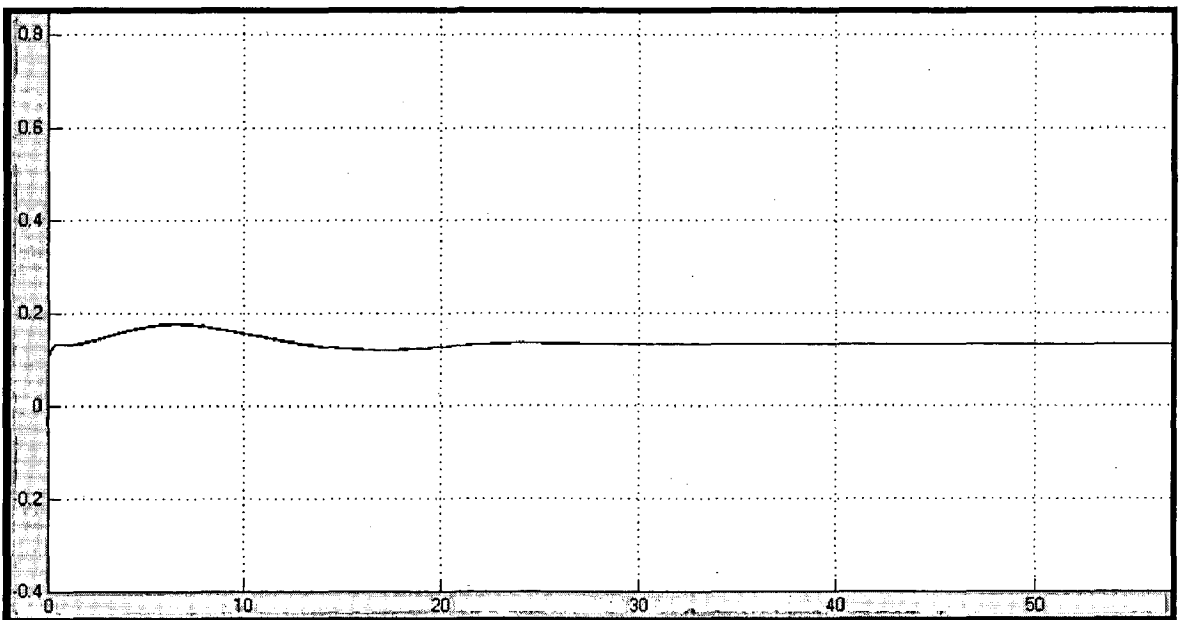


Fig. (4.9) V_d (p.u.)

When 50 MW active power and 50 MVAR Reactive Power Load is applied at 1 p.u. Head then due to increase in excitation voltage d-transformation voltage become 0.131 p.u.

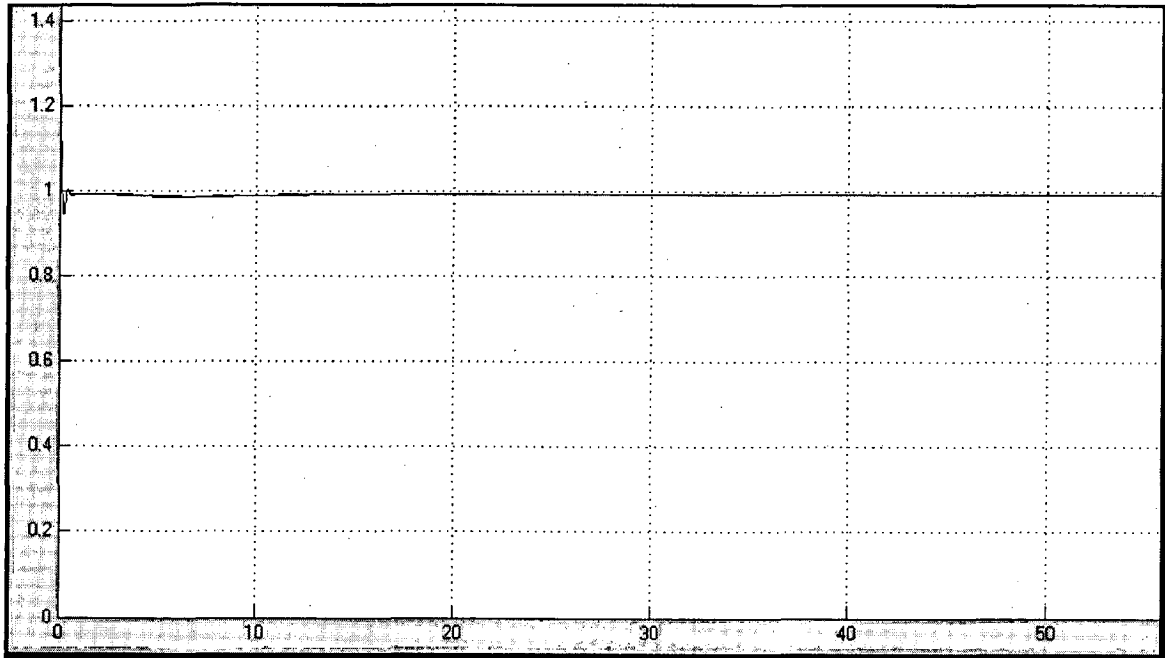


Fig. (4.10) V_q (p.u.)

When 50 MW active power and 50 MVAR Reactive Power Load is applied at 1 p.u. Head then due to increase in excitation voltage q-transformation becomes 0.993 p.u.

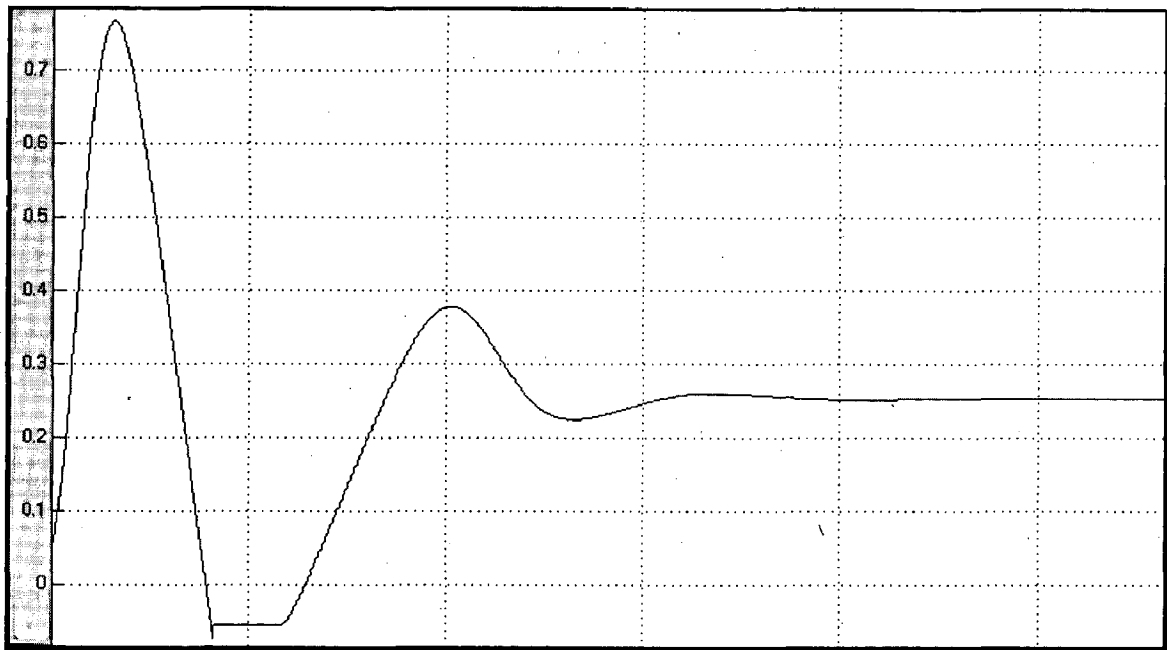


Fig. (4.11) Mechanical Power P_m (p.u.)

When 50 MW active power and 50 MVAR Reactive Power Load is applied at 1 p.u. Head then mechanical power demand becomes 0.252 p.u.

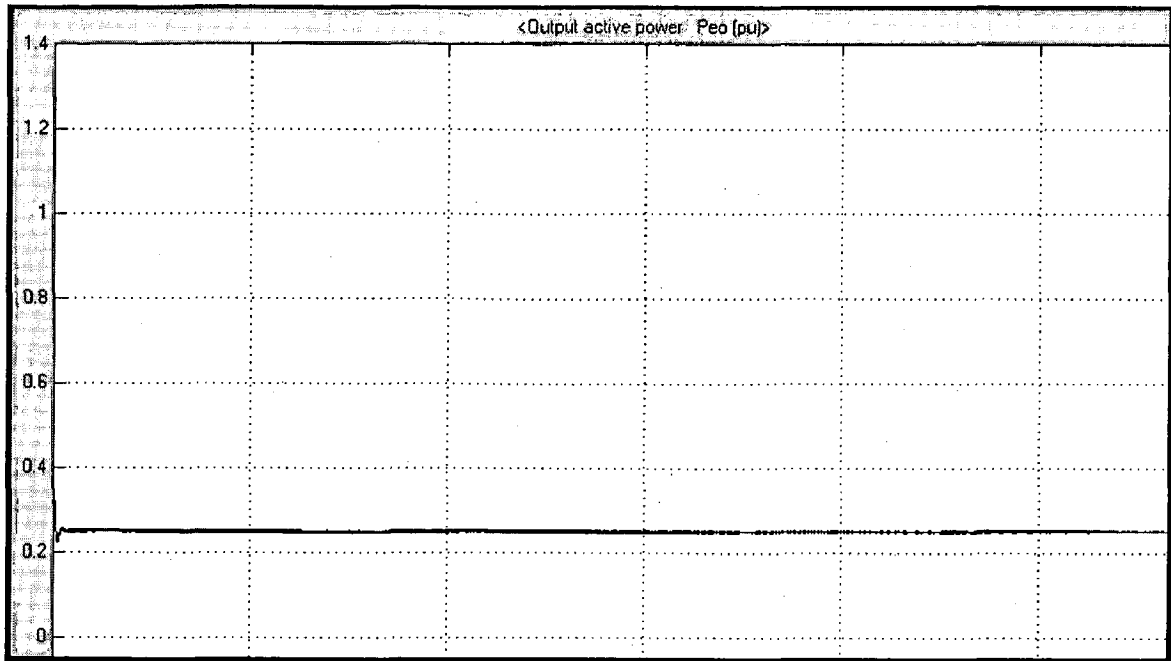


Fig. (4.12) Electrical Power P_{eo} (p.u.)

When 50 MW active power and 50 MVAR Reactive Power Load is applied at 1 p.u. Head then Electrical power demand becomes 0.25 p.u.

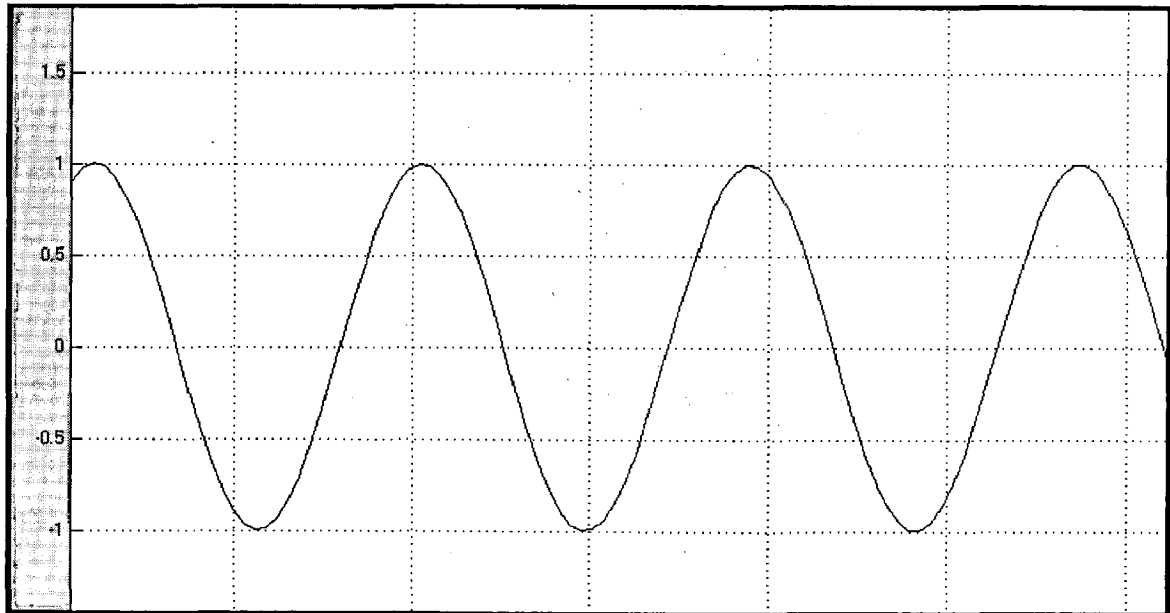


Fig. (4.13) Stator Voltage

When 50 MW active power and 50 MVAR Reactive Power Load is applied at 1 p.u. Head then also stator voltage does not affect and remain constant as 1 p.u. in magnitude.

4.7.2 When Load is increased to 60 MW Active Power from 50 MW and 50 MVAR Reactive Power is applied at 1 p.u. Head. Here X- axis represent time (sec.)

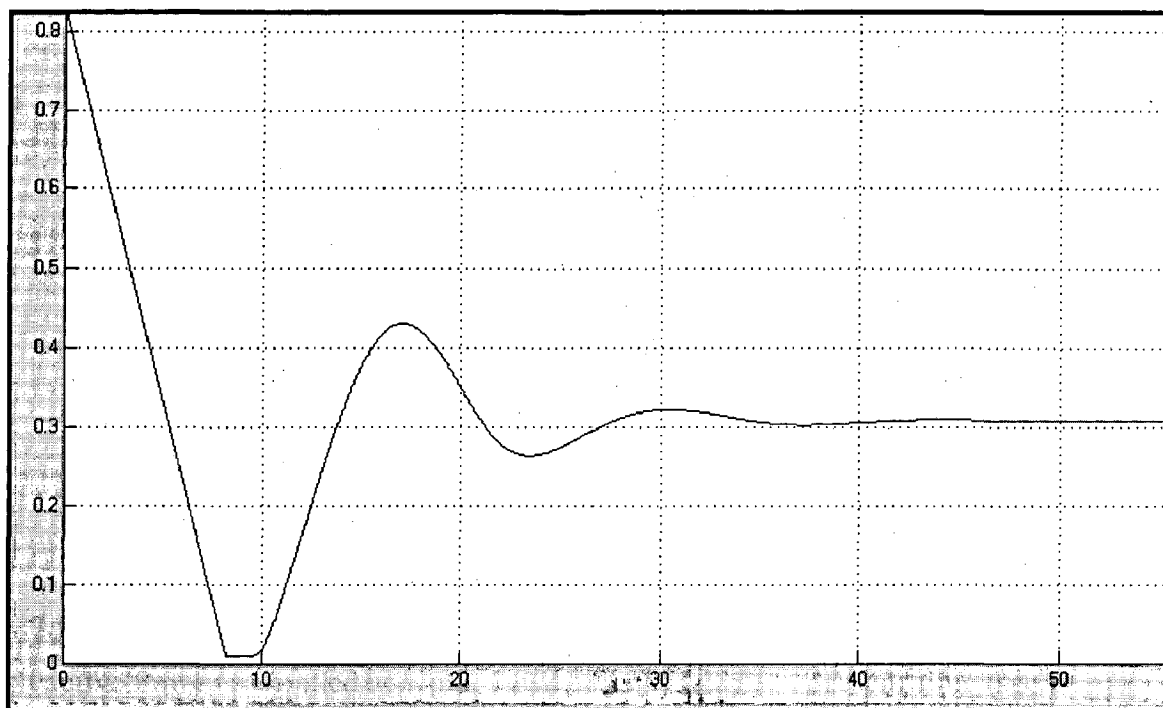


Fig. (4.14) Gate (p.u.)

When Load is increased to 60 MW active power from 50 MW and 50 MVAR Reactive Power Load is applied at 1 p.u. Head then at that moment gate opening increases form 0.2655 p.u. to 0.3068 p.u. to maintain constant speed.

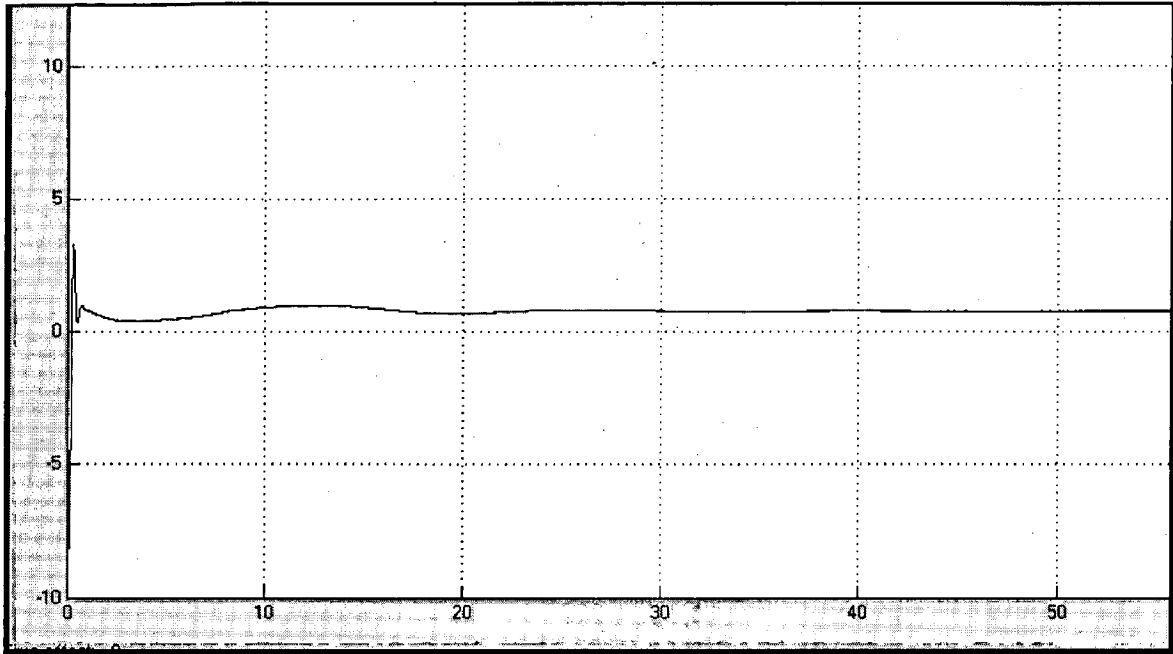


Fig. (4.15) Excitation Voltage V_f (p.u.)

When Load is increased to 60 MW active power from 50 MW and 50 MVAR Reactive Power Load is applied at 1 p.u. Head then Excitation Voltage increases to 0.77 p.u. from 0.745 p.u

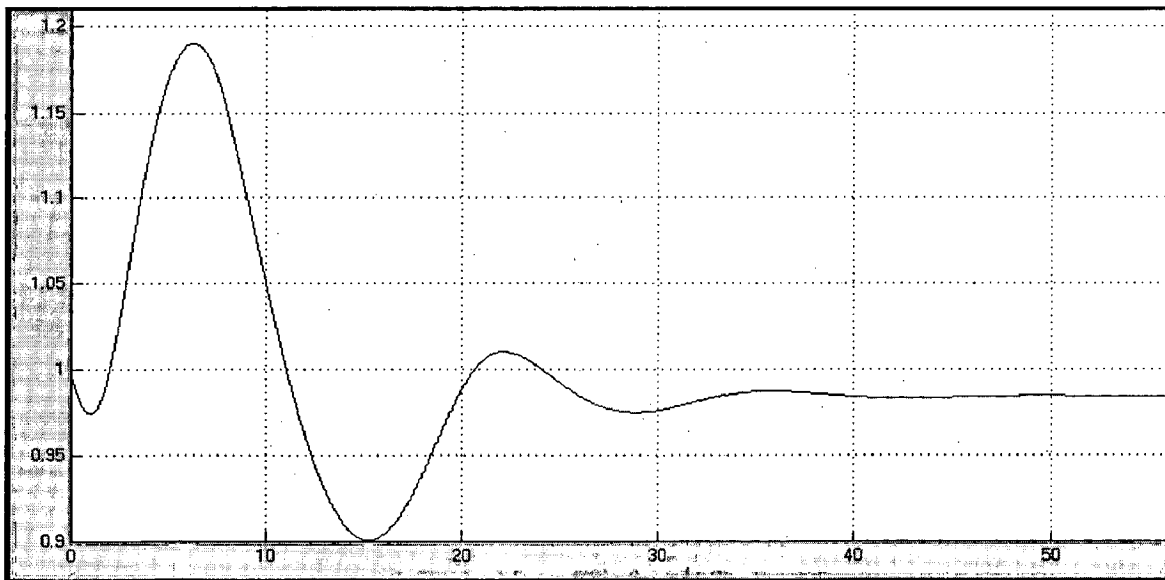


Fig. (4.16) Rotor Speed (p.u.)

When Load is increased to 60 MW active power from 50 MW and 50 MVAR Reactive Power Load is applied at 1 p.u. Head then at that moment speed decrease from 1 p.u. to 0.9845 p.u.

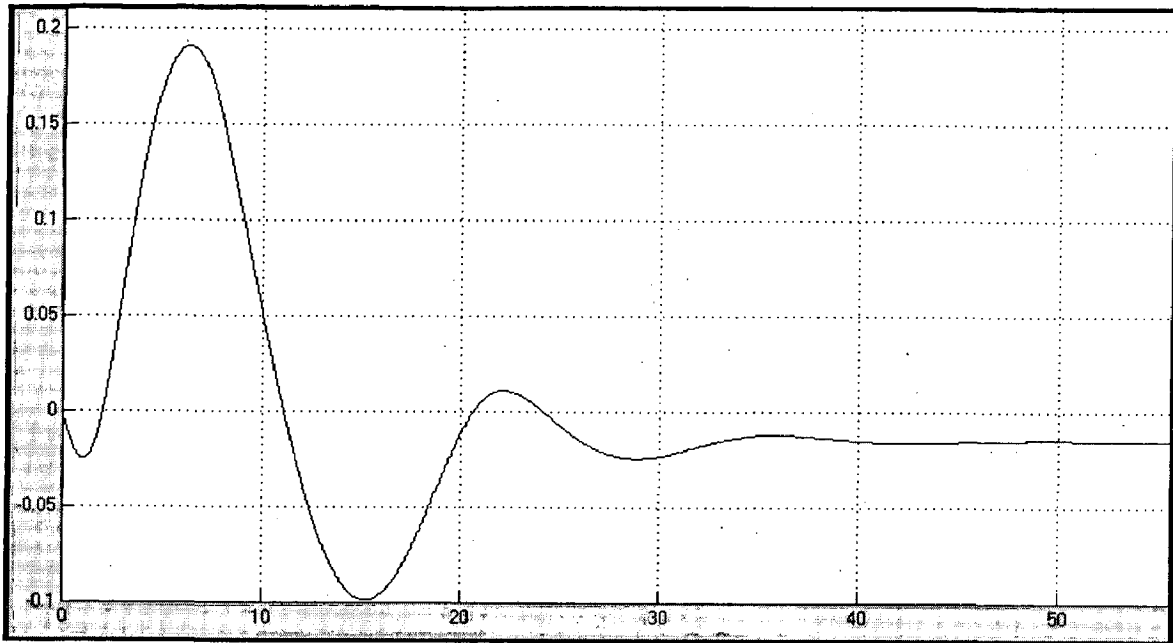


Fig. (4.17) Speed Deviation (p.u.)

When Load is increased to 60 MW active power from 50 MW and 50 MVAR Reactive Power Load is applied at 1 p.u. Head then speed deviation decrease from 0 p.u. to - 0.0153 p.u.

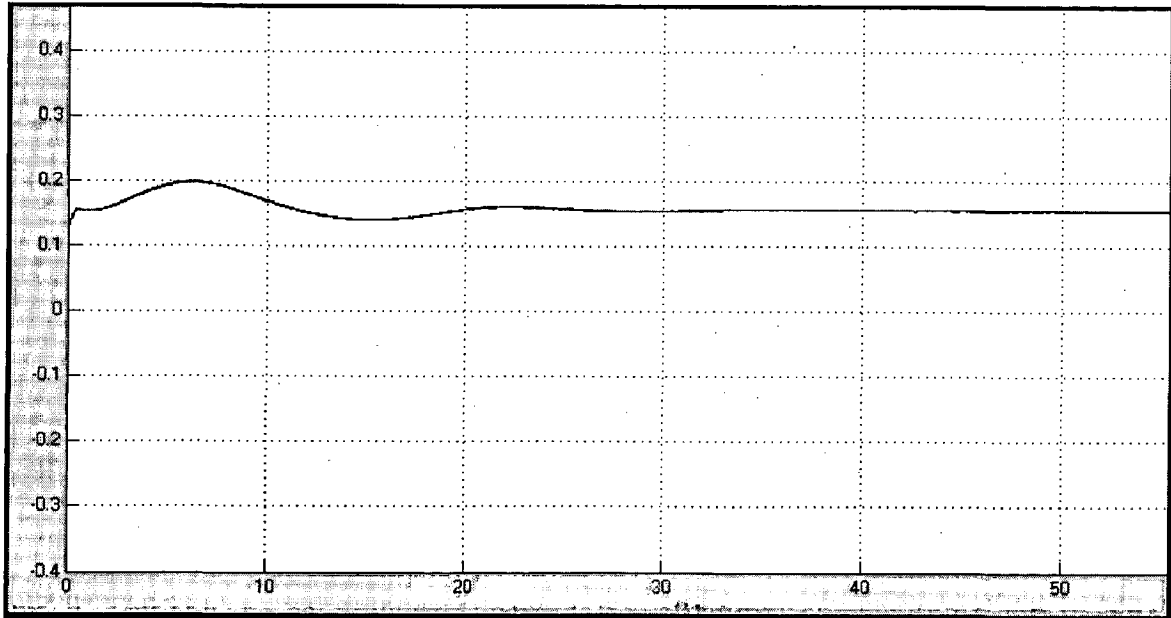


Fig. (4.18) V_d (p.u.)

When Load is increased to 60 MW active power from 50 MW and 50 MVAR Reactive Power Load is applied at 1 p.u. Head then due to increase in excitation voltage d-transformation voltage increases to 0.155 p.u. from 0.131 p.u.

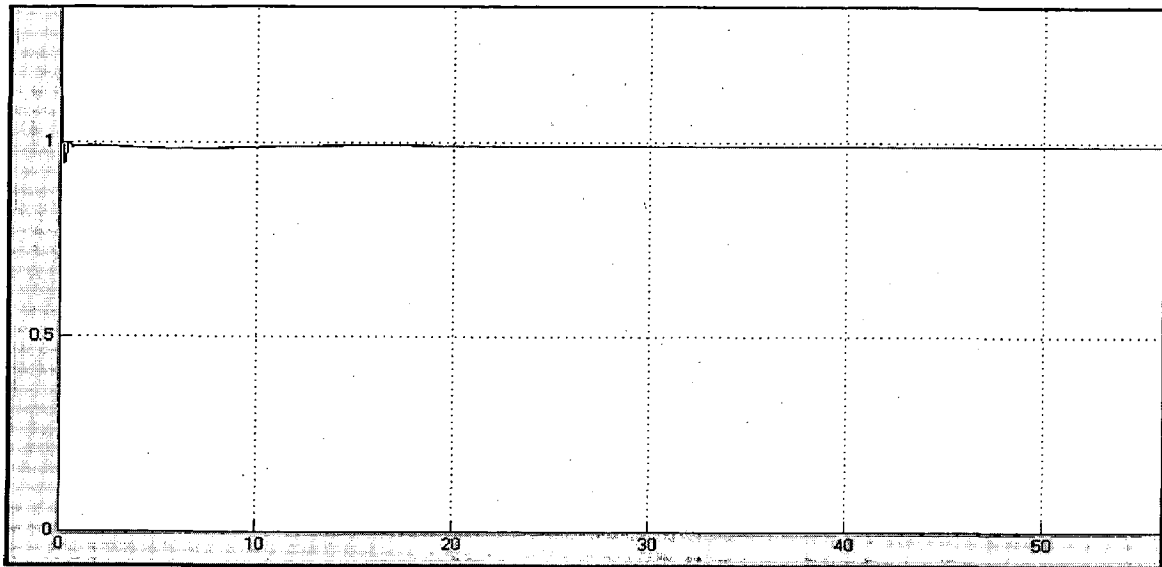


Fig. (4.19) V_q (p.u.)

When Load is increased to 60 MW active power from 50 MW and 50 MVAR Reactive Power Load is applied at 1 p.u. Head then due to increase in excitation voltage q-transformation voltage increases to 0.988 p.u. from 0.993 p.u.

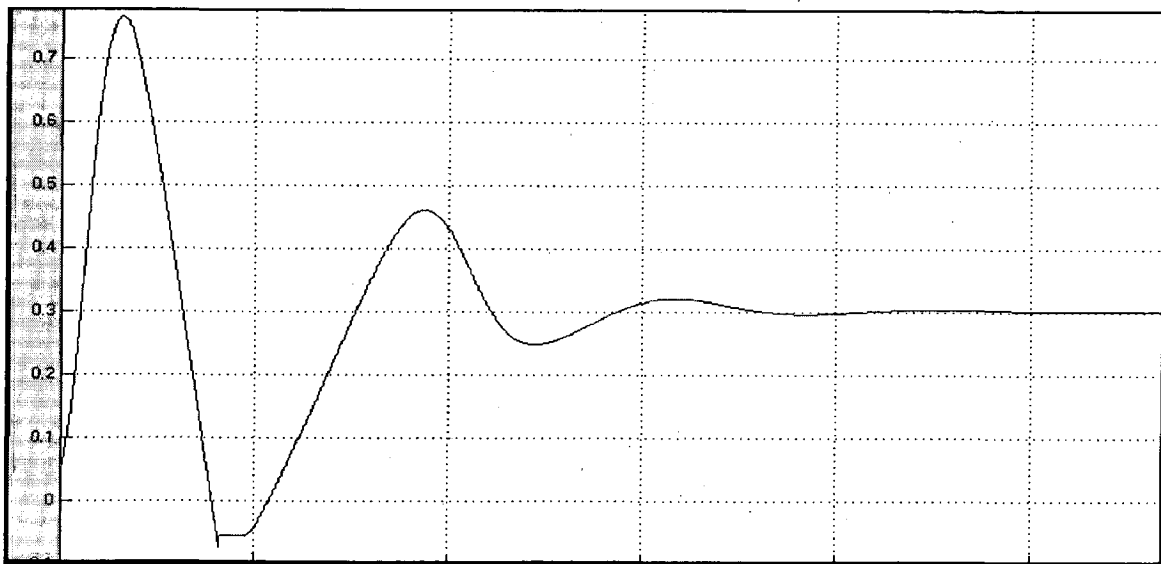


Fig.(4.20) Mechanical Power P_m (p.u.)

When Load is increased to 60 MW active power from 50 MW and 50 MVAR Reactive Power Load is applied at 1 p.u. Head then mechanical power demand increases to 0.3017 p.u. from 0.252 p.u.

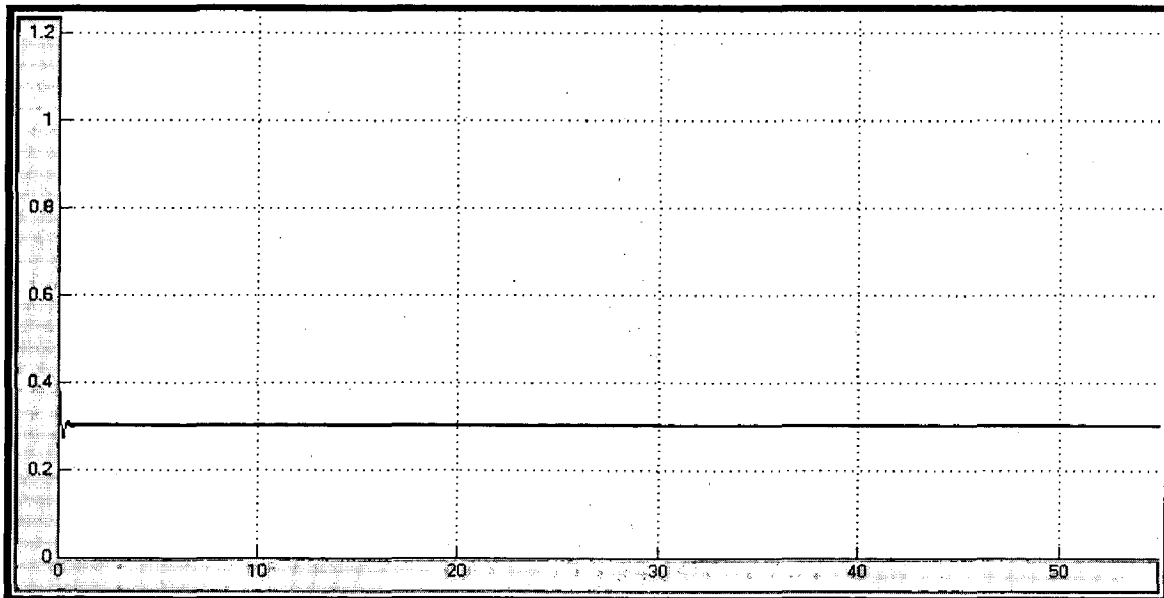


Fig. (4.21) Electrical Power P_{co} (p.u.)

When Load is increased to 60 MW active power from 50 MW and 50 MVAR Reactive Power Load is applied at 1 p.u. Head then Electrical power demand increases to 0.3 p.u. from 0.25 p.u.

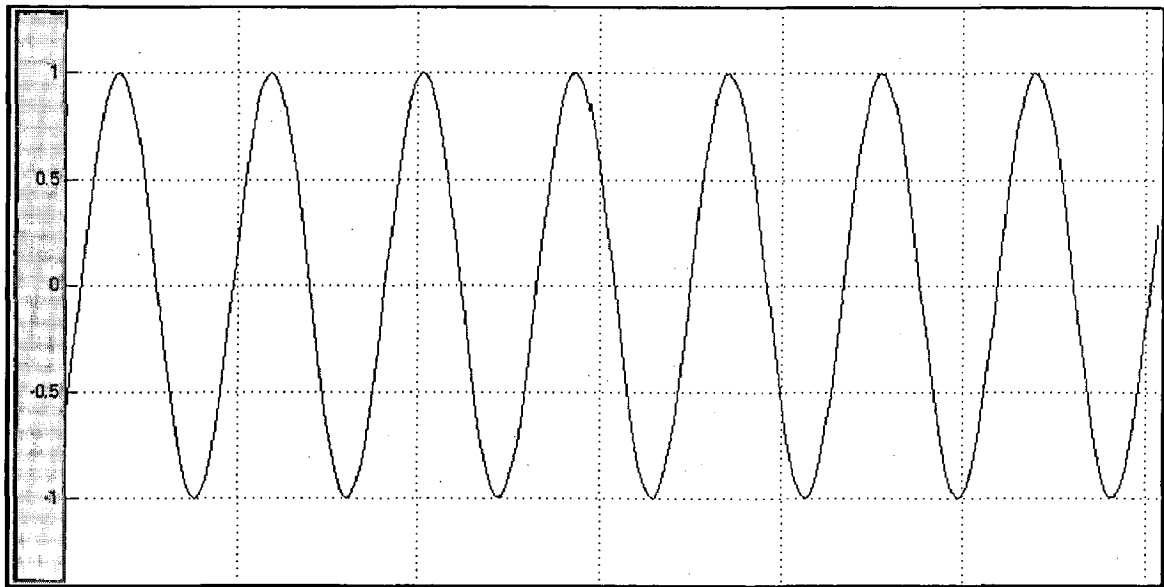


Fig. (4.22) Voltage

When Load is increased to 60 MW active power from 50 MW and 50 MVAR Reactive Power Load is applied at 1 p.u. Head then also stator voltage does not effect and remain constant as 1 p.u. in magnitude.

4.7.3 When Head is varied to 0.9 p.u. from 1 p.u. at 50 MW Active Power and 50 MVAR Reactive Power Load. Head Here X- axis represent time (sec.)

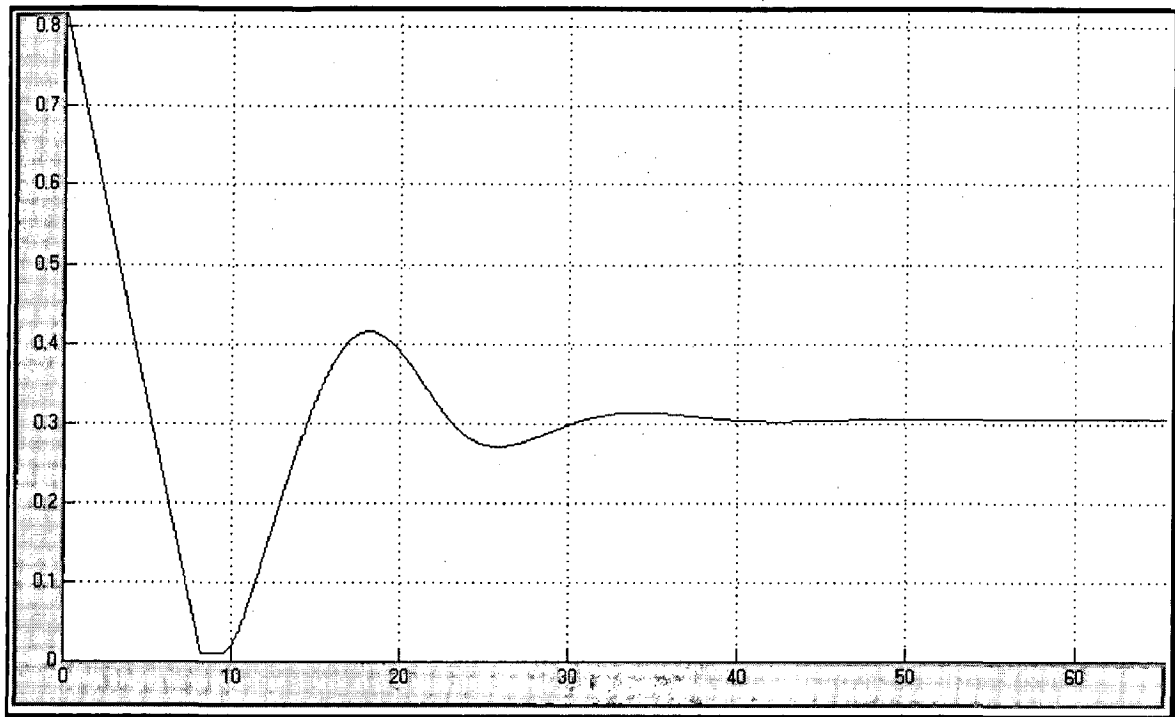


Fig. (4.23) Gate (p.u.)

When Head is varied to 0.9 p.u. from 1 p.u. at 50 MW Active Power and 50 MVAR Reactive Power Load then at that moment gate opening increases from 0.2655 p.u. to 0.3045 p.u.

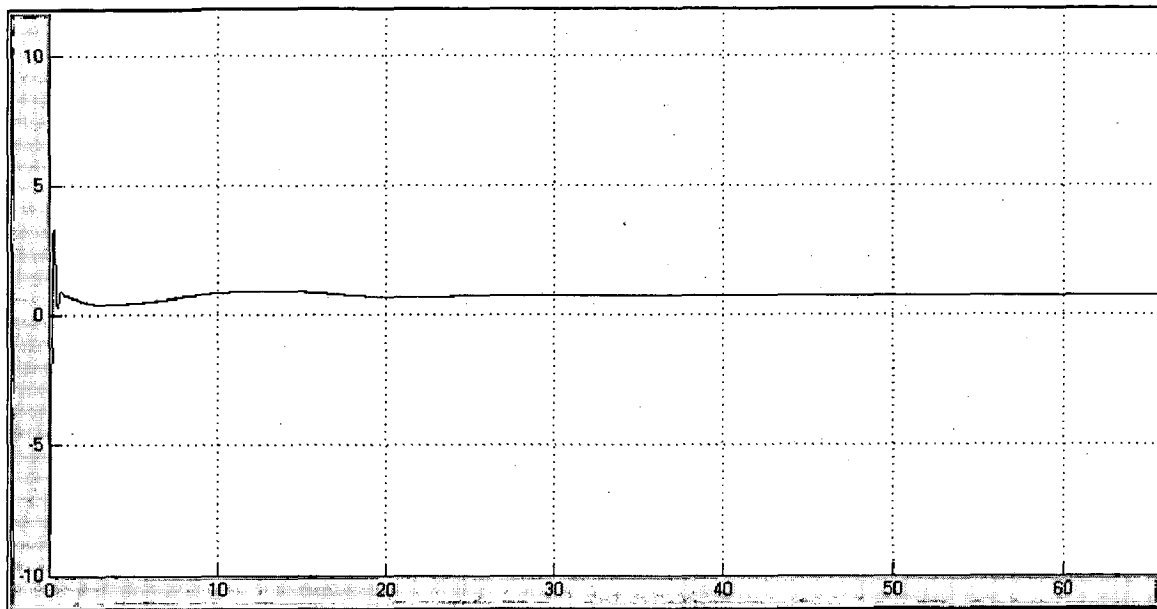


Fig. (4.24) Excitation Voltage V_f (p.u.)

When Head is varied to 0.9 p.u. from 1 p.u. at 50 MW Active Power and 50 MVAR Reactive Power Load then Excitation Voltage approximately remain same upto 0.745 p.u.

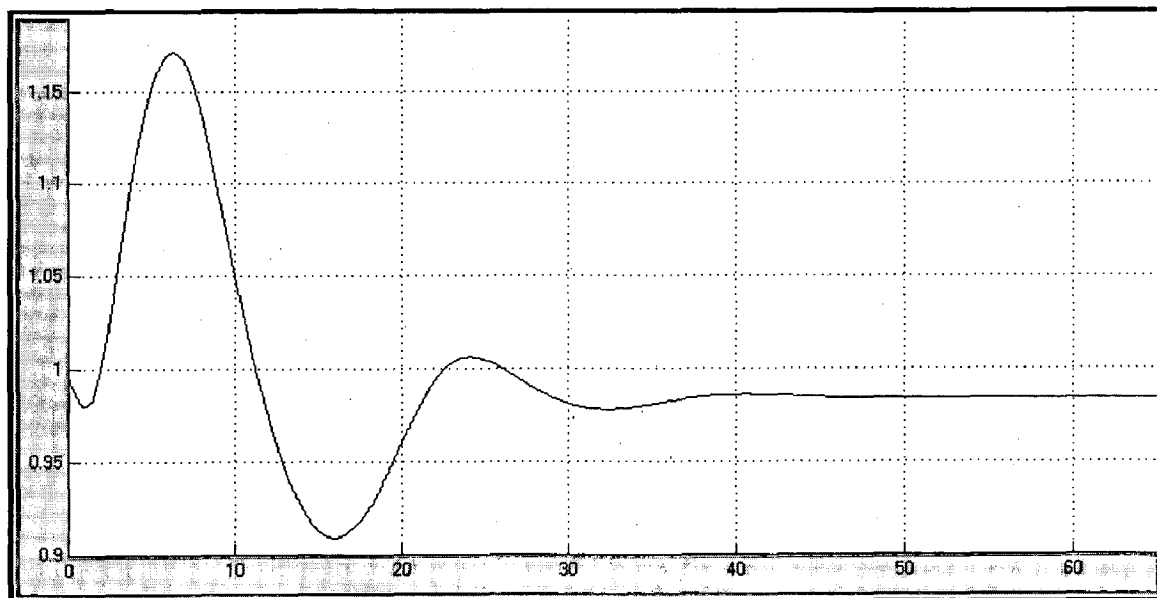


Fig. (4.25) Rotor Speed (p.u.) \

When Head is varied to 0.9 p.u. from 1 p.u. at 50 MW Active Power and 50 MVAR Reactive Power Load then at that moment speed decrease from 1 p.u. to 0.9848 p.u.

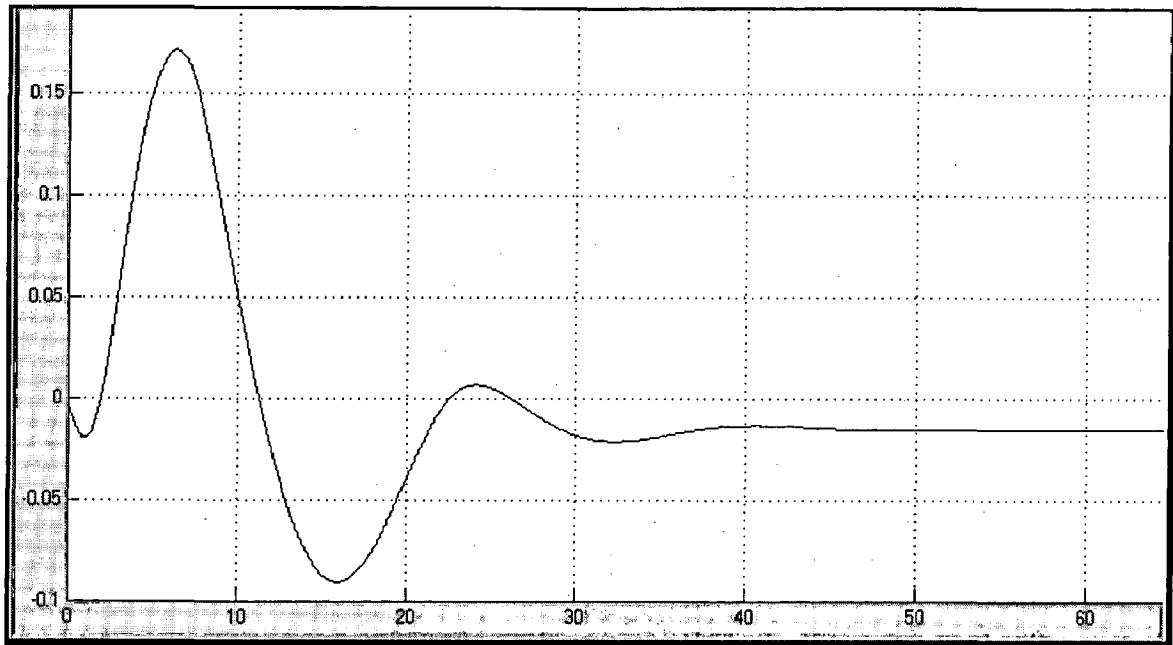


Fig. (4.26) Speed Deviation (p.u.)

When Head is varied to 0.9 p.u. from 1 p.u. at 50 MW Active Power and 50 MVAR Reactive Power Load then speed deviation decrease from 0 p.u. to -0.0153 p.u.

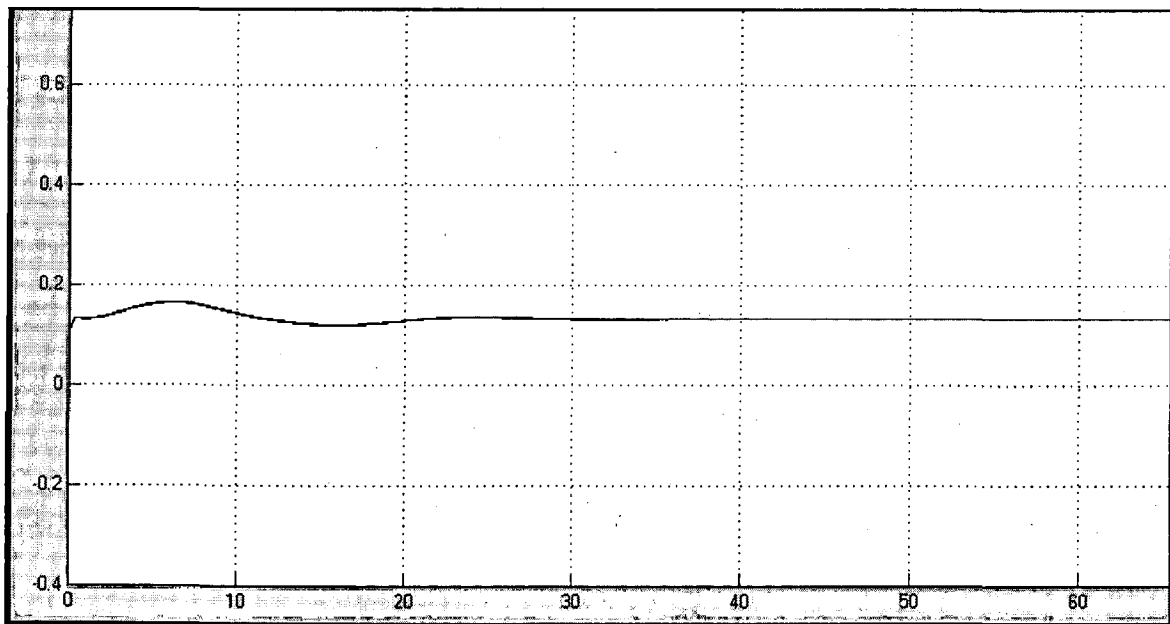


Fig. (4.27) V_d (p.u.)

When Head is varied to 0.9 p.u. from 1 p.u. at 50 MW Active Power and 50 MVAR Reactive Power Load then d-transformation voltage remains constant to 0.131 p.u.

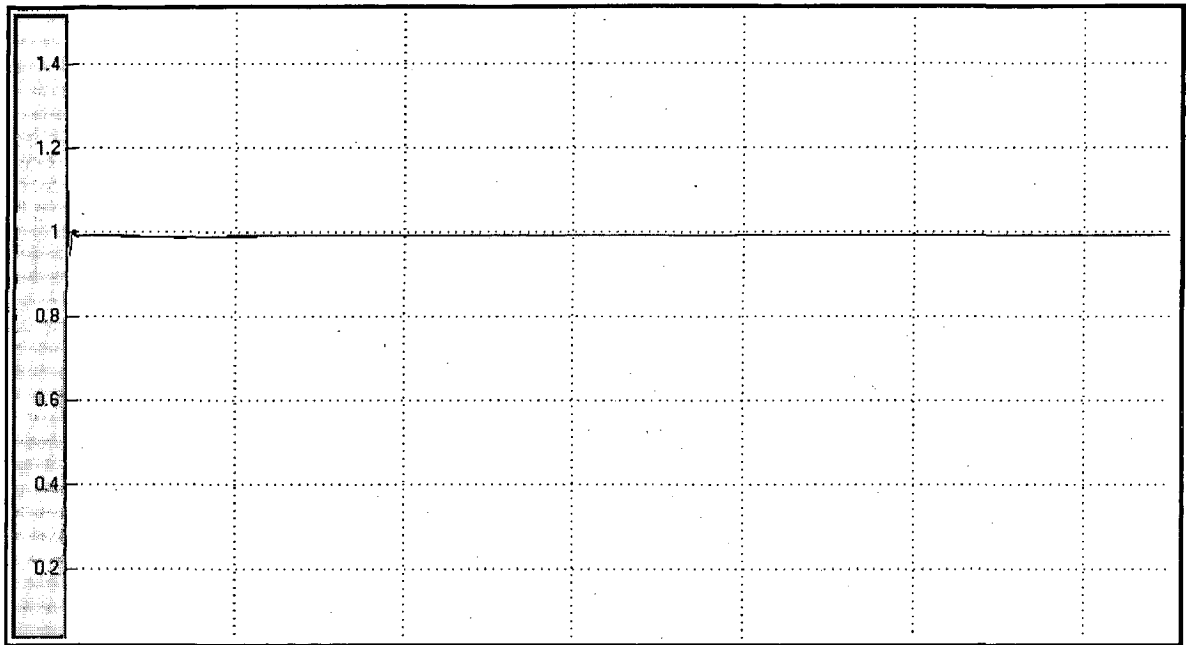


Fig. (4.28) V_q (p.u.)

When Head is varied to 0.9 p.u. from 1 p.u. at 50 MW Active Power and 50 MVAR Reactive Power Load then q-transformation voltage remain constant to 0.993 p.u.

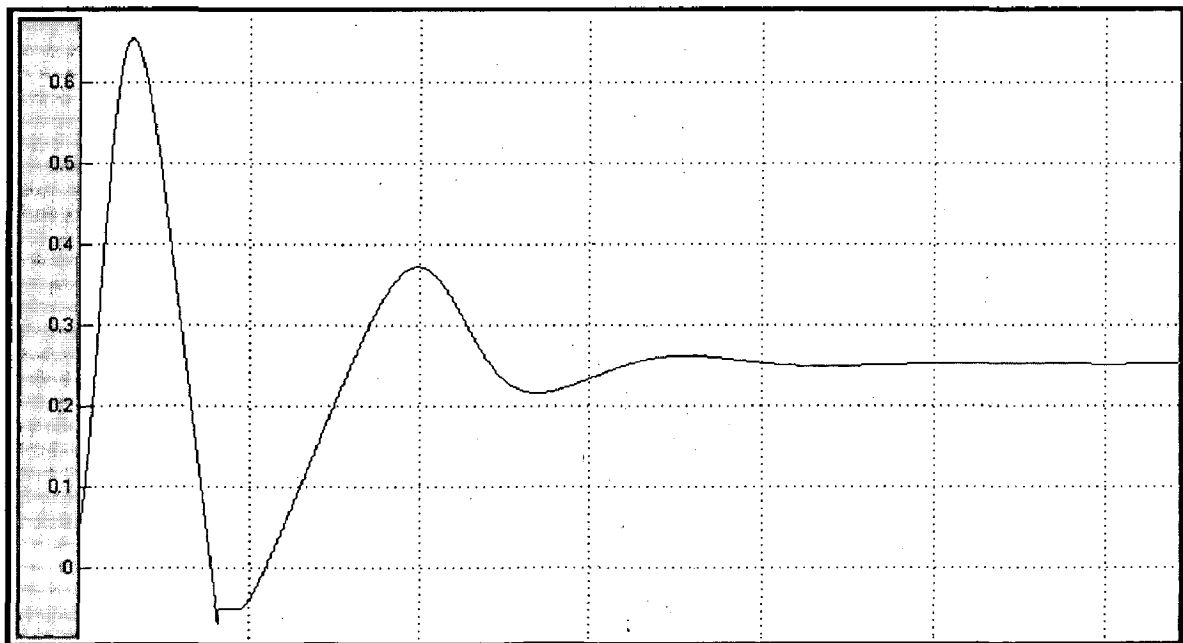


Fig. (4.29) Mechanical Power P_m (p.u.)

When Head is varied to 0.9 p.u. from 1 p.u. at 50 MW Active Power and 50 MVAR Reactive Power Load then mechanical power demand remain same at 0.252 p.u.

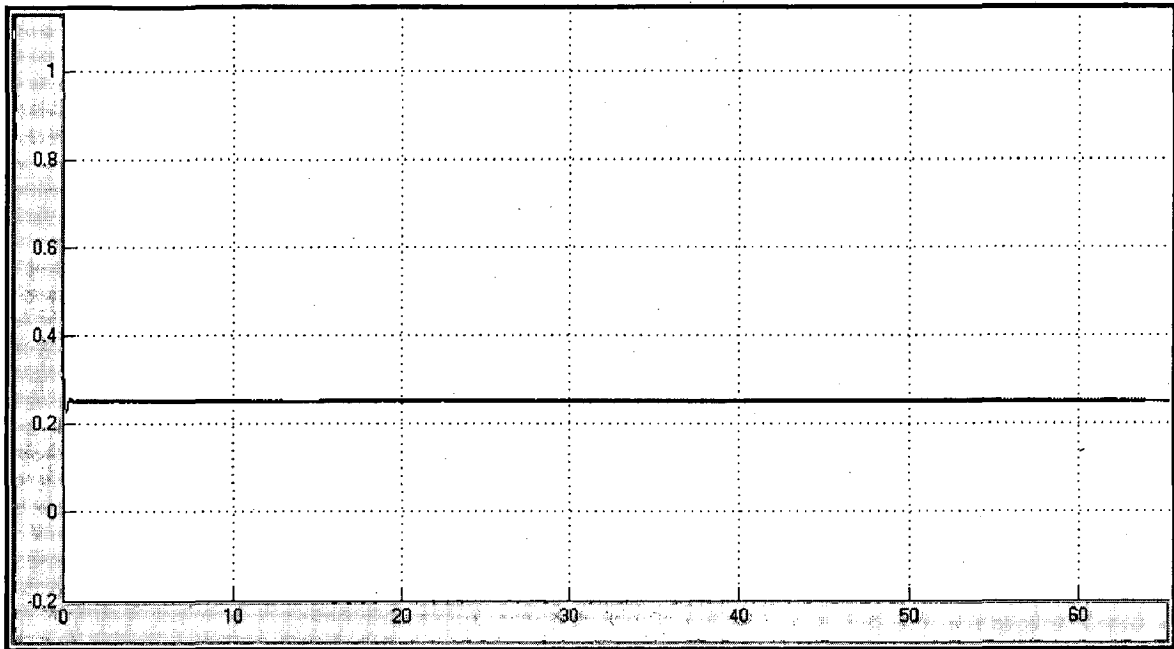


Fig. (4.30) Electrical Power P_{eo} (p.u.)

When Head is varied to 0.9 p.u. from 1 p.u. at 50 MW Active Power and 50 MVAR Reactive Power Load then Electrical power demand remain same to 0.25 p.u.

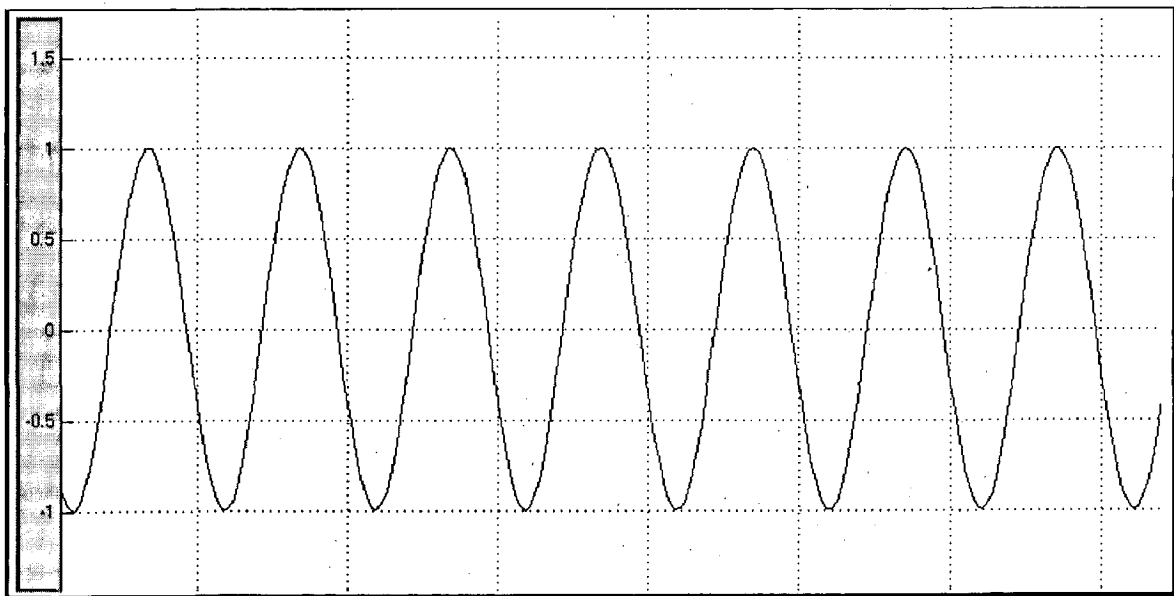


Fig. (4.31) Voltage

When Head is varied to 0.9 p.u. from 1 p.u. at 50 MW Active Power and 50 MVAR Reactive Power Load then also stator voltage does not effect and remain constant as 1 p.u. in magnitude..

4.7.4 When Load is increased to 60 MW active power from 50 MW and 50 MVAR
Reactive Power Load is applied at 0.9 p.u. Head Here X- axis represent time (sec.)

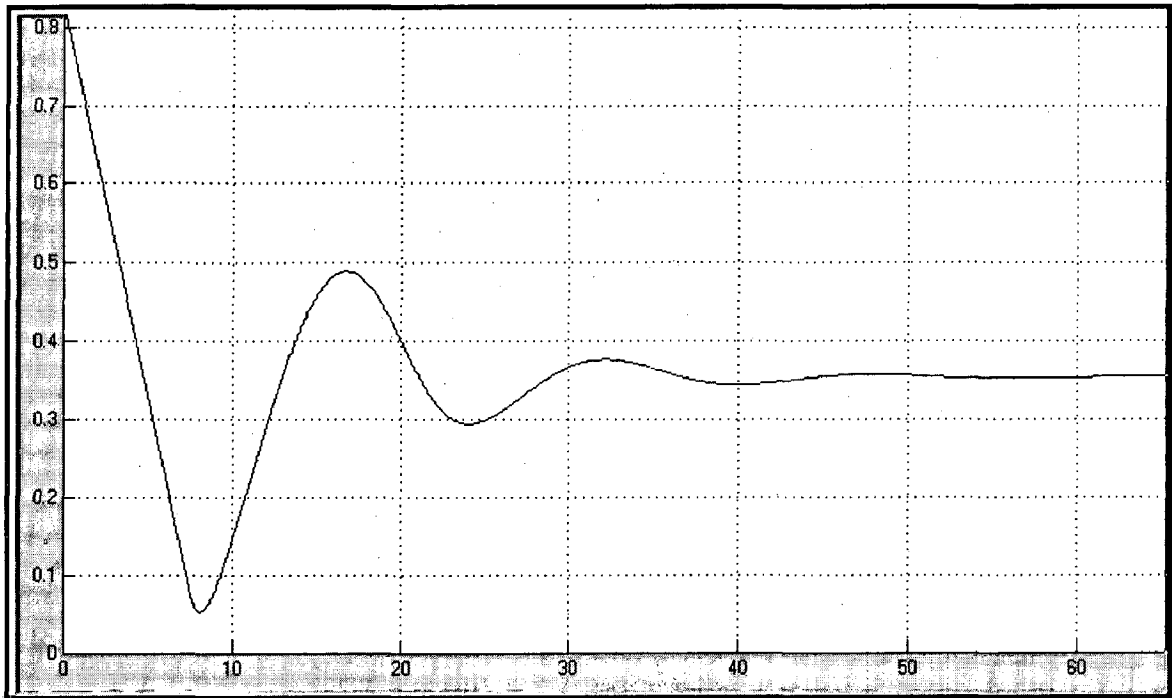


Fig. (4.32) Gate (p.u.)

When Load is increased to 60 MW active power from 50 MW and 50 MVAR Reactive Power Load is applied at 0.9 p.u. Head then at that moment gate opening increases from 0.3045 p.u. to 0.3527 p.u.

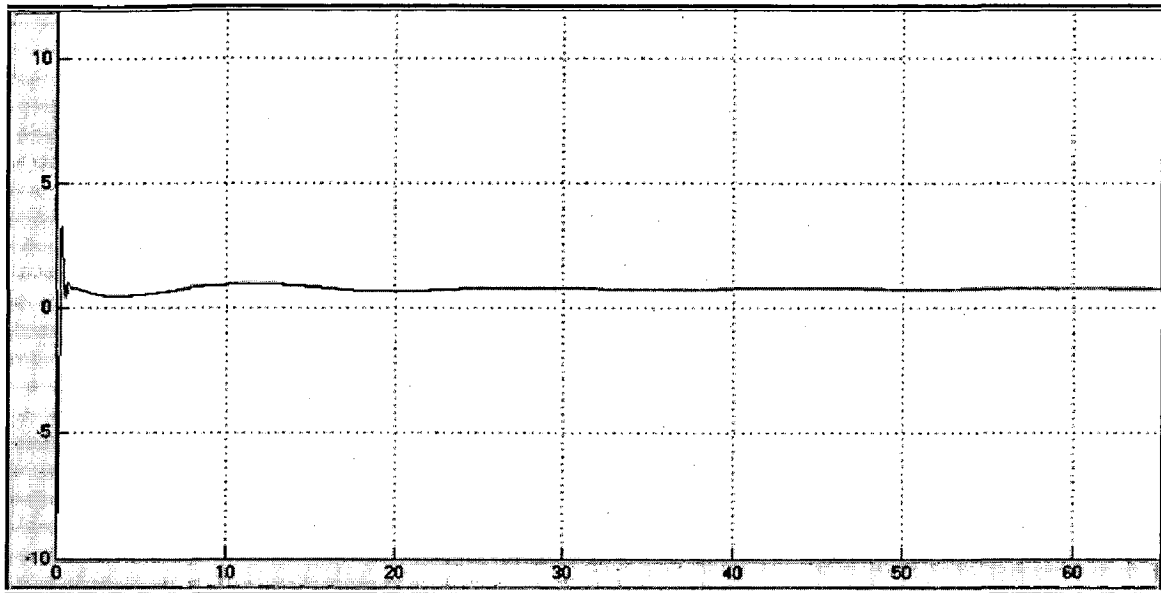


Fig. (4.33) Excitation Voltage V_f (p.u.)

When Load is increased to 60 MW active power from 50 MW and 50 MVAR Reactive Power Load is applied at 0.9 p.u. Head then Excitation Voltage increases to 0.77 p.u. from 0.745 p.u. It is used to increase rotor speed.

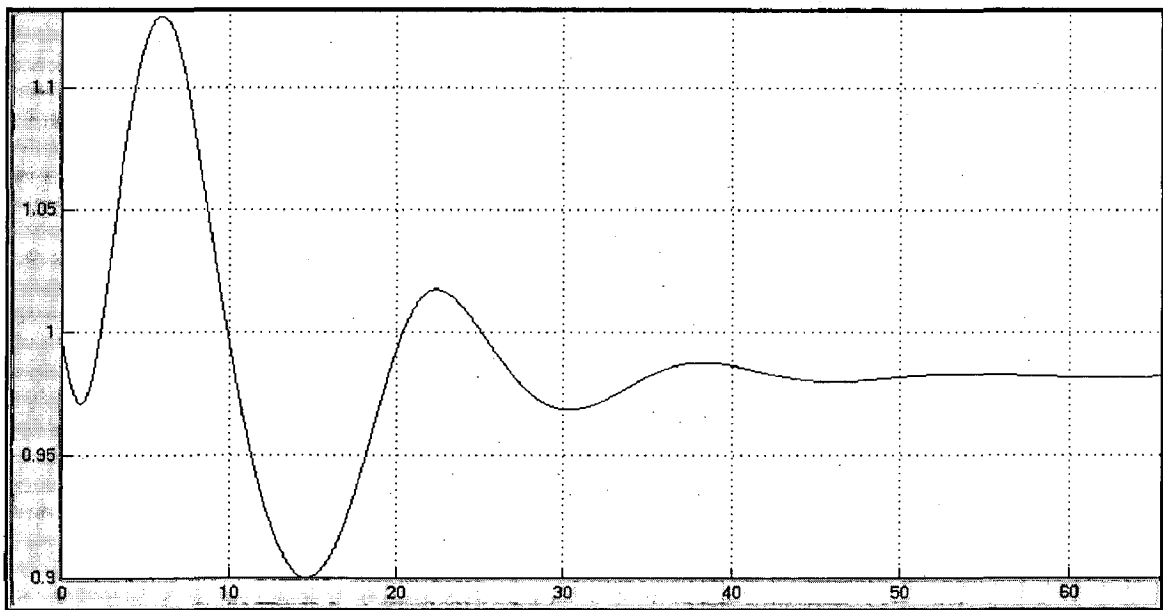


Fig. (4.34) Rotor Speed (p.u.)

When Load is increased to 60 MW active power from 50 MW and 50 MVAR Reactive Power Load is applied at 0.9 p.u. Head then at that moment speed decreases from 1 p.u. to 0.9825 p.u.

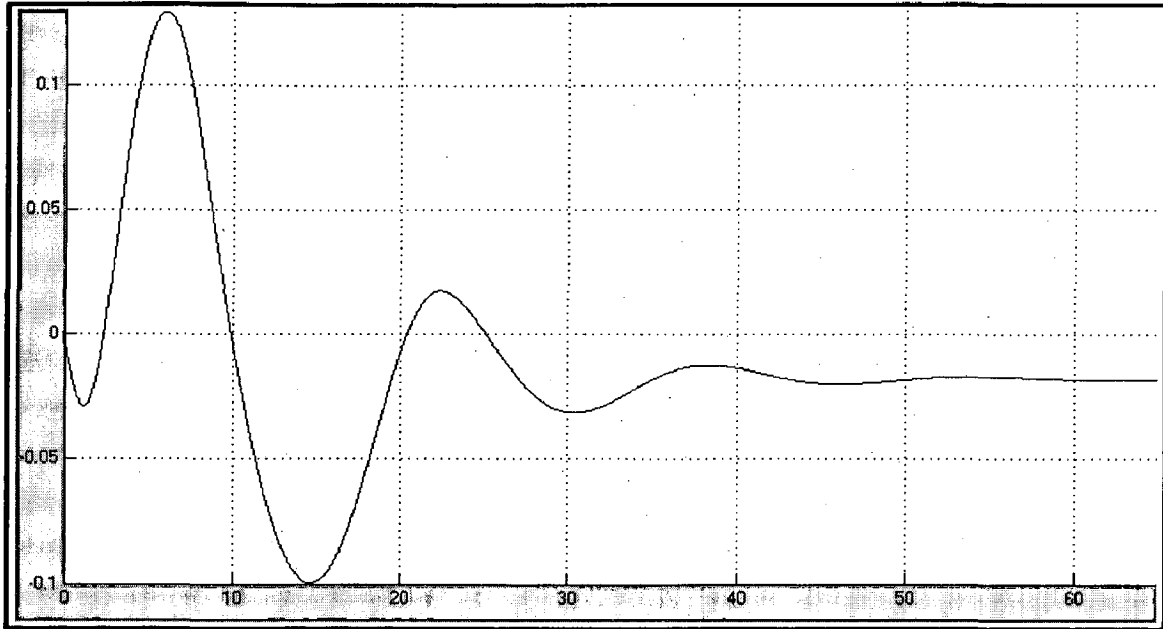


Fig. (4.35) Speed Deviation (p.u.)

When Load is increased to 60 MW active power from 50 MW and 50 MVAR Reactive Power Load is applied at 0.9 p.u. Head then speed deviation decreases from 0 p.u. to - 0.017 p.u.

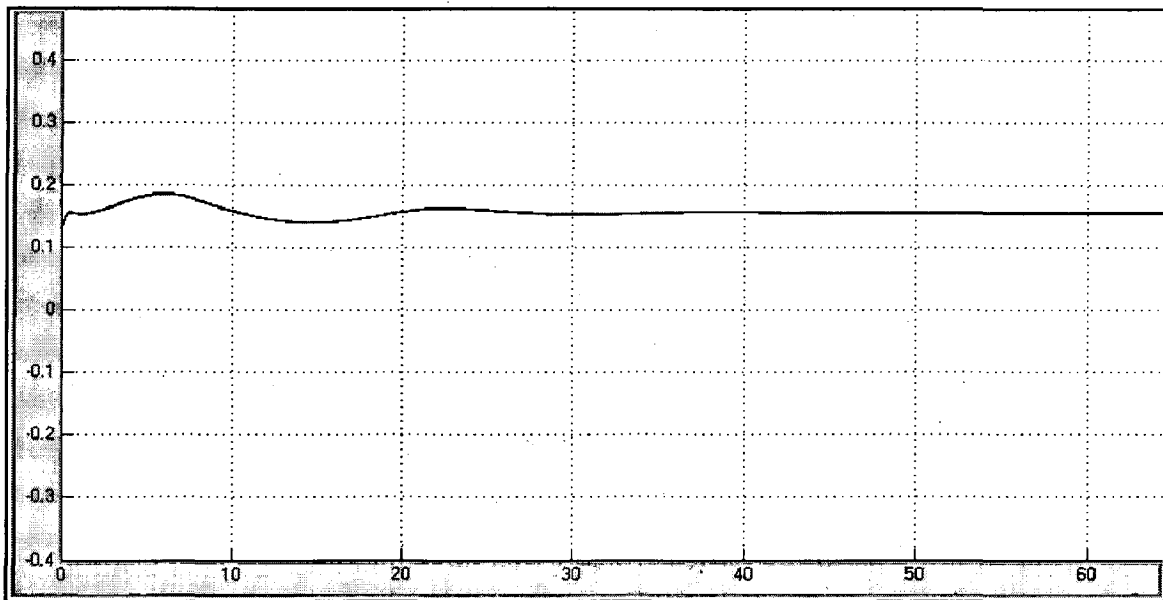


Fig.(4.36) V_d (p.u.)

When Load is increased to 60 MW active power from 50 MW and 50 MVAR Reactive Power Load is applied at 0.9 p.u. Head then due to increase in excitation voltage d-transformation voltage increases to 0.155 p.u. from 0.131 p.u.

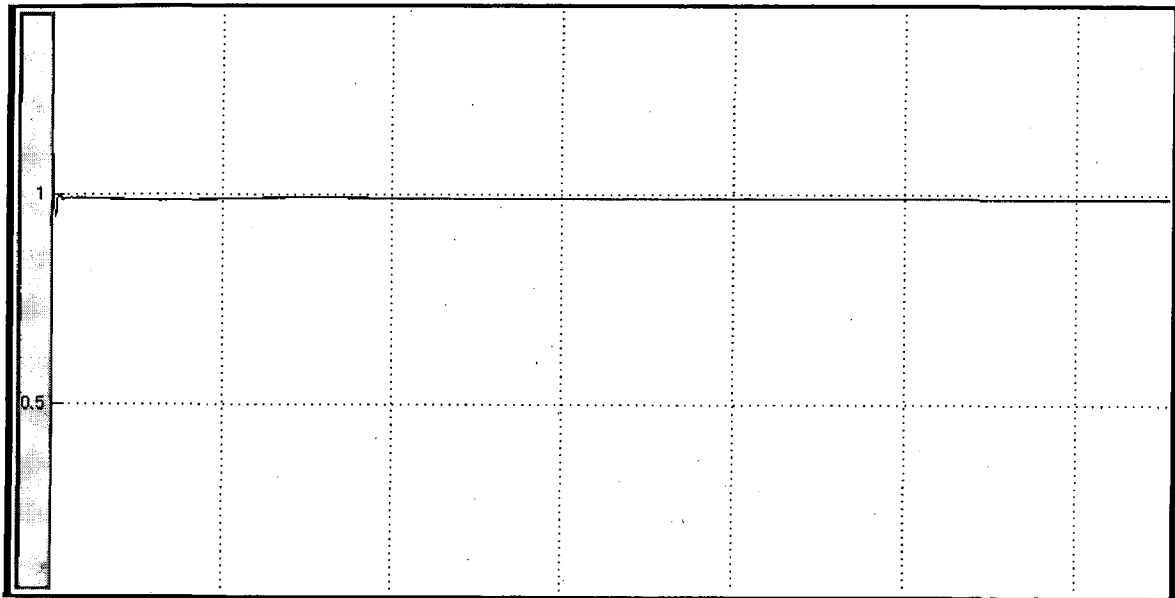


Fig. (4.37) V_q (p.u.)

When Load is increased to 60 MW active power from 50 MW and 50 MVAR Reactive Power Load is applied at 0.9 p.u. Head then due to increase in excitation voltage q-transformation voltage decreases to 0.9885 p.u. from 0.993 p.u.

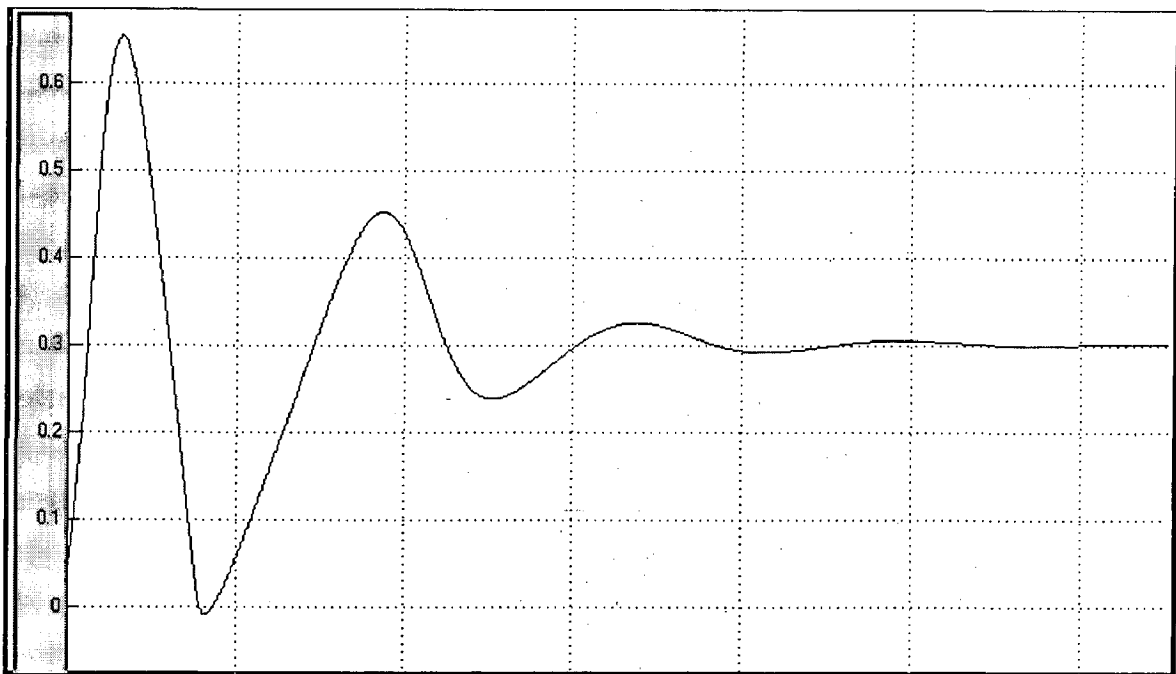


Fig. (4.38) Mechanical Power P_m (p.u.)

When Load is increased to 60 MW active power from 50 MW and 50 MVAR Reactive Power Load is applied at 0.9 p.u. Head then mechanical power demand increases to 0.3017 p.u. from 0.252 p.u.

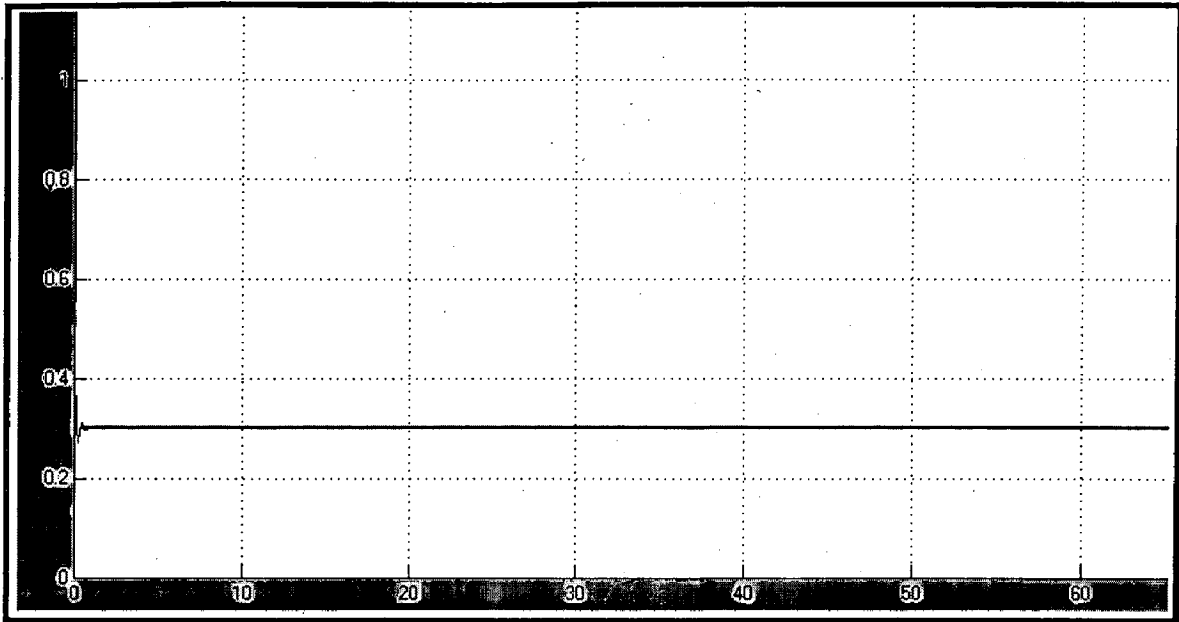


Fig. (4.39) Electrical Power P_{eo} (p.u.)

When Load is increased to 60 MW active power from 50 MW and 50 MVAR Reactive Power Load is applied at 0.9 p.u. Head then Electrical power demand increases to 0.3 p.u. from 0.25 p.u.

4.7.5 When Head is varied to 0.8 p.u. from 0.9 p.u. at 50 MW Active Power and 50 MVAR Reactive Power Load. Here X- axis represent time (sec.)

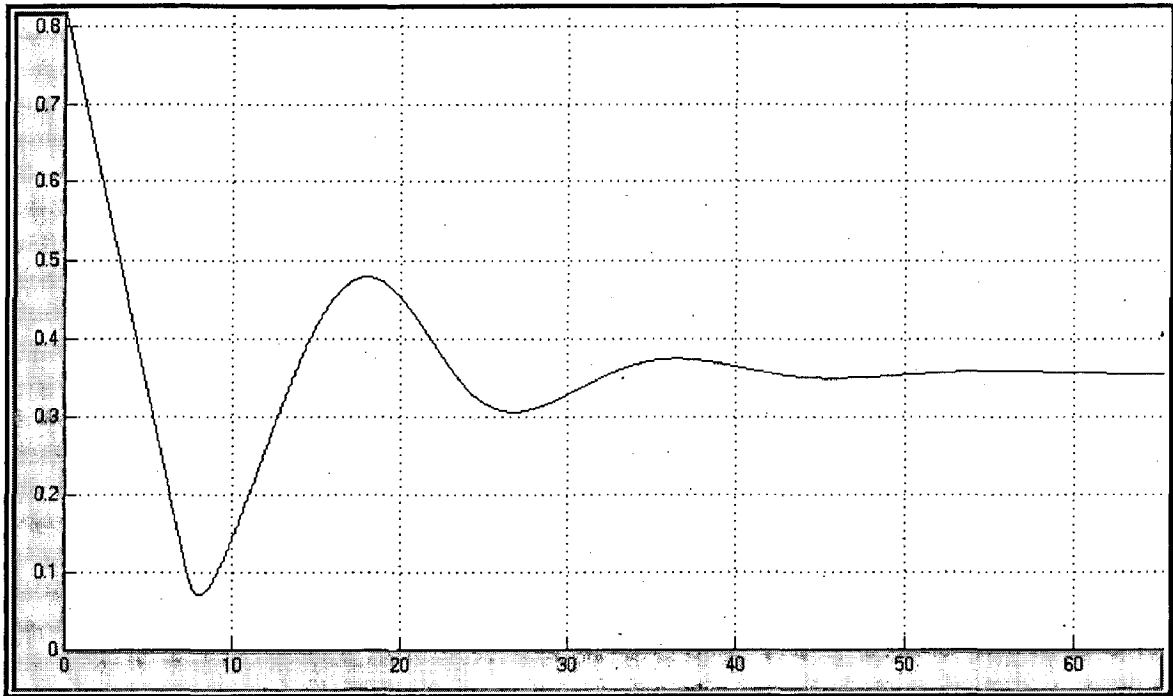


Fig. (4.40) Gate (p.u.)

When Head is varied to 0.8 p.u. from 0.9 p.u. at 50 MW Active Power and 50 MVAR Reactive Power Load then at that moment gate opening increases from 0.3045 p.u. to 0.355 p.u.

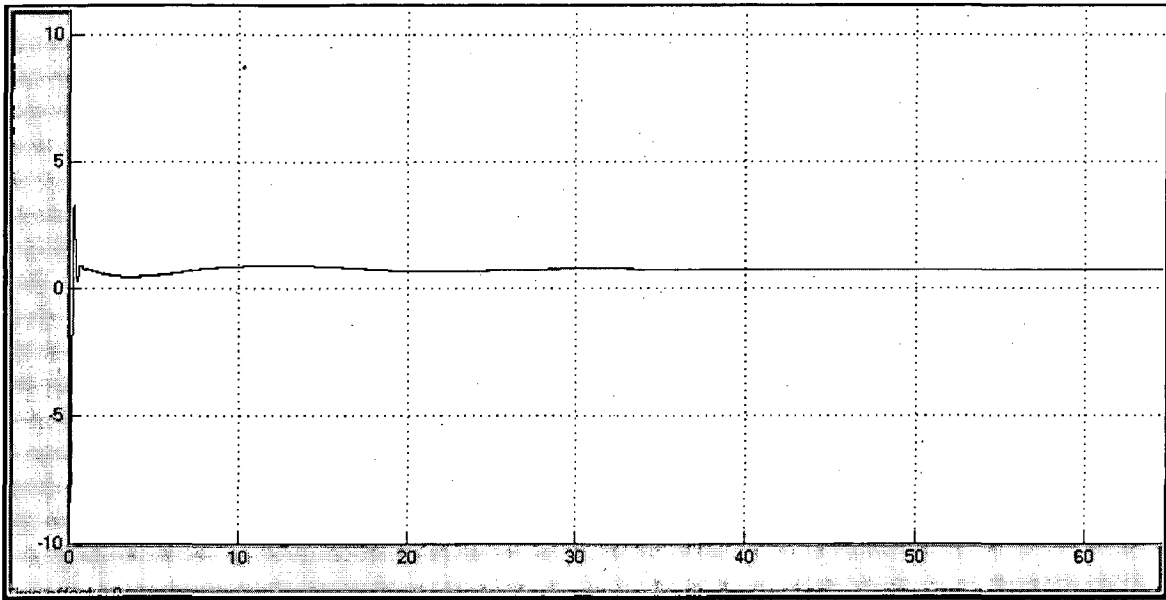


Fig. (4.41) Excitation Voltage V_f (p.u.)

When Head is varied to 0.8 p.u. from 0.9 p.u. at 50 MW Active Power and 50 MVAR Reactive Power Load then Excitation Voltage remain constant to 0.745 p.u.

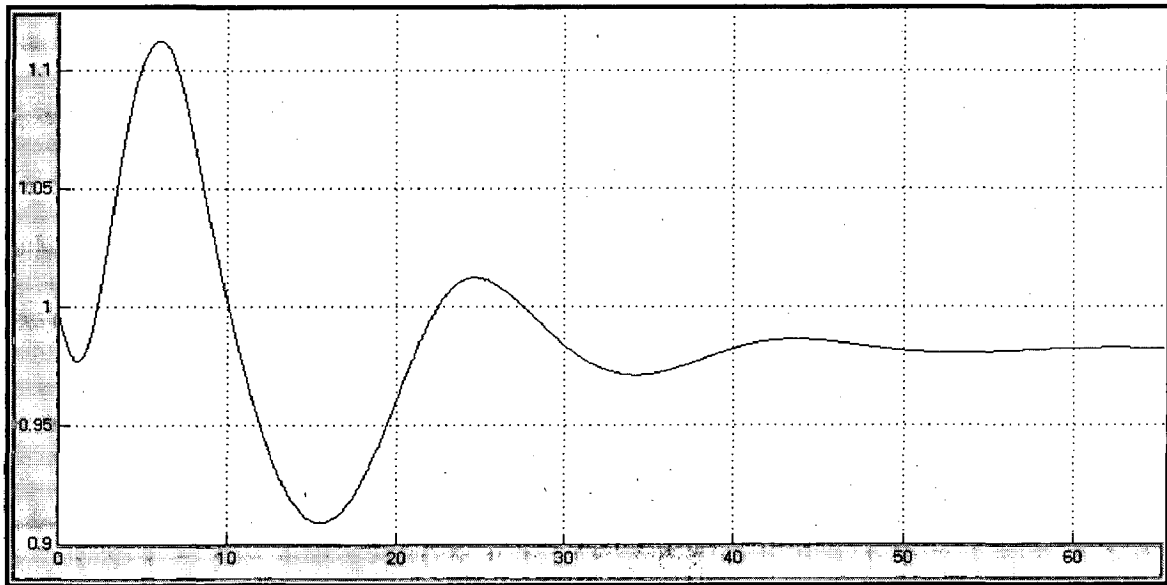


Fig. (4.42) Rotor Speed (p.u.)

When Head is varied to 0.8 p.u. from 0.9 p.u. at 50 MW Active Power and 50 MVAR Reactive Power Load then at that moment rotor speed decreases from 1 p.u. to 0.983 p.u.

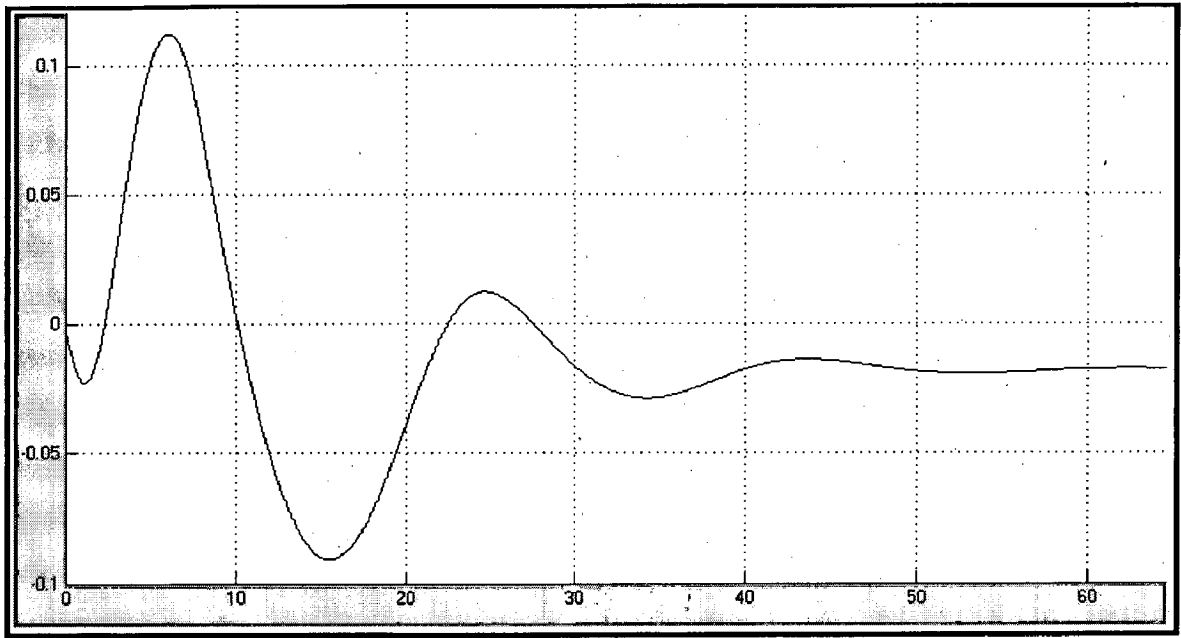


Fig. (4.43) Speed Deviation (p.u.)

When Head is varied to 0.8 p.u. from 0.9 p.u. at 50 MW Active Power and 50 MVAR Reactive Power Load then speed deviation decreases from 0 p.u. to -0.017 p.u.

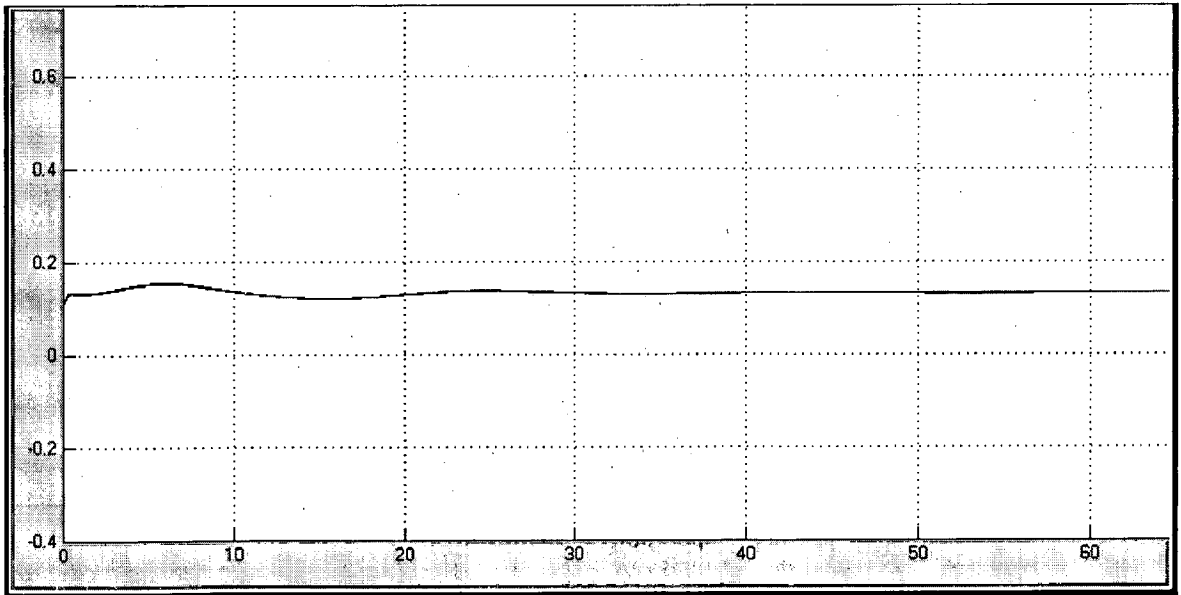


Fig. (4.44) V_d (p.u.)

When Head is varied to 0.8 p.u. from 0.9 p.u. at 50 MW Active Power and 50 MVAR Reactive Power Load then d-transformation voltage remain constant to 0.131 p.u.

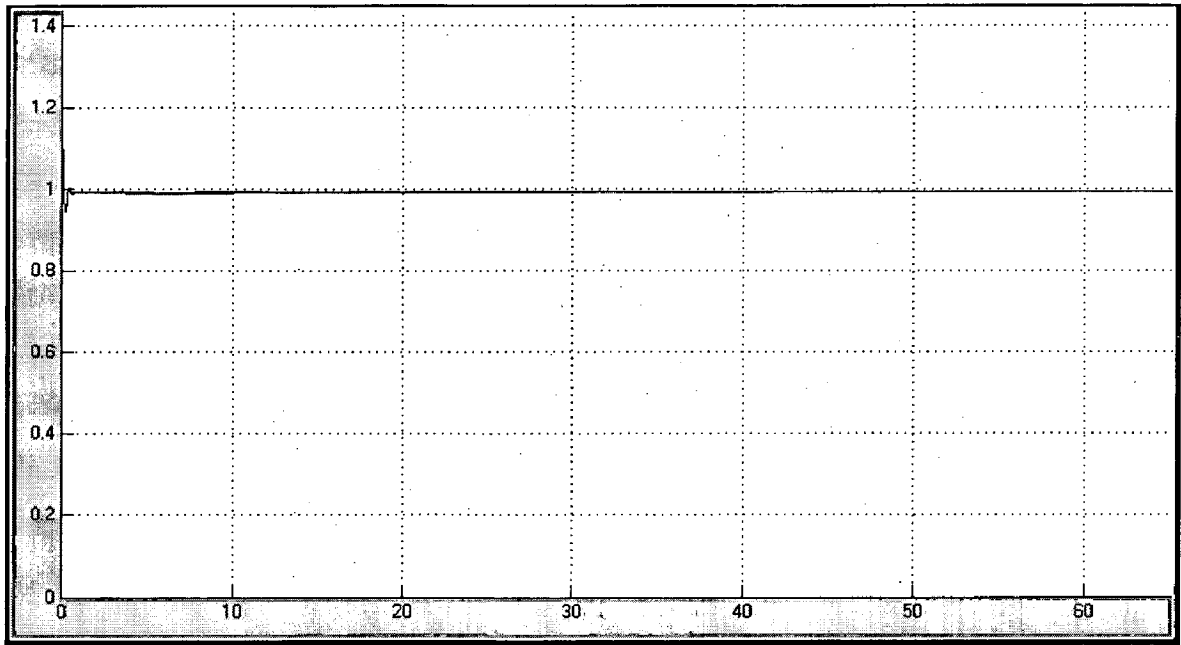


Fig. (4.45) V_q (p.u.)

When Head is varied to 0.8 p.u. from 0.9 p.u. at 50 MW Active Power and 50 MVAR Reactive Power Load then q -transformation voltage remain constant to 0.993 p.u.

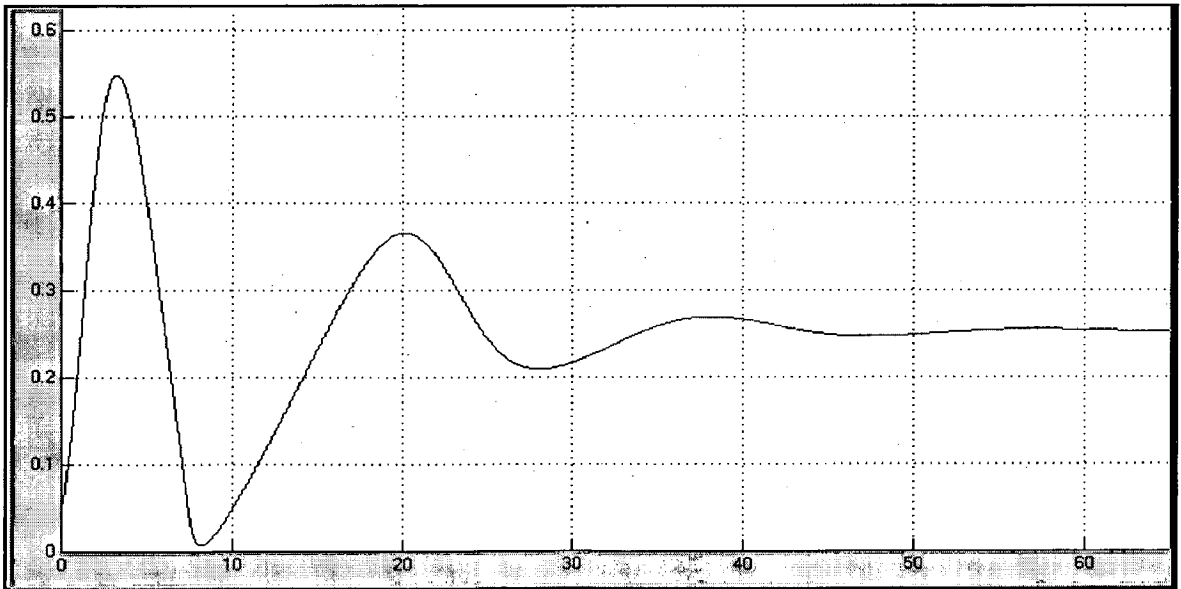


Fig. (4.46) Mechanical Power P_m (p.u.)

When Head is varied to 0.8 p.u. from 0.9 p.u. at 50 MW Active Power and 50 MVAR Reactive Power Load then mechanical power demand remain constant to 0.252 p.u.

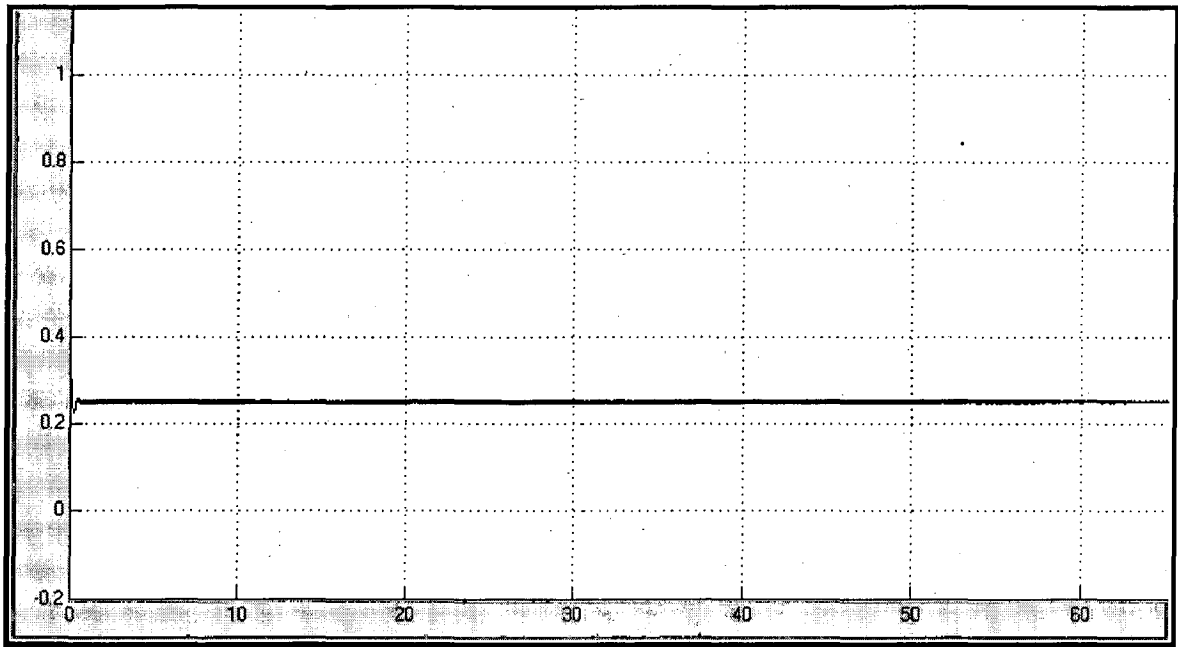


Fig. (4.47) Electrical Power P_{co} (p.u.)

When Head is varied to 0.8 p.u. from 0.9 p.u. at 50 MW Active Power and 50 MVAR Reactive Power Load then Electrical power demand remain constant to 0.25 p.u.

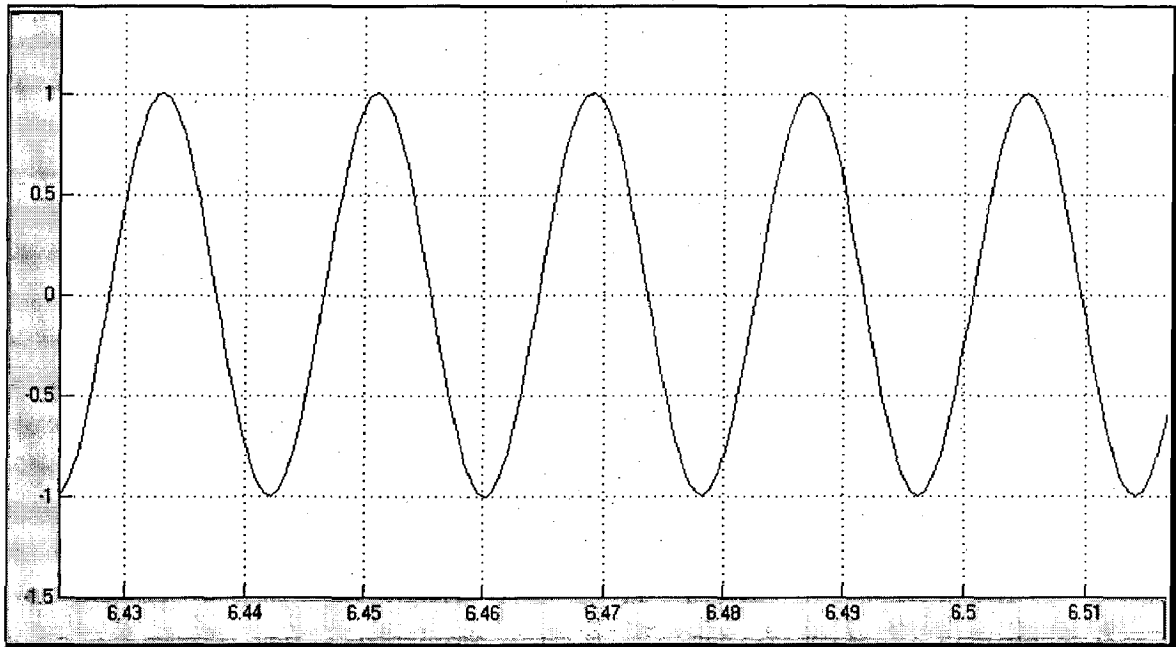


Fig. (4.48) Voltage

When Head is varied to 0.8 p.u. from 0.9 p.u. at 50 MW Active Power and 50 MVAR Reactive Power Load then also stator voltage does not effect and remain constant as 1 p.u. in magnitude.

4.7.6 When Head is varied to 0.7 p.u. from 0.8 p.u. at 50 MW Active Power and 50 MVAR Reactive Power Load. Here X- axis represent time (sec.)

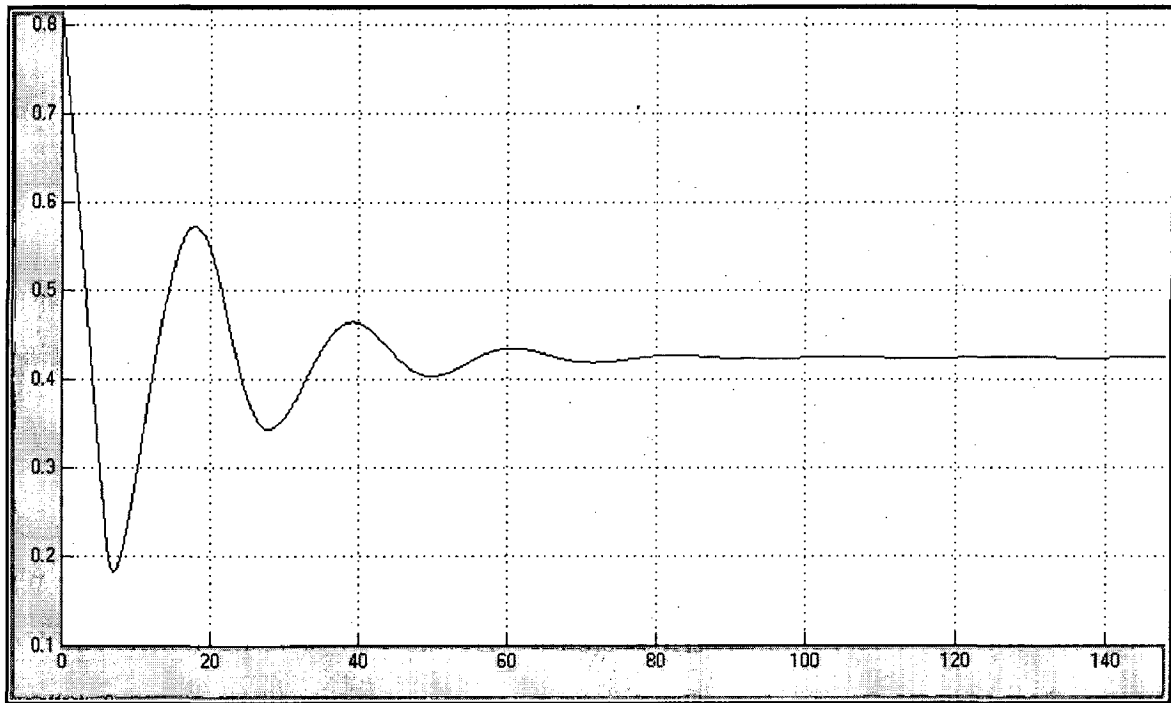


Fig. (4.49) Gate Opening (p. u.)

When Head is varied to 0.7 p.u. from 0.8 p.u. at 50 MW Active Power and 50 MVAR Reactive Power Load then at that moment gate opening increases from 0.355 p.u. to 0.425 p.u.

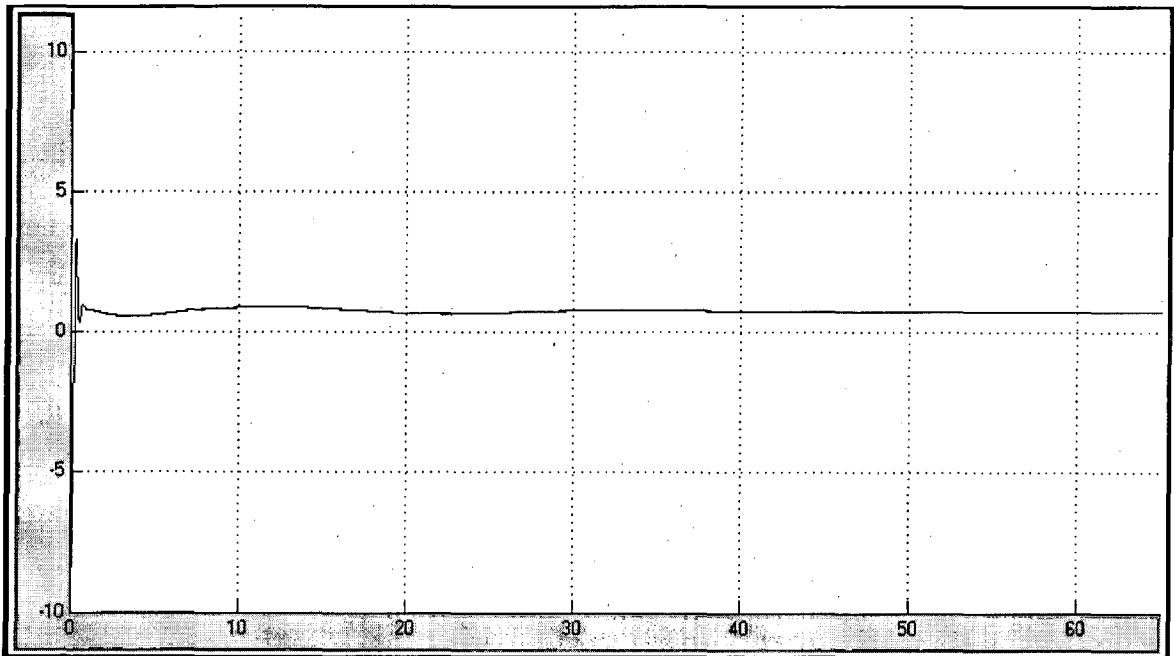


Fig. (4.50) Excitation Voltage V_f (p.u.)

When Head is varied to 0.7 p.u. from 0.8 p.u. at 50 MW Active Power and 50 MVAR Reactive Power Load then Excitation Voltage remain constant to 0.755 p.u.

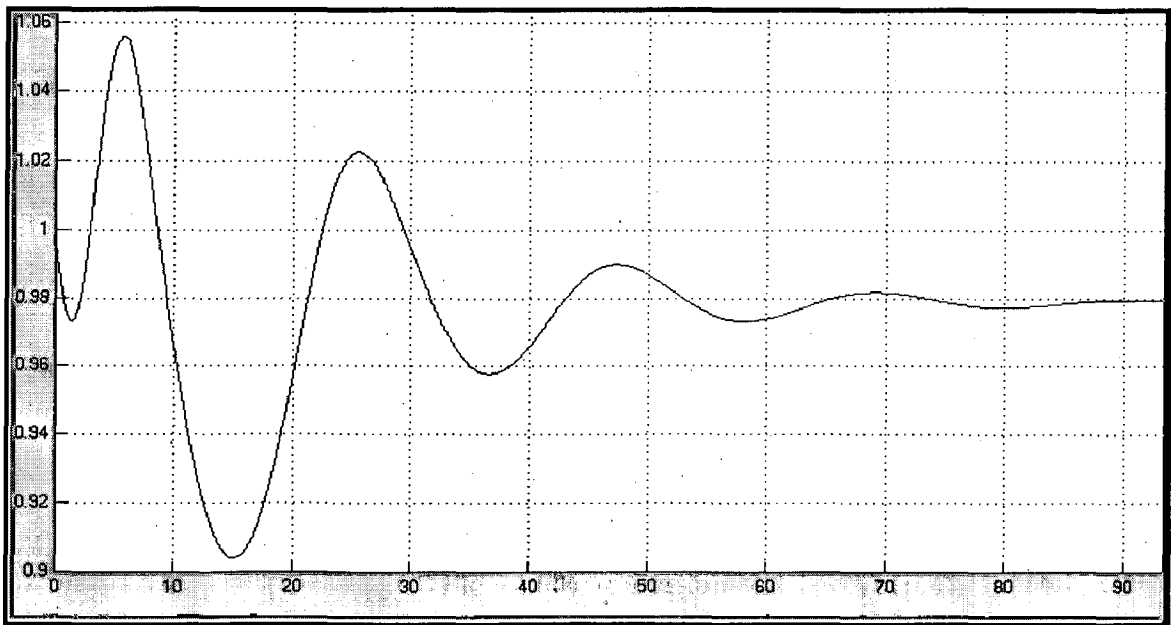


Fig. (4.51) Rotor Speed (p.u.)

When Head is varied to 0.7 p.u. from 0.8 p.u. at 50 MW Active Power and 50 MVAR Reactive Power Load then at that moment speed decreases from 1 p.u. to 0.9787 p.u.

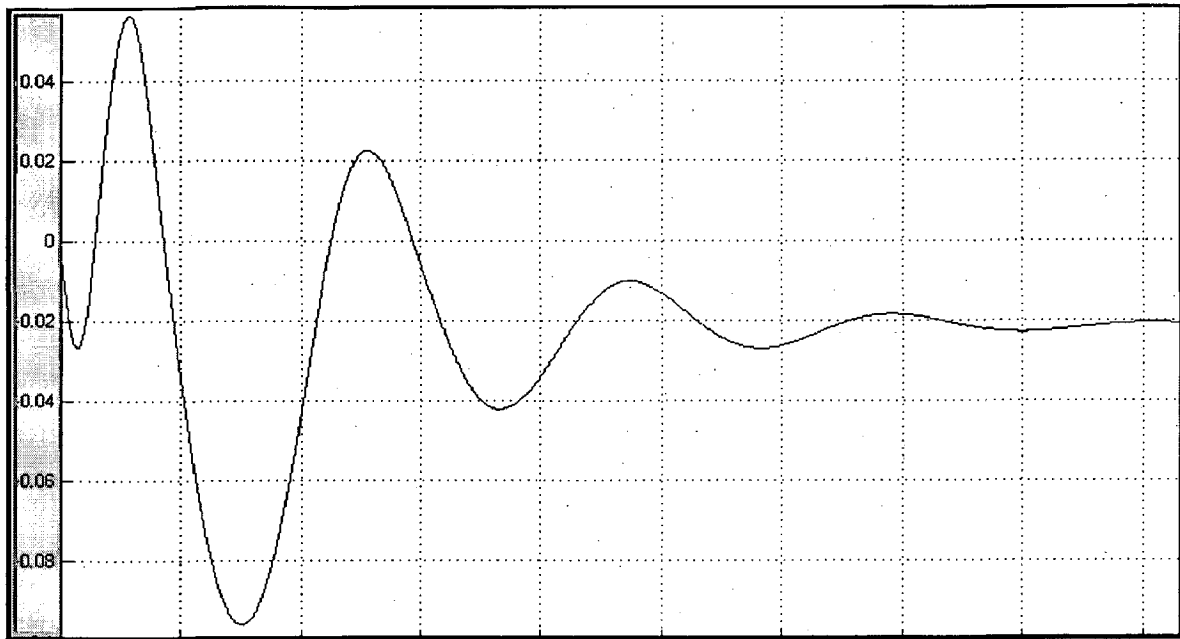


Fig. (4.52) Speed Deviation (p.u.)

When Head is varied to 0.7 p.u. from 0.8 p.u. at 50 MW Active Power and 50 MVAR Reactive Power Load then speed deviation decreases from 0 p.u. to -0.0213 p.u.

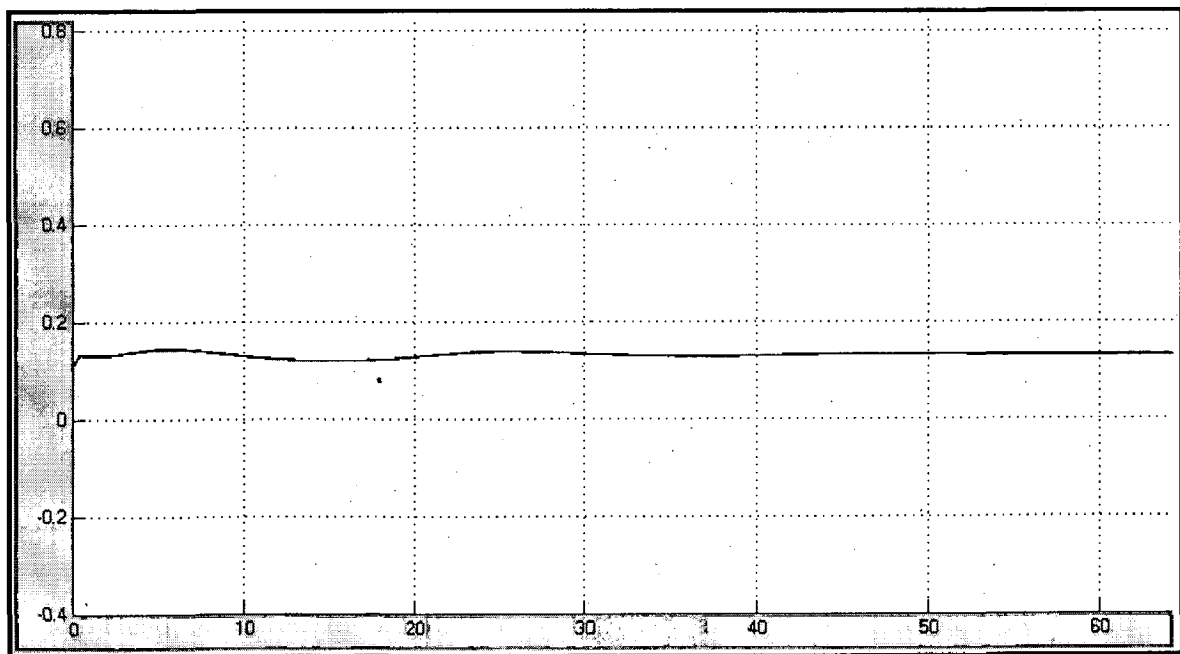


Fig. (4.53) V_d (p.u.)

When Head is varied to 0.7 p.u. from 0.8 p.u. at 50 MW Active Power and 50 MVAR Reactive Power Load then d-transformation voltage remain constant at 0.13 p.u.

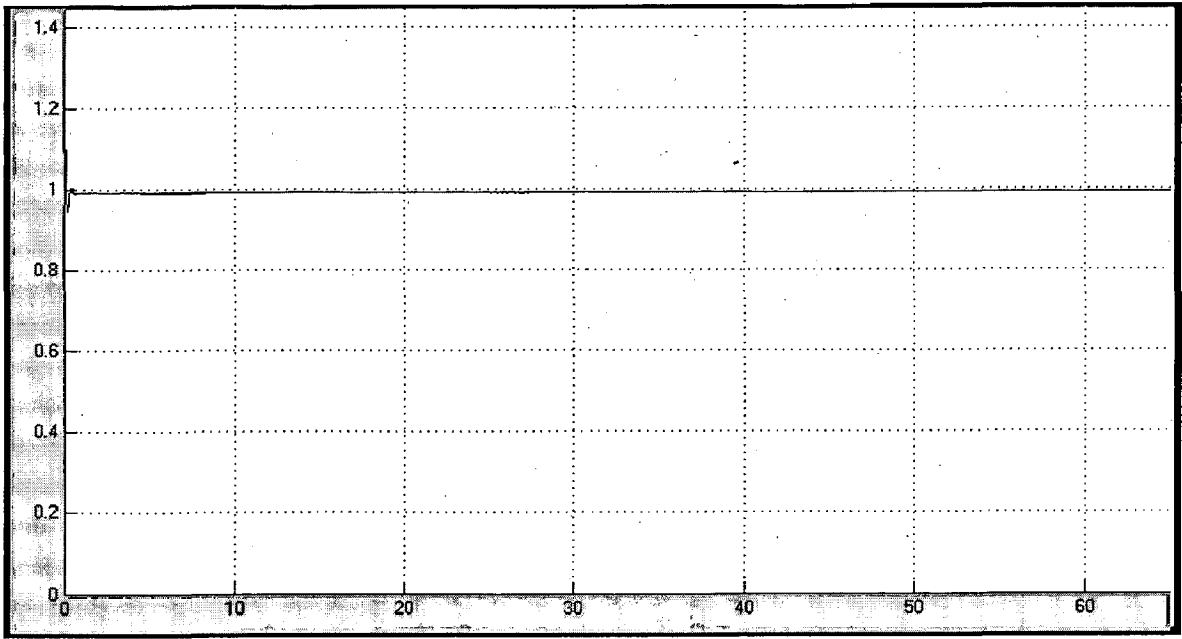


Fig. (4.54) V_q (p.u.)

When Head is varied to 0.7 p.u. from 0.8 p.u. at 50 MW Active Power and 50 MVAR Reactive Power Load then q-transformation voltage remain constant at 0.992 p.u.

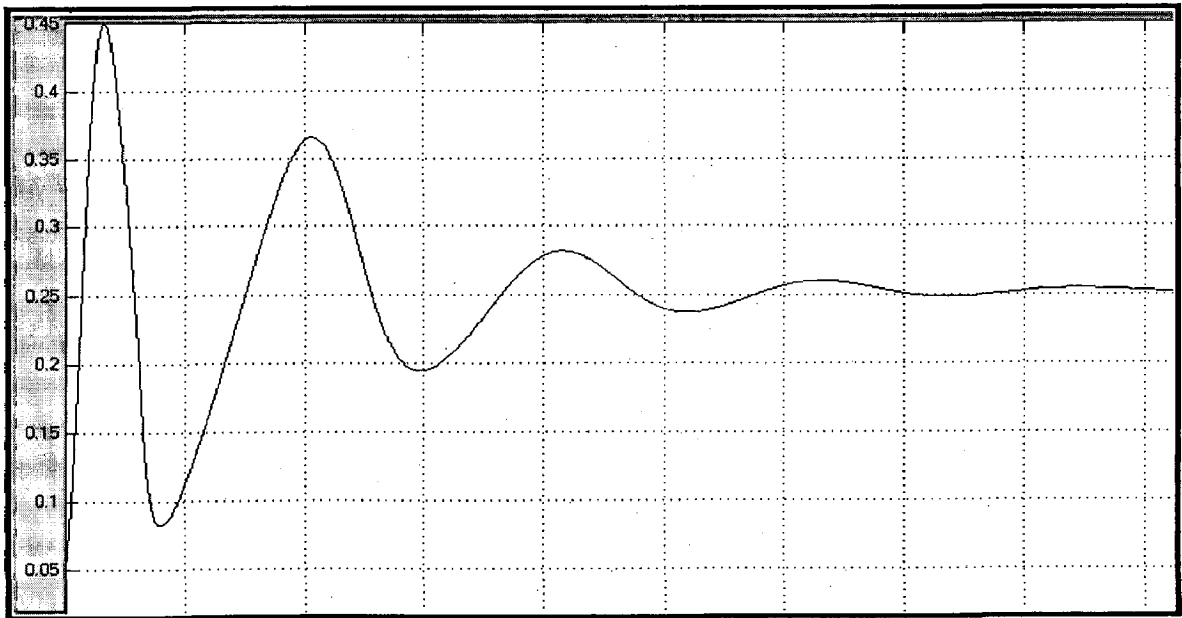


Fig.(4.55) Mechanical Power P_m (p.u.)

When Head is varied to 0.7 p.u. from 0.8 p.u. at 50 MW Active Power and 50 MVAR Reactive Power Load then mechanical power demand remain constant to 0.252 p.u.

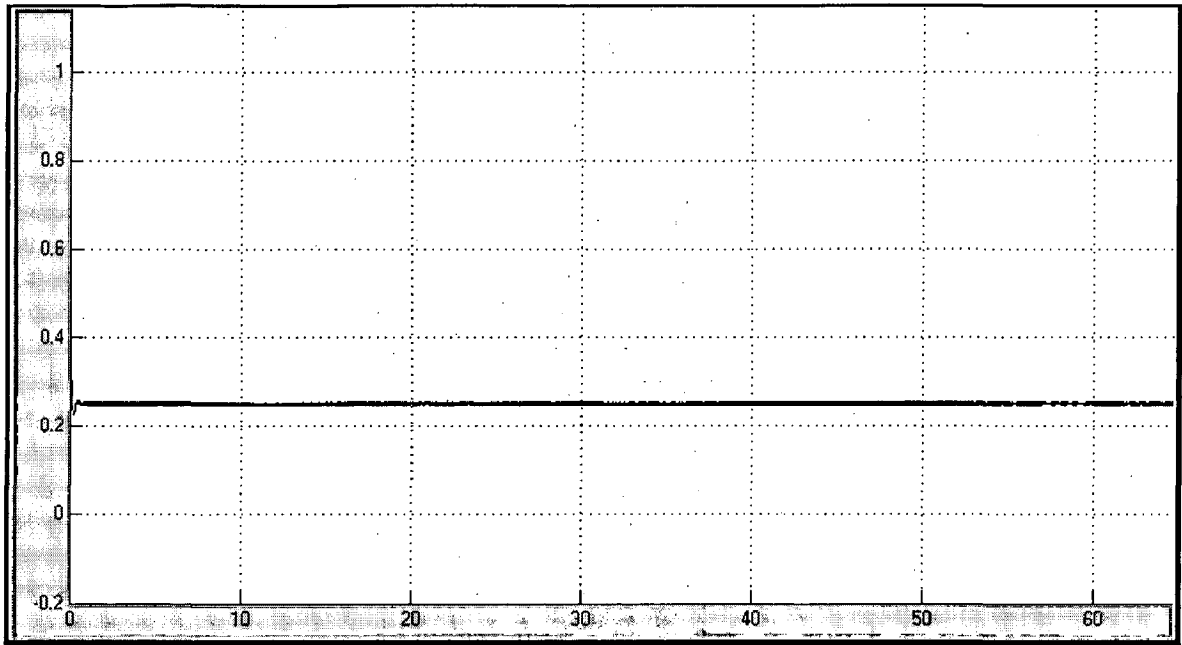


Fig. (4.56) Electrical Power P_{eo} (p.u.)

When Head is varied to 0.7 p.u. from 0.8 p.u. at 50 MW Active Power and 50 MVAR Reactive Power Load then Electrical power demand remain constant to 0.25 p.u.

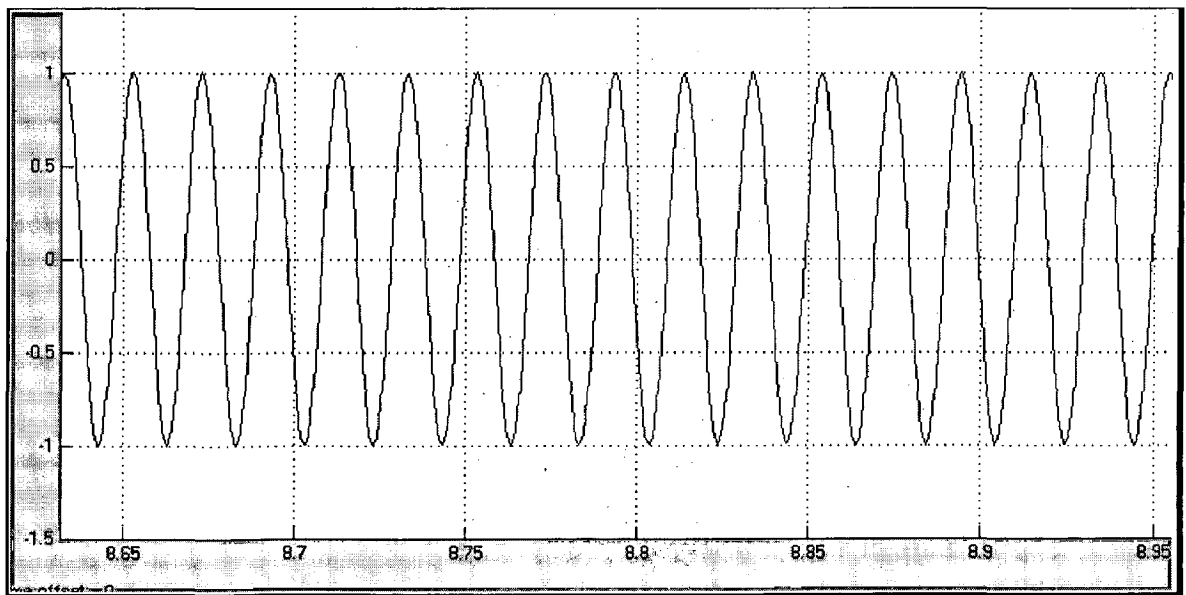


Fig. (4.57) Voltage

When Head is varied to 0.7 p.u. from 0.8 p.u. at 50 MW Active Power and 50 MVAR Reactive Power Load then also stator voltage does not effect and remain constant as 1 p.u. in magnitude..

4.7.7 When Head is varied to 0.6 p.u. from 0.7 p.u. at 50 MW Active Power and 50 MVAR Reactive Power Load. Here X- axis represent time (sec.)

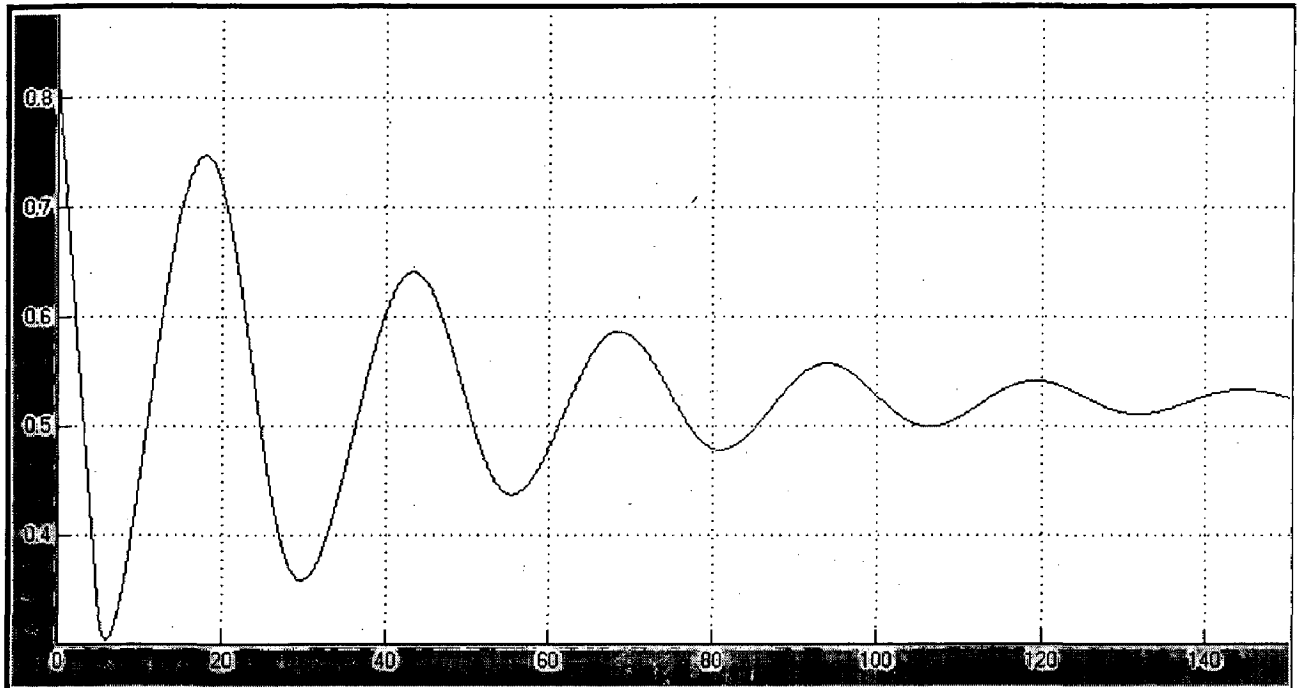


Fig. (4.58) Gate (p.u.)

When Head is varied to 0.6 p.u. from 0.7 p.u. at 50 MW Active Power and 50 MVAR Reactive Power Load then at that moment gate opening increases from 0.425 p.u. to 0.52 p.u. Here 0.16 is gate opening at no load condition

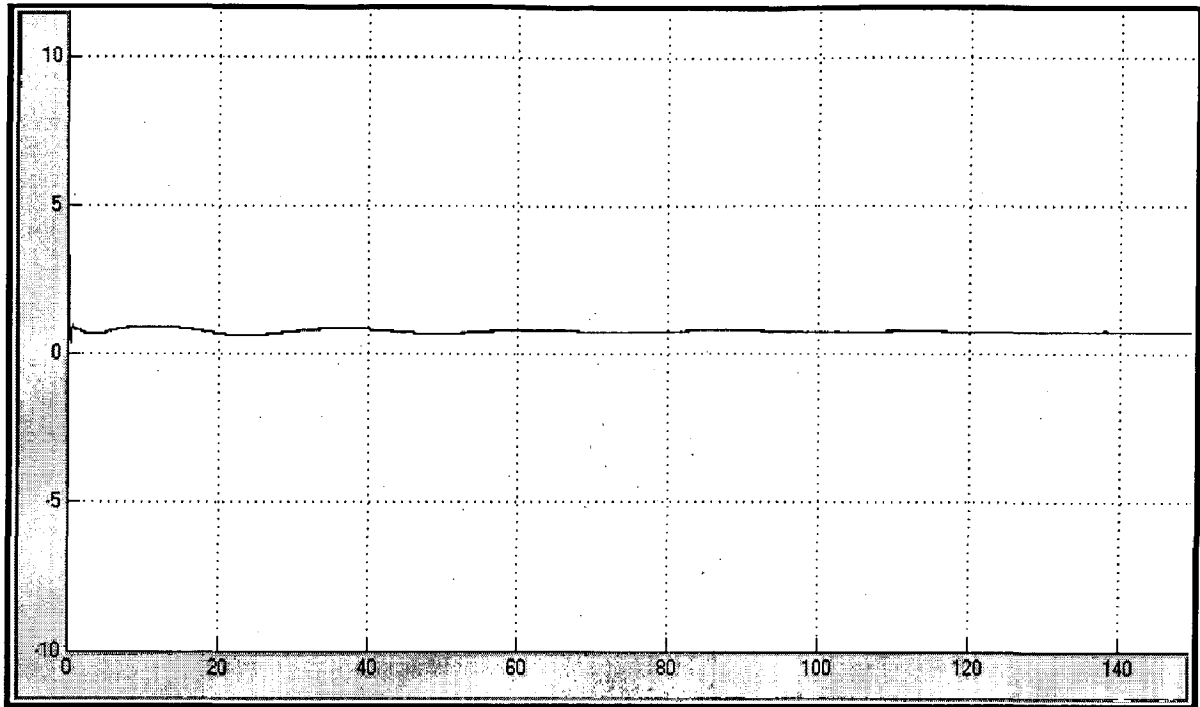


Fig. (4.59) Excitation Voltage V_f (p.u.)

When Head is varied to 0.6 p.u. from 0.7 p.u. at 50 MW Active Power and 50 MVAR Reactive Power Load then Excitation Voltage remain constant to 0.75 p.u.

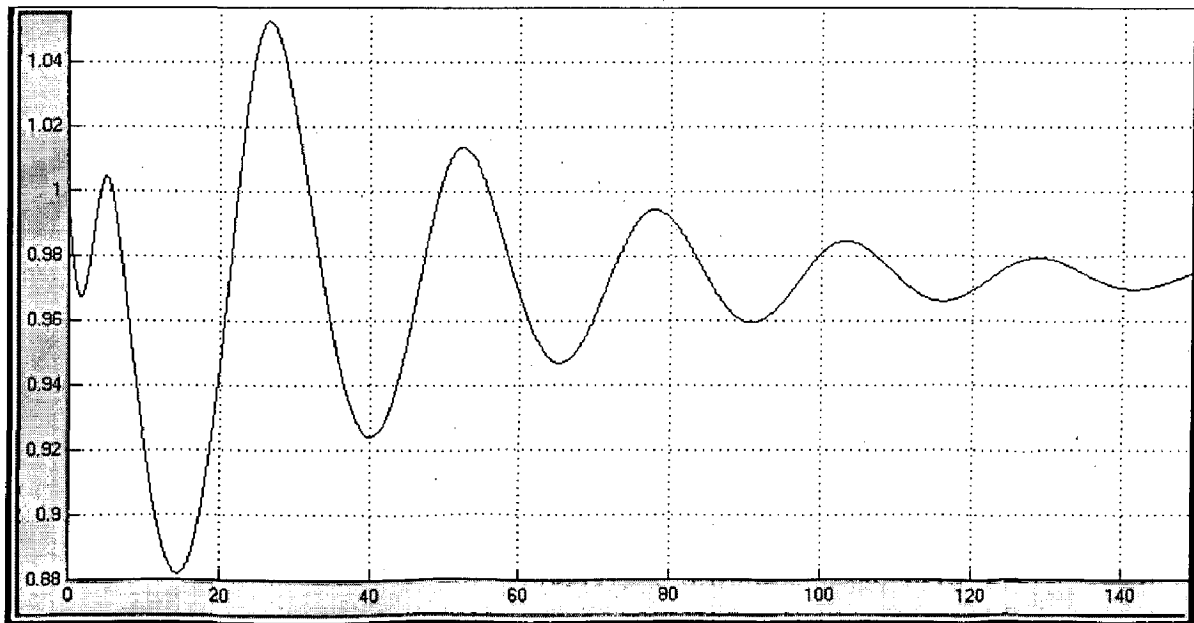


Fig. (4.60) Rotor Speed (p.u.)

When Head is varied to 0.6 p.u. from 0.7 p.u. at 50 MW Active Power and 50 MVAR Reactive Power Load then at that moment rotor speed decreases from 1 p.u. to 0.97 p.u.

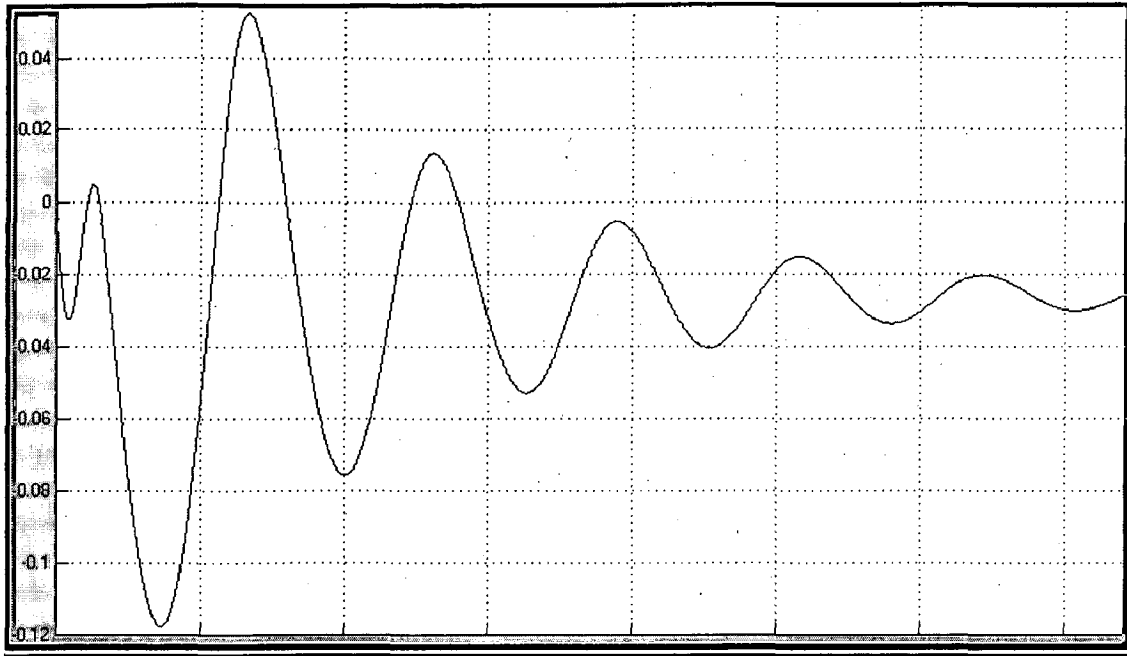


Fig (4.61)_Speed Deviation (p.u.)

When Head is varied to 0.6 p.u. from 0.7 p.u. at 50 MW Active Power and 50 MVAR Reactive Power Load then speed deviation decreases from 0 p.u. to -0.03 p.u.

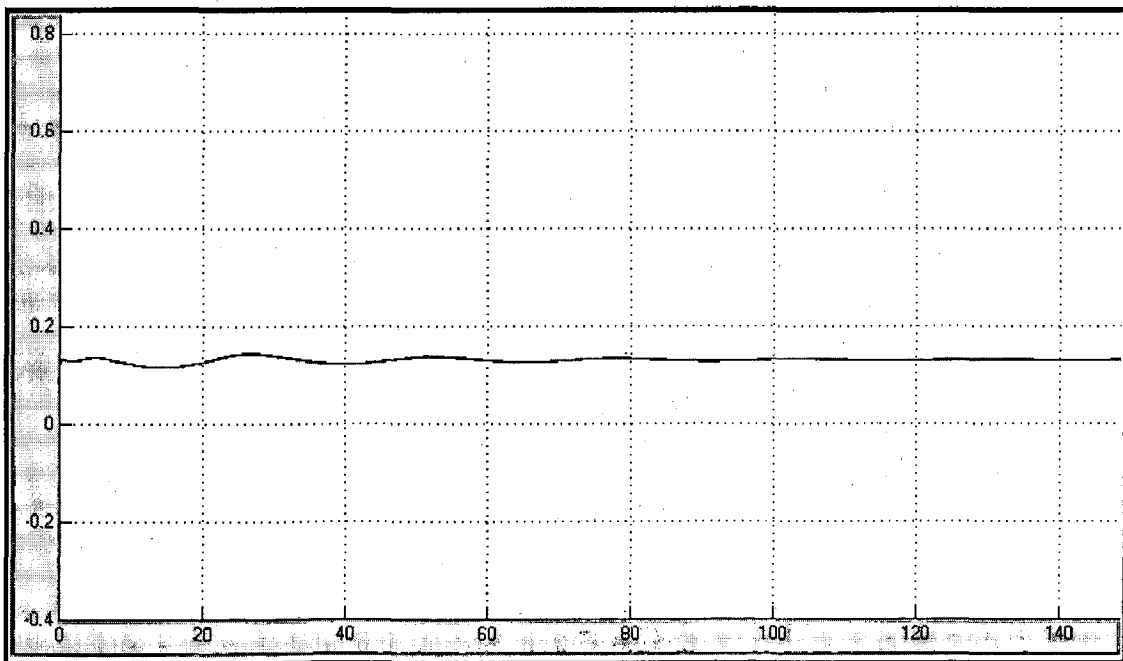


Fig. (4.62) V_d (p.u.)

When Head is varied to 0.6 p.u. from 0.7 p.u. at 50 MW Active Power and 50 MVAR Reactive Power Load then d-transformation voltage remain constant to 0.13 p.u.

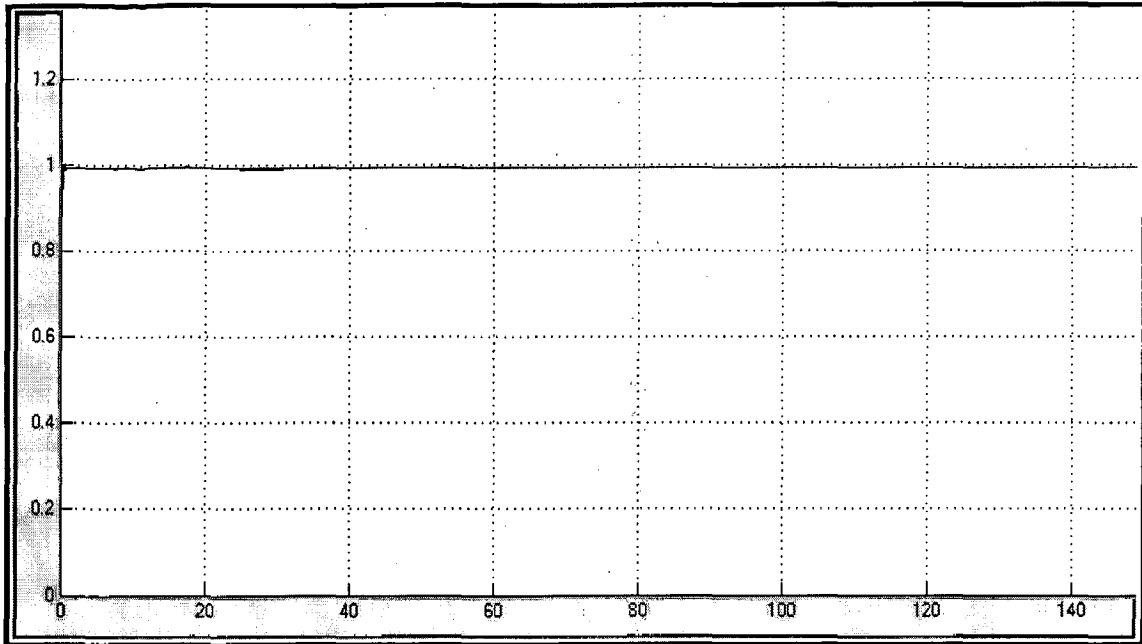


Fig (4.63) V_q (p.u.)

When Head is varied to 0.6 p.u. from 0.7 p.u. at 50 MW Active Power and 50 MVAR Reactive Power Load then q-transformation voltage remain constant to 0.992 p.u.

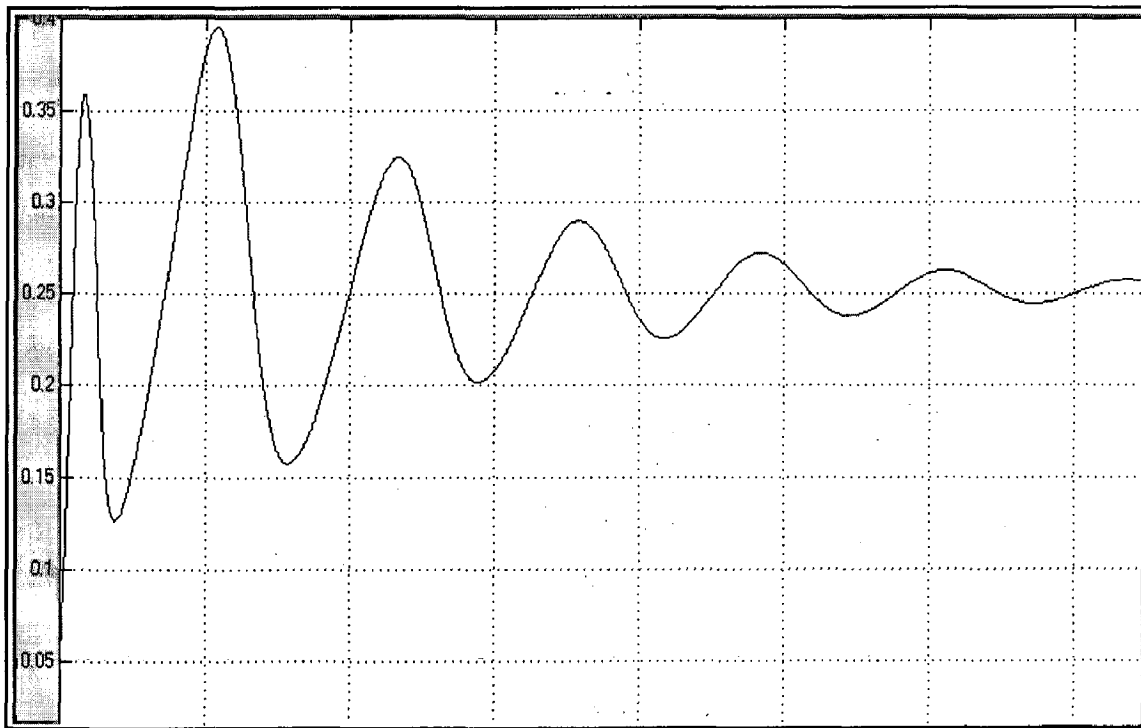


Fig. (4.64) Mechanical Power P_m (p.u.)

When Head is varied to 0.6 p.u. from 0.7 p.u. at 50 MW Active Power and 50 MVAR Reactive Power Load then mechanical power demand remain constant to 0.252 p.u.

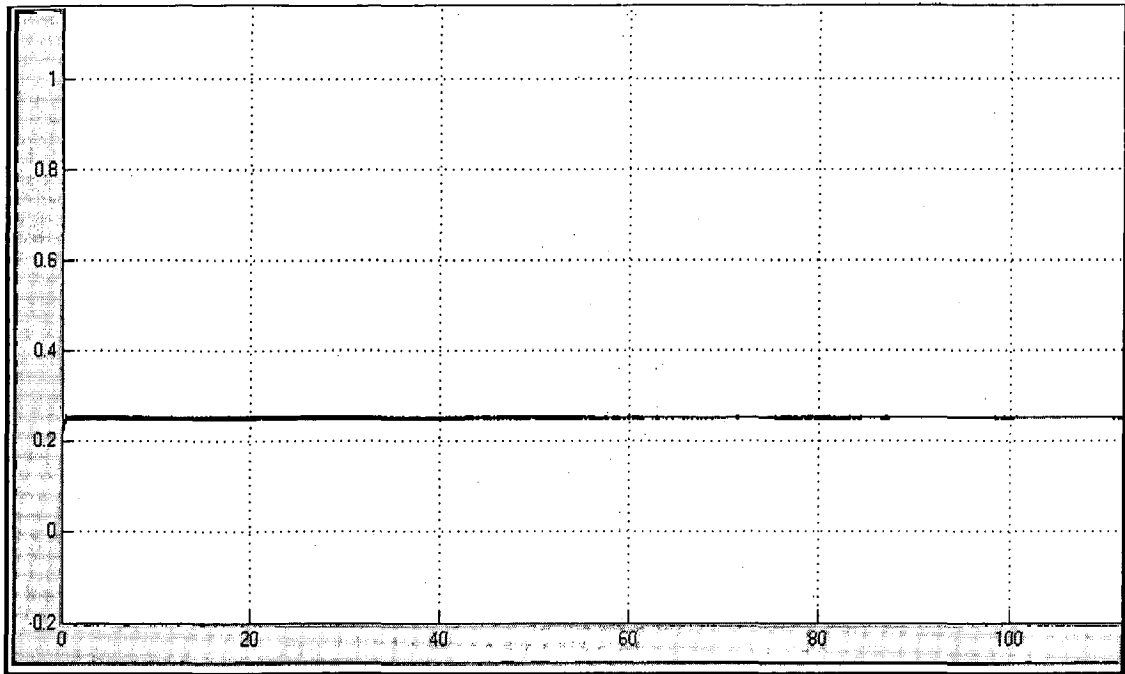


Fig (4.65) Electrical Power P_{eo} (p.u.)

When Head is varied to 0.6 p.u. from 0.7 p.u. at 50 MW Active Power and 50 MVAR Reactive Power Load then Electrical power demand remain constant to 0.25 p.u.

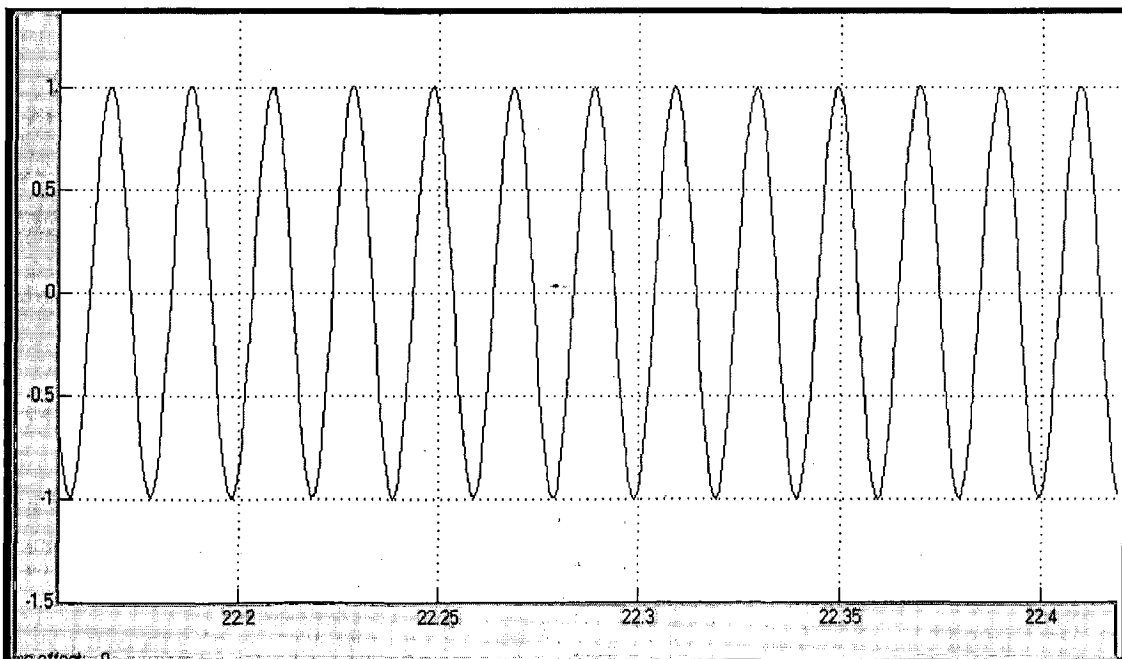


Fig. (4.66) , Voltage

When Head is varied to 0.6 p.u. from 0.7 p.u. at 50 MW Active Power and 50 MVAR Reactive Power Load then also stator voltage does not effect and remain constant as 1 p.u. in magnitude..

5. CONCLUSION

The general principles of the variable speed generator for application in the field of hydro power generation have been presented. The behavior of a variable speed generator installation of 200 MVA has been simulated in steady state as well as transient operations. The above described variable speed generator system has been simulated with a software package MATLAB. Simulation output is obtained for mechanical power, active power, speed, gate opening, excitation voltage etc. at different load power conditions. Their transient response and steady state response are studied, and then stability is studied. This study is extended for different Head and discharge conditions also. Thus variable speed generator for hydro power plant at varying head and discharge conditions is performed well.

6. REFERENCE

- Alan K. Wallace, Rene Spee, Gerald C. Alexander, “Adjustable Speed Drive and Variable Speed Generation System with Reduced Power Converter Requirements” (IEEE paper 1993)
- Yuzo ITOH and Nobuhito NOZAWA, “The Design of Control Configuration of Variable Speed Generator System” (IEEE paper 1997)
- R.Kobayashi, A.Yokoyama , S. Ogawa, S.C.Verma, “Power Interchange Control of Frequency Converter using Adjustable Speed Generator/Motor Taking Into Account Multiple Power Flow Conditions”(IEEE paper 2000)
- Krzysztof Kulesza ABB Corporate Research, “Advance Control Schema for Variable Speed Wind Turbine” (IEEE paper 2008)
- Tin Luu and Adel Nasiri, “Output Power Maximizing of a wind Turbine by Adjusting Rotor Speed” (IEEE paper 2008)
- Danial Schafer and Prof. Jean-Jacques Simond, “Adjustable speed Asynchronous Machine in Hydro Power Plants and its Advantages for the Electric Grid Stability”
- Prabha Kundur, “Power System Stability and Control”
- K R Padiyar, “Power System Dynamics stability and Control”